

Measurement of flow harmonics with multi-particle cumulants in Pb+Pb collisions at $\sqrt{s_{\text{NN}}} = 2.76$ TeV with the ATLAS detector

ATLAS Collaboration*

CERN, 1211 Geneva 23, Switzerland

Received: 20 August 2014 / Accepted: 22 October 2014 / Published online: 26 November 2014

© CERN for the benefit of the ATLAS collaboration 2014. This article is published with open access at Springerlink.com

Abstract ATLAS measurements of the azimuthal anisotropy in lead–lead collisions at $\sqrt{s_{\text{NN}}} = 2.76$ TeV are shown using a dataset of approximately $7 \mu\text{b}^{-1}$ collected at the LHC in 2010. The measurements are performed for charged particles with transverse momenta $0.5 < p_{\text{T}} < 20$ GeV and in the pseudorapidity range $|\eta| < 2.5$. The anisotropy is characterized by the Fourier coefficients, v_n , of the charged-particle azimuthal angle distribution for $n = 2-4$. The Fourier coefficients are evaluated using multi-particle cumulants calculated with the generating function method. Results on the transverse momentum, pseudorapidity and centrality dependence of the v_n coefficients are presented. The elliptic flow, v_2 , is obtained from the two-, four-, six- and eight-particle cumulants while higher-order coefficients, v_3 and v_4 , are determined with two- and four-particle cumulants. Flow harmonics v_n measured with four-particle cumulants are significantly reduced compared to the measurement involving two-particle cumulants. A comparison to v_n measurements obtained using different analysis methods and previously reported by the LHC experiments is also shown. Results of measurements of flow fluctuations evaluated with multi-particle cumulants are shown as a function of transverse momentum and the collision centrality. Models of the initial spatial geometry and its fluctuations fail to describe the flow fluctuations measurements.

1 Introduction

The anisotropy of charged-particle azimuthal angle distributions in heavy-ion collisions has been a subject of extensive experimental studies at RHIC [1–6] and more recently at the LHC [7–24]. The results provide conclusive evidence that the hot and dense matter produced in these collisions behaves collectively and has properties resembling those of a nearly perfect fluid [25].

The final-state anisotropy is a global property of particle production that arises from the initial spatial asymmetry of the collision region in a plane transverse to the beam axis for heavy-ion collisions with a non-zero impact parameter. It is characterized by the coefficients, v_n , of the Fourier expansion of the measured azimuthal angle distributions [1,26]:

$$v_n \equiv \langle e^{in(\phi - \Psi_n)} \rangle = \langle \cos [n(\phi - \Psi_n)] \rangle, \quad (1)$$

where n is the order of the Fourier harmonic, referred to as flow harmonic, ϕ is the azimuthal angle of the outgoing particle, Ψ_n defines the azimuthal angle of the n th-order symmetry plane of the initial geometry [15], and the angled brackets denote an average over charged particles in an event. Due to the symmetry in the azimuth of the plane defined by Ψ_n , all sine terms of the Fourier expansion vanish. For evaluation of the coefficients v_n in the “event-plane” method, the initial plane of symmetry is estimated from the measured correlations between particles, using the so-called sub-event method [26]. As a consequence, only the two-particle correlations are exploited in the determination of v_n (see Eq. 1). This leads to a problem of disentangling all-particle flow and contributions from particle correlations unrelated to the initial geometry, known as non-flow correlations. These non-flow effects include correlations due to energy and momentum conservation, resonance decays, quantum interference phenomena and jet production. They generally involve only a small number of produced particles. In order to suppress non-flow correlations, methods that use genuine multi-particle correlations, estimated using cumulants, were proposed [27–30].

Calculating multi-particle correlations in large-multiplicity heavy-ion collisions at high energies is limited by the computing requirements needed to perform nested loops over thousand of particles per event to analyse all particle multiplets. To avoid this problem, the generating function formalism [27–29] is exploited to calculate multi-particle cumulants, and the results obtained are presented in this paper. An alternative approach was proposed in Ref. [30] to express

* e-mail: atlas.publications@cern.ch

multi-particle correlations in terms of the moments of the flow vector, Q_n , and is used in this paper as a cross-check of multi-particle cumulants obtained with the generating function method. The cumulant approach to measure flow harmonics also provides the possibility to study event-to-event fluctuations in the amplitudes of different harmonics, which can be related to the fluctuations in the initial transverse shape of the interaction region [31–33].

The cumulant method has been used to measure the anisotropic flow in NA49 [34], STAR [35] and recently also at the LHC experiments [7, 9, 20, 23]. The results show that the Fourier coefficients determined with four-particle cumulants are smaller than those derived with two-particle cumulants due to the suppression in the former of non-flow two-particle correlations. In this paper, the method is used to measure flow harmonics in lead–lead collisions at $\sqrt{s_{NN}} = 2.76$ TeV with the ATLAS detector. The elliptic flow v_2 is measured using two-, four-, six- and eight-particle cumulants. For v_3 and v_4 measurements the two- and four-particle cumulants are exploited.

This paper is organized as follows. Section 2 describes the ATLAS detector, trigger, and offline event selections. Section 3 contains a description of additional selection criteria for events and charged-particle tracks. Section 4 gives details of the Monte Carlo simulation samples used to derive the tracking efficiency and fake-track rates. The analysis method and procedure is outlined in Sect. 5. Section 6 contains a discussion of the systematic errors. Results are presented in Sect. 7. Section 8 is devoted to summary and conclusions.

2 The ATLAS detector and trigger

The results presented in this paper were obtained from a sample of minimum-bias lead–lead collisions at $\sqrt{s_{NN}} = 2.76$ TeV recorded by ATLAS in 2010 and corresponding to an integrated luminosity of approximately $7 \mu\text{b}^{-1}$. The measurements were performed using the ATLAS inner detector and forward calorimeters [36]. The inner detector covers the complete azimuthal range and extends over the pseudorapidity region $|\eta| < 2.5$.¹ The inner detector silicon tracker, used in this analysis for track reconstruction, consists of layers of pixel and microstrip detectors (SCT) immersed in a 2 T axial magnetic field. The forward calorimeters (FCal) use liquid argon with copper-tungsten absorbers to perform both the electromagnetic and hadronic energy measurements

¹ ATLAS uses a right-handed coordinate system with its origin at the nominal interaction point (IP) in the centre of the detector and the z -axis along the beam pipe. The x -axis points from the IP to the centre of the LHC ring, and the y -axis points upward. Cylindrical coordinates (r, ϕ) are used in the transverse plane, ϕ being the azimuthal angle around the beam pipe. The pseudorapidity is defined in terms of the polar angle θ as $\eta = -\ln \tan(\theta/2)$.

with copper-tungsten/liquid argon technology, and also provide complete coverage in azimuth for $3.2 < |\eta| < 4.9$. The trigger system was used to select minimum-bias lead–lead collisions. It required a coincidence of signals recorded in both zero-degree calorimeters (ZDC), located symmetrically at $z = \pm 140$ m, and in the minimum-bias trigger scintillator (MBTS) counters at $z = \pm 3.6$ m.

3 Event and track selections

Additional offline event selections were also applied, requiring a time difference between the two MBTS counters of less than 3 ns and at least one primary vertex reconstructed using charged-particle tracks. Events satisfying the above-described selections were also required to have a reconstructed primary vertex within 100 mm of the nominal centre of the ATLAS detector.

The precision silicon tracking detectors were used to reconstruct charged-particle trajectories with a minimum p_T of 0.5 GeV. Special track-quality criteria are imposed to deal with high particle densities in Pb+Pb collisions. Tracks are required to have at least eight hits in the SCT, at least two pixel hits and a hit in the pixel layer closest to the interaction point if expected. A track must have no missing pixel hits and no missing SCT hits, when a hit is expected. The transverse and longitudinal impact parameters with respect to the vertex, $|d_0|$ and $|z_0 \sin \theta|$ respectively, were each required to be less than 1 mm. Specifically for this analysis it was also required that $|d_0/\sigma_{d_0}| < 3$ and $|z_0 \sin \theta/\sigma_z| < 3$, where σ_{d_0} and σ_z are the uncertainties on d_0 and $z_0 \sin \theta$, respectively, as obtained from the covariance matrix of the track fit. The latter requirements improve both the tracking performance at high p_T and the purity of the track sample. The number of reconstructed tracks per event is denoted $N_{\text{ch}}^{\text{rec}}$. For this analysis, the additional requirement of $N_{\text{ch}}^{\text{rec}} \geq 10$ for tracks with $0.5 < p_T < 5$ GeV was imposed to allow the measurement of correlations involving as many as eight particles.

The correlation between the summed transverse energy (ΣE_T^{FCal}) measured in the FCal and $N_{\text{ch}}^{\text{rec}}$ was investigated in order to identify background events. Events having an $N_{\text{ch}}^{\text{rec}}$ vs. ΣE_T^{FCal} correlation distinctly different from that for the majority of Pb+Pb collisions were removed. The removed events, less than 0.01 % of the sample, were found to contain multiple Pb+Pb collisions. After applying all selection requirements, the data sample consists of about 35×10^6 Pb+Pb collision events.

The summed transverse energy is used to define the centrality of the collision. A detailed analysis of the ΣE_T^{FCal} distribution [15] showed that the fraction of the total inelastic cross-section sampled by the trigger and event selection requirements is $(98 \pm 2) \%$. The ΣE_T^{FCal} distribution was divided into centrality intervals, each representing a per-

centile fraction of all events after accounting for the 2 % inefficiency in recording the most peripheral collisions. The analysis is performed in narrow centrality intervals: 1 % centrality bins for the 20 % of events with the largest ΣE_T^{FCal} , and 5 % centrality bins for the remaining events. These narrow centrality intervals are then combined into wider bins to ensure sufficiently small statistical uncertainties on the measured flow harmonics. The 20 % of events with the smallest ΣE_T^{FCal} (most peripheral collisions) are not considered in this analysis, due to the inefficiency in the event triggering and the correspondingly large uncertainties of measurements performed for these low-multiplicity collisions. For each centrality interval, a standard Glauber Monte Carlo model [37,38] is used to estimate the average number of participating nucleons, $\langle N_{\text{part}} \rangle$, which provides an alternative measure of the collision centrality.

4 Monte Carlo simulations

A Monte Carlo (MC) sample was used in the analysis to determine tracking efficiencies and rates of falsely reconstructed tracks (fake-track rates). The HIJING event generator [39] was used to produce minimum-bias Pb+Pb collisions. Events were generated with the default parameters, except for the jet quenching, which was turned off. Flow harmonics were introduced into HIJING at the generator level by changing the azimuthal angle of each particle [1] in order to produce an anisotropic azimuthal angle distribution consistent with previous ATLAS v_n ($n = 2-6$) measurements [15,16]. The detector response simulation [40] uses the GEANT4 package [41] with data-taking conditions corresponding to those of the 2010 Pb+Pb run and simulated events are reconstructed in the same way as the data.

The tracking efficiency, $\epsilon(p_T, \eta)$, and the fake-track rate $f(p_T, \eta)$ are determined [42] using the Monte Carlo sample described above. The MC reproduces the measured centrality dependence of the track-quality parameters. The efficiency is found to depend weakly on the collision centrality. For the lowest transverse momenta (0.5–0.6 GeV), the efficiency at $|\eta| < 1$ is of the order of 50 % and falls to about 30 % at high $|\eta|$. For higher transverse momenta it reaches about 70 % at $|\eta| < 1$ and drops to about 50 % at high $|\eta|$. The rate of falsely reconstructed tracks (the fake-track rate) is typically below 1 %. It increases to 3–7 % for the lowest transverse momenta in the most central collisions.

5 Analysis procedure

Fourier coefficients, v_n , are measured using $2k$ -particle correlations [27–29] defined as:

$$\begin{aligned} \langle \text{corr}_n\{2k\} \rangle &= \langle \langle e^{in(\phi_1 + \dots + \phi_k - \phi_{1+k} - \dots - \phi_{2k})} \rangle \rangle \\ &= \langle v_n\{2k\}^{2k} \rangle, \end{aligned} \tag{2}$$

where the notation $v_n\{2k\}$ is used for the v_n flow harmonic derived from the $2k$ -particle correlations, and k is an integer. Azimuthal angles of particles forming a $2k$ -particle cluster are denoted by ϕ_l , where $l = 1, \dots, 2k$. The double angled brackets denote an average, first over charged particles in an event, and then over events, while the single angled brackets denote averaging over events. The multi-particle correlation, $\langle \text{corr}_n\{2k\} \rangle$, includes contributions from the collective anisotropic flow and from non-flow effects (see Sect. 1). It was proposed in Refs. [27–29] to exploit the cumulant expansion of multi-particle correlations in order to reduce the non-flow contribution. The anisotropic flow related to the initial geometry is a global, collective effect involving correlations between all outgoing particles. Thus, in the absence of non-flow effects, $v_n\{2k\}$ is expected to be independent of k . On the other hand, most of the non-flow correlations, such as resonance decays or interference effects, contribute only to correlations between small numbers of particles. The idea of using $2k$ -particle cumulants is to suppress the non-flow contribution by eliminating the correlations which act between fewer than $2k$ particles. More specifically, the cumulant of e.g. the four-particle correlations, defined as:

$$c_n\{4\} = \langle \text{corr}_n\{4\} \rangle - 2\langle \text{corr}_n\{2\} \rangle^2, \tag{3}$$

measures the genuine four-particle correlations. So, if the non-flow contribution is only due to the two-particle correlations, then $c_n\{4\}$ directly measures flow harmonics. Similarly, using the cumulant of the six-particle correlations allows one to remove contributions from two- and four-particle correlations. The different cumulants provide independent estimates of the same flow harmonic v_n , with the estimate based on correlations among many particles being more precise due to the suppressed non-flow correlations. In the absence of non-flow correlations, cumulants of different order should give the same estimate of v_n .

The generating function formalism for calculating $2k$ -particle cumulants (GFC method) was proposed in Ref. [29]. With this method, the number of required computing operations is proportional to the number of particles per event. The cumulant generating function of multi-particle azimuthal correlations, $C_n(z)$, is defined in the plane of a complex variable z as:

$$\begin{aligned} C_n(z) &= \langle N \rangle \\ &\times \left(\left\langle \prod_{j=1}^N \left[1 + \frac{w_j(z e^{in\phi_j} + z^* e^{-in\phi_j})}{N} \right] \right\rangle^{1/\langle N \rangle} - 1 \right), \end{aligned} \tag{4}$$

where the angled brackets represent the average over events in a given centrality interval, and the product runs over

the N particles within a given Pb+Pb event [27–29]. The weighting factors, w_j , are used in this analysis to correct for any non-uniformity in the azimuthal angle distribution of reconstructed tracks. The weights are obtained from the data using the two-dimensional distribution in the η – ϕ plane of all reconstructed tracks. For each bin j in $(\delta\eta, \delta\phi) = (0.1, 2\pi/64)$ a weight is calculated as $w_j = \langle N(\delta\eta) \rangle / N(\delta\eta, \delta\phi)$, where $\langle N(\delta\eta) \rangle$ is the average number of tracks in the $\delta\eta$ slice to which this bin belongs, while $N(\delta\eta, \delta\phi)$ is the number of tracks in the $(\delta\eta, \delta\phi)$ bin.

The expansion of the cumulant generating function in powers of $|z|$ provides the cumulant $c_n\{2k\}$, which is equal to the coefficient of the term $|z|^{2k}/k!^2$ of this expansion. In practice, to construct the $c_n\{2k\}$ cumulant the power series is truncated to order $|z|^{2k}$ and $C_n(z)$ is computed at a discrete set of interpolating points $z_{p,q} = x_{p,q} + iy_{p,q}$ [29], where:

$$x_{p,q} = r_0 \sqrt{p} \cdot \cos\left(\frac{2q\pi}{q_{\max}}\right), \tag{5}$$

$$y_{p,q} = r_0 \sqrt{p} \cdot \sin\left(\frac{2q\pi}{q_{\max}}\right). \tag{6}$$

For this analysis, the parameters $p = 1, \dots, 5$ and $q = 0, \dots, q_{\max} - 1$ with $q_{\max} = 11$ were chosen as recommended in Ref. [29]. The r_0 parameter ($r_0 \equiv |z|/\sqrt{p}$) should be as small as possible, chosen such that the results remain stable under its variation. The r_0 values used were chosen to be 4.0, 2.2, 1.6, 1.1 and 1.0 for centrality intervals 0–5 %, 5–10 %, 10–20 %, 20–30 % and 30–80 %, respectively. For these values, the cumulants are found to be stable when varying r_0 between $r_0/2$ and $2r_0$. The only differences, up to about 2 %, were seen when using the eight-particle cumulants to calculate the elliptic flow harmonic and are accounted for in the systematic uncertainty on $v_2\{8\}$.

An alternative method to calculate multi-particle correlations and cumulants in a single pass over all particles in each event, referred to as the QC method, was proposed in Ref. [30]. In this method, the expressions for the multi-particle correlations are derived in terms of the moments of the flow vector Q_n , defined as $Q_n = \sum_{j=1}^N w_j e^{in\phi_j}$, where the index n denotes the order of the flow harmonic, the sum runs over all N particles in an event and w_j are weights as defined above. The QC method is used to calculate the cumulants, $c_n\{2k\}$, which are compared with the cumulants obtained from the GFC method.

A practical application of the cumulant method involves two main steps [27–29]. First, the reference $2k$ -particle cumulants, $c_n\{2k\}$, are derived from the cumulant generating function calculated from particles measured over a broad range of transverse momentum and pseudorapidity. This step is equivalent to the event-plane estimate in the standard method (see Eq. 1) and the reference cumulants play a similar role to the event-plane resolution correction [26]. In

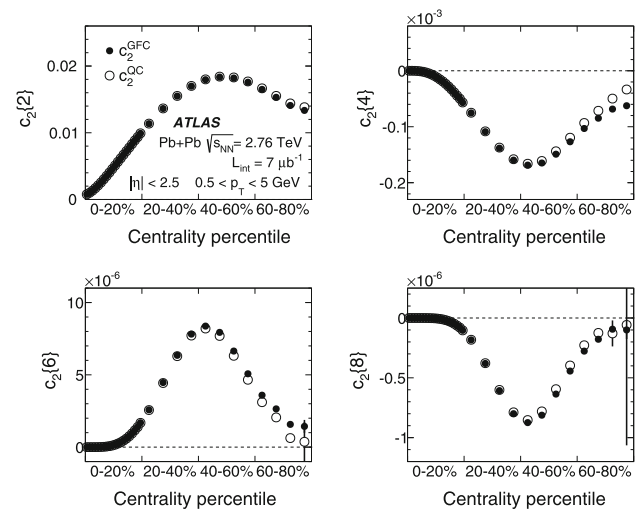


Fig. 1 Multi-particle cumulants for the second-order flow harmonic, $c_2\{2k\}$ for $k = 1, 2, 3, 4$, obtained with the GFC [29] and QC [30] methods shown as a function of centrality. The horizontal axis ranges from central collisions (0–20 %) to more peripheral collisions (60–80 %)

the next step, the differential flow is calculated in p_T and η bins using cumulants, denoted $d_n\{2k\}$, computed from a differential generating function. To determine the $d_n\{2k\}$ cumulants, each charged particle from a p_T and η bin is correlated with $2k - 1$ reference particles. The differential flow harmonics $v_n\{2k\}(p_T, \eta)$, are then calculated with respect to the reference cumulants as prescribed in Refs. [28,29]:

$$v_n\{2\}(p_T, \eta) = \frac{d_n\{2\}}{\sqrt{c_n\{2\}}}, \tag{7}$$

$$v_n\{4\}(p_T, \eta) = \frac{-d_n\{4\}}{\sqrt[3]{-c_n\{4\}}}, \tag{8}$$

$$v_n\{6\}(p_T, \eta) = \frac{d_n\{6\}/4}{\sqrt[5]{c_n\{6\}/4}}, \tag{9}$$

$$v_n\{8\}(p_T, \eta) = \frac{-d_n\{8\}/33}{\sqrt[7]{-c_n\{8\}/33}}. \tag{10}$$

In order to calculate the reference cumulants, $c_n\{2k\}$, all charged particles with pseudorapidities $|\eta| < 2.5$ and transverse momenta $0.5 < p_T < 5$ GeV are used in this analysis. The results for c_2 are shown as a function of centrality in Fig. 1 for two-, four-, six- and eight-particle cumulants obtained from the GFC and QC methods. The figure shows that the two methods yield consistent results over a wide range of collision centralities. Differences, up to ~ 20 %, are observed only for the most peripheral collisions. For the most central (0–2 %) Pb+Pb collisions, the cumulants $c_n\{2k\}$ for $k > 1$ are, within sizeable statistical errors, consistent with zero. However, they have incorrect signs, which prevents the calculation of flow harmonics due to the square-root function in the denominator of Eqs. (8), (9) and (10).

For higher flow harmonics, the cumulants $c_3\{2k\}$ and $c_4\{2k\}$ obtained from both the GFC and QC methods are

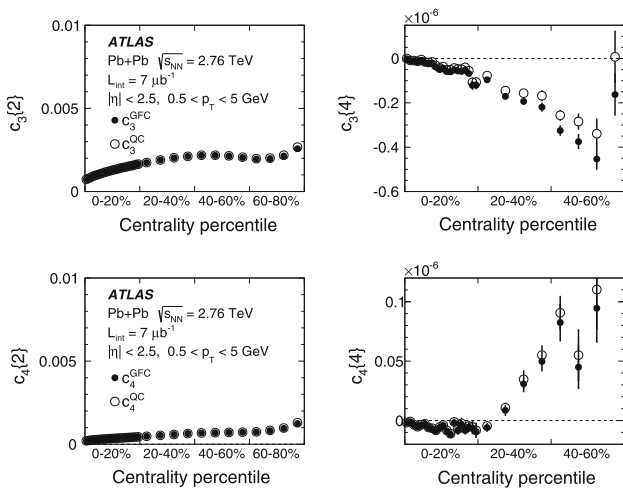


Fig. 2 *Top*: multi-particle cumulants for the third-order flow harmonic, $c_3\{2k\}$ for $k = 1, 2$ obtained with the GFC [29] and QC [30] methods shown as a function of centrality. *Bottom*: the same for the fourth-order flow harmonics, $c_4\{2k\}$

consistent with zero for $k > 2$. Therefore, only two- and four-particle cumulants can be used to derive third- and fourth-order flow coefficients. Figure 2 shows the centrality dependence of the two- and four-particle cumulants, obtained from the GFC and QC methods, for $n = 3$ and $n = 4$. The figure demonstrates an overall good agreement between the cumulants calculated using the two different methods. In the case of four-particle cumulants, the centrality range of the method’s applicability is limited to 0–60 % for $n = 3$ and 0–25 % for $n = 4$.

The differential flow harmonics, $v_n\{2k\}(p_T, \eta)$, are determined using the differential cumulants $d_n\{2k\}$ and Eqs. (7)–(10) in bins of transverse momentum and pseudorapidity for events from a given centrality interval. The pseudorapidity range $|\eta| < 2.5$ is divided into 50 bins of width 0.1 each. In transverse momentum, 28 bins of variable width, covering the p_T range from 0.5 GeV to 20 GeV, are used. These differential flow harmonics can then be integrated over wider phase-space bins or the full range in either pseudorapidity or transverse momentum, or both. In this integration procedure, the harmonics $v_n\{2k\}(p_T, \eta)$ measured in each small bin are weighted by the charged-particle multiplicity in that bin, corrected for tracking efficiency and fake-track rate, using the MC-determined corrections $\epsilon(p_T, \eta)$ and $f(p_T, \eta)$ as described in Sect. 4.

6 Systematic uncertainties

The systematic uncertainties on the measurements presented in this paper are evaluated by varying different aspects of the analysis and comparing the results obtained to the baseline results for the transverse momentum, pseudorapidity and

centrality dependence of v_2, v_3 and v_4 . The following sources are considered as potential contributors to the systematic uncertainty on the measured flow harmonics.

An overall scale uncertainty on flow harmonics comes from the uncertainty in the fraction of the total inelastic cross-section accepted by the trigger and the event selection criteria. It is evaluated by varying the centrality bin definitions, using the modified selections on ΣE_T^{FCal} , which account for the 2 % uncertainty in the sampled fraction of the cross-section.

All formulas applied in the analysis are valid under the assumption that the sine terms in the Fourier expansion vanish due to the azimuthal symmetry of the initial geometry. However, due to some distortions in the detector acceptance and non-uniformities in the measured azimuthal angle distributions, a residual sine term may be present. The magnitude of the sine term is calculated as the imaginary part of the differential generating function. The deviation from zero of the average sine term with respect to $\langle v_n \rangle$ is treated as the systematic uncertainty. Some detector distortions may lead to an asymmetry between positive and negative η hemispheres, and the difference between the flow harmonics measured at positive and negative pseudorapidities is also considered as a systematic uncertainty.

A small contribution to the systematic uncertainty, only for $v_2\{8\}$, comes from the stability of the results with respect to the assumed value of the r_0 parameter (see discussion in the previous section). The correction applied to ensure the uniformity of the azimuthal angle distribution of reconstructed tracks (via weights w_j) is also checked by comparing the baseline results to those obtained with $w_j \equiv 1$. The contribution to the systematic uncertainty related to the track-quality definition is evaluated by comparing results obtained with more restrictive or less restrictive requirements. Both the transverse and longitudinal impact parameter cuts, $|d_0|$ and $|z_0 \sin \theta|$, are changed by ± 0.5 mm with respect to the nominal value of 1 mm and the significance cuts, $|d_0/\sigma_{d_0}| < 3$ and $|z_0 \sin \theta/\sigma_z| < 3$, are changed by ± 1 .

The analysis procedure is also checked through MC studies by comparing the observables at the generator/particle level with those obtained in the MC simulated sample for which the same analysis chain and correction procedure is used as for the data. The measured flow harmonics in data agree qualitatively with the reconstructed MC harmonics and show similar trends as a function of η . In the phase-space region where tracking performance suffers from low efficiency and high fake-track rates ($p_T < 1.5$ GeV and $|\eta| > 1$), systematic differences are observed between the flow harmonics calculated at the generator level and at the reconstruction level after the corrections. In general, in this phase-space region, the reconstructed flow harmonics are smaller than the generator-level ones and show an η dependence, not present at the generator level. To account for this η -dependent bias,

Table 1 Relative systematic and statistical uncertainties ($|\Delta v_2|/v_2$, in percent) for v_2 measured with four-particle cumulants for three centrality intervals: 2–5 %, 15–20 % and 60–80 %. A single entry is given

Centrality bin		2–5 %		15–20 %		60–80 %	
		Syst. [%]	Stat. [%]	Syst. [%]	Stat. [%]	Syst. [%]	Stat. [%]
$v_2\{4\}$ vs. p_T	$0.5 \leq p_T \leq 1.5$ GeV	3.5	2.9	5.8–1.2	0.1	1.3–1.7	1.2–1.4
	$1.5 < p_T < 20$ GeV	3.5	2.5–30	1.2–1.0	0.1–41	1.8–5.4	1.3–76
$v_2\{4\}$ vs. η	$ \eta \leq 1$	3.8	1.8	1.6	0.1	2.4	0.9
	$1 < \eta < 2.5$	6.0	2.7	5.0	0.1	2.3	1.0
$v_2\{4\}$ vs. N_{part}		4.1	0.5	3.0	0.1	2.0	0.3

the MC closure test is considered as part of the systematic uncertainty.

A significant systematic uncertainty on the transverse momentum dependence of v_2 due to the centrality bin definitions was found. In the most peripheral 60–80 % centrality interval it is of the order of 5 % for $v_2\{4\}$ and rises to 14 % for $v_2\{8\}$. For the most central collisions the uncertainty is in the range 1–2 %. At low p_T , below 1.5 GeV, the systematic uncertainty due to the Monte Carlo closure is significant in the most central collisions, and reaches 8 % for $v_2\{2\}$. For $v_2\{2k\}$ with $k > 1$ it is at the level of 3–4 %. The MC closure at p_T above 1.5 GeV gives 4 % for the most central collisions, and stays typically below 1 % for other collision centralities. The r_0 stability adds about 2 % uncertainty only for $v_2\{8\}$. All other considered sources give contributions well below 1 % to the systematic uncertainty on the p_T dependence of v_2 . For higher-order flow harmonics, the systematic uncertainty on the transverse momentum dependence is mainly due to the non-zero sine term and the MC closure. The former contributes up to 5 % (15 %) for $v_3\{4\}$ ($v_4\{4\}$) and about 1 % for $v_3\{2\}$ and $v_4\{2\}$. The uncertainty due to the MC closure is less than 6 % for v_3 , and increases to 13 % for v_4 . Contributions from other sources are of the order of 1–2 %.

The systematic uncertainty on the pseudorapidity dependence of v_2 is dominated by the MC closure at $|\eta| > 1$ (up to 7 % for $v_2\{2\}$ in the most central collisions). For v_2 calculated with six- and eight-particle cumulants, significant contributions come also from the sine term (up to 15 %), η asymmetry (up to 10 %) and tracking (about 5 %) for the most central collisions. Other contributions are well below 1 %. For higher-order flow harmonics, the sine term contributes about 3 % (13 %) for v_3 (v_4) for $|\eta| < 2.5$. The MC closure at high η ($|\eta| > 1$) contributes up to 7 % (10 %) for $v_3\{2\}$ ($v_4\{2\}$) and less than 2 % for $v_3\{4\}$ and $v_4\{4\}$. For $|\eta| < 1$ it is about 1 %. Other sources give contributions up to 4 %.

The systematic uncertainty on the centrality dependence of v_2 due to the centrality bin definition is 1–2 %. For the most central collisions, the Monte Carlo closure gives a contribution of 4 %. The r_0 stability adds about 2 % only for $v_2\{8\}$. Contributions from all other sources are below 1 %.

where the uncertainty only varies by a small amount over the selected p_T or η range. Otherwise the range in uncertainties is provided corresponding to the range in p_T or η

Table 2 Relative systematic and statistical uncertainties ($|\Delta v_n|/v_n$, in percent) for v_3 and v_4 measured with four-particle cumulants averaged over the accessible centrality ranges 0–60 % and 0–25 %, respectively. A single entry is given where the uncertainty only varies by a small amount over the p_T range from 0.5 to 20 GeV or η range from –2.5 to 2.5. Otherwise the range in uncertainties is provided corresponding to the range in p_T or η

Measurement	Syst. [%]	Stat. [%]
$v_3\{4\}$ vs. p_T	6.2–4.8	19–26
$v_3\{4\}$ vs. η	3.7	8
$v_3\{4\}$ vs. N_{part}	3.3	16
$v_4\{4\}$ vs. p_T	16	46–34
$v_4\{4\}$ vs. η	13	23
$v_4\{4\}$ vs. N_{part}	5.4	31

For higher-order flow harmonics, the sine term and MC closure each contribute about 3 %, while all other sources contribute less than 1 %.

The total systematic uncertainty is the sum in quadrature of all the individual contributions. For illustration, Table 1 shows the total systematic uncertainties on $v_2\{4\}$ for three representative centrality intervals: 2–5 %, 15–20 % and 60–80 %. For higher-order flow harmonics, the systematic uncertainties are listed in Table 2. For comparison, the statistical uncertainties on v_n are also listed. It can be seen that the uncertainties on the measured v_2 at high p_T and on v_3 and v_4 over the whole kinematic range, are dominated by large statistical errors.

In addition to the evaluation of the systematic uncertainty, further cross-checks are performed. The comparison between cumulants calculated with the GFC and QC methods is discussed in detail in Sect. 5. The analysis is performed separately for negatively and positively charged particles and the resulting v_n coefficients are found to be consistent within their statistical and systematic uncertainties. Furthermore, the consistency of $v_2\{2k\}$ for $k > 1$ measured for same-sign particles and all combinations of charged particles confirms the global collective feature of the measured effect. Consistency is also observed between measurements obtained from

sub-samples collected early and late during the data-taking period. The analysis also evaluates a potential bias which may be due to the large spread in charged-particle multiplicities in centrality intervals defined by ΣE_T^{FCal} . For this purpose, in a given centrality bin selected by ΣE_T^{FCal} , the analysis is restricted to events with multiplicities limited to a very narrow range (corresponding to $\pm RMS/2$ around the mean multiplicity) and compared to the analysis performed for the full range of multiplicities. Both give v_n harmonics consistent with each other within their statistical and systematic uncertainties.

7 Results

7.1 Transverse momentum dependence of flow harmonics

The transverse momentum dependence of $v_2\{2\}$, $v_2\{4\}$, $v_2\{6\}$ and $v_2\{8\}$ is shown in Fig. 3 in 14 centrality intervals as indicated in the plots. The v_2 coefficients are integrated over the full pseudorapidity range $|\eta| < 2.5$. The elliptic flow mea-

surements, $v_2\{EP\}$, obtained with the event-plane method [26] are also shown. For this comparison, the measurements from Ref. [15] were reanalysed with the same track-quality requirements and centrality intervals as for the present analysis. The event-plane v_2 is systematically smaller than $v_2\{2\}$ since it is less affected by short-range two-particle correlations, which are partially removed from $v_2\{EP\}$ due to the separation between the phase-space region where the event plane angle is determined ($3.2 < |\eta| < 4.9$) and the phase space where charged-particle momenta are reconstructed ($|\eta| < 2.5$). This effect is particularly pronounced at high transverse momenta, where $v_2\{2\}$ is strongly influenced by jet-related correlations. At lower transverse momenta, the difference between $v_2\{2\}$ and $v_2\{EP\}$ can also be attributed to flow fluctuations. The difference between $v_2\{EP\}$ and $v_2\{4\}$ is mainly due to flow fluctuations. The $v_2\{2k\}$ for $k > 1$ is systematically smaller than $v_2\{2\}$, consistent with the expected suppression of non-flow effects in v_2 obtained with cumulants of more than two particles. The results for $v_2\{2k\}$ with $k > 1$ agree with each other, within the uncertainties, for all centrality intervals, indicating that already the four-particle

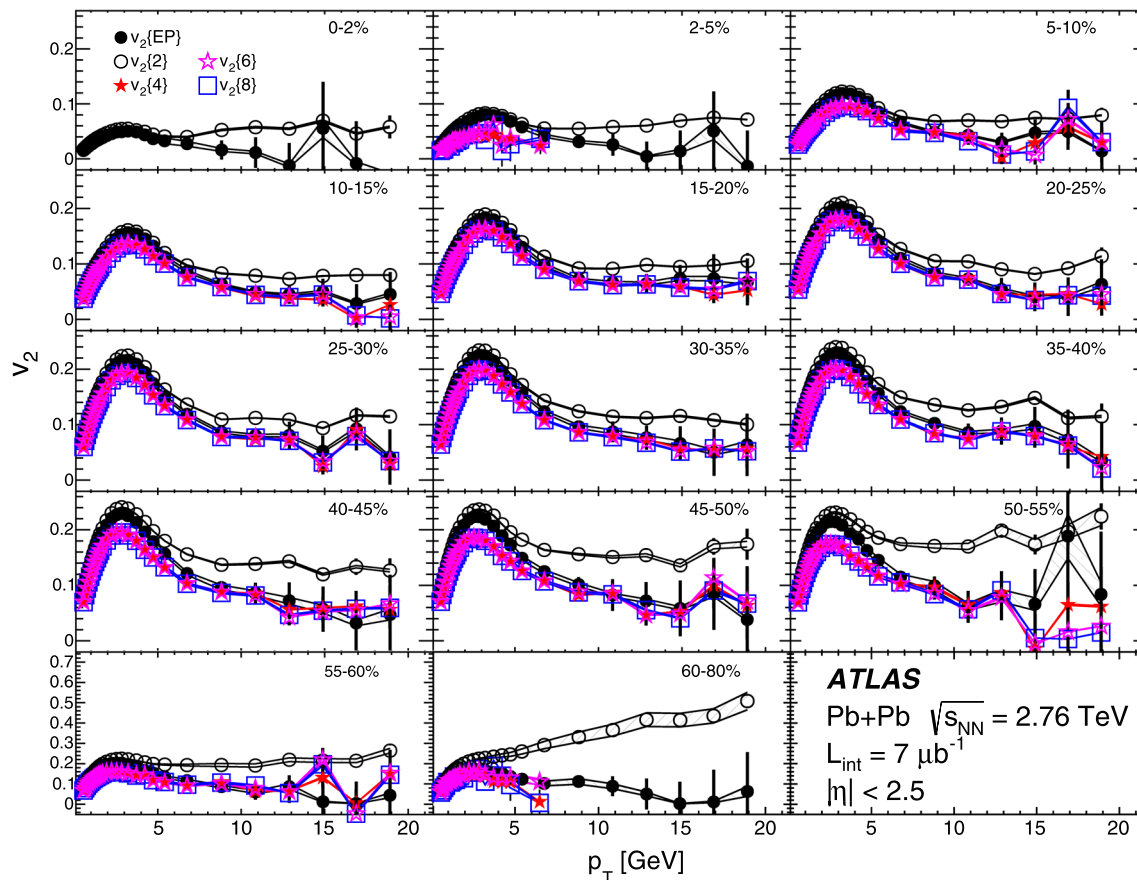


Fig. 3 The second flow harmonic calculated with the two-, four-, six-, and eight-particle cumulants measured over the full pseudorapidity range, $|\eta| < 2.5$, as a function of transverse momentum in different centrality intervals, indicated on the plots. For the most central colli-

sions (0–2 % centrality class) the results are available only for $v_2\{2\}$. For comparison the $v_2\{EP\}$ measurements obtained with the event-plane method are also shown. Statistical uncertainties are shown as bars and systematic uncertainties as bands

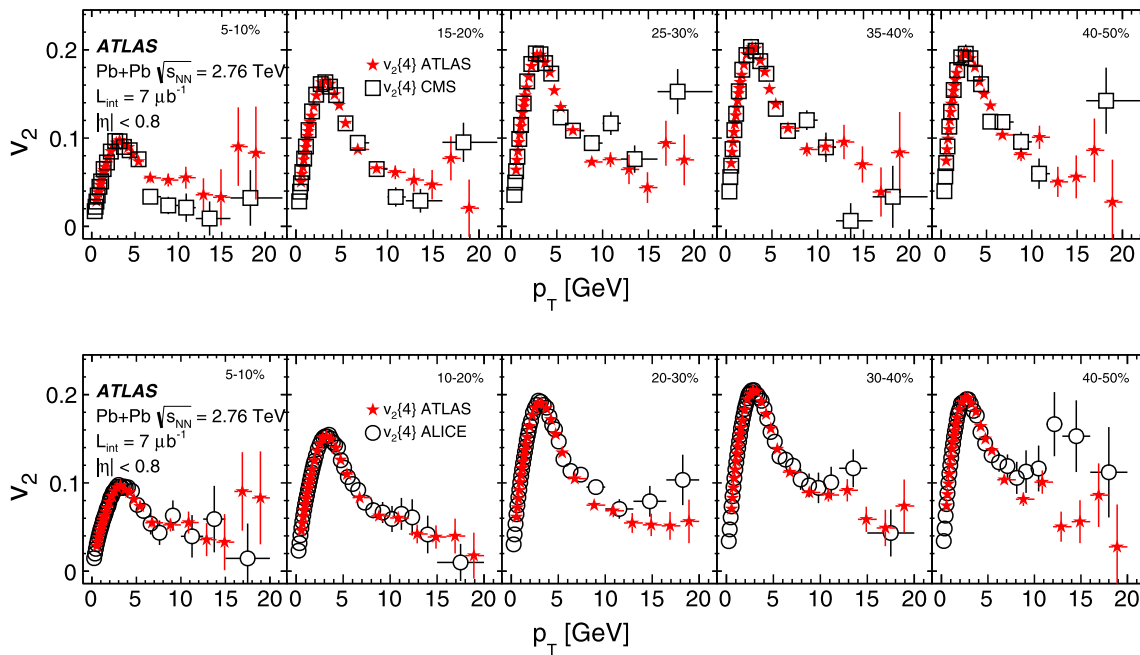


Fig. 4 Comparison of the ATLAS and CMS [20] (*top panel*), and ATLAS and ALICE [9] (*bottom panel*) measurements of $v_2\{4\}$ for selected centrality intervals at $|\eta| < 0.8$. The *error bars* denote statistical and systematic uncertainties added in quadrature

cumulants efficiently suppress non-flow correlations. As a function of transverse momentum, the second flow harmonic first increases with p_T up to $p_T \approx 2-3$ GeV, then gradually decreases for p_T values up to about 6 GeV. This trend is consistent with hydrodynamic predictions for a collective expansion of the created system [43, 44]. Beyond p_T of about 10 GeV, a much weaker v_2 dependence on p_T is observed. Interestingly the coefficients $v_2\{2k\}$ for $k > 1$ remain significant at high transverse momenta, up to about 20 GeV, over a broad centrality range, except the most peripheral and the most central collisions. These large values of $v_2\{4\}$, $v_2\{6\}$ and $v_2\{8\}$ at high transverse momenta may reflect both the anisotropy of the initial geometry and the path-length dependence of the parton energy loss in the dense, strongly interacting medium [45].

Figure 4 shows the comparison of our results for $v_2\{4\}$ integrated over $|\eta| < 0.8$ as a function of p_T , to these coefficients measured by the CMS [20] and ALICE [9] experiments in several centrality intervals. The results on the elliptic flow harmonic measured with four-particle cumulants are consistent within uncertainties for the three experiments.

The transverse momentum dependence of the higher-order harmonics, v_3 and v_4 , is shown in Fig. 5 and compared to the results obtained with the event-plane method. Due to the large uncertainties on the harmonics measured with four-particle cumulants, especially for events with low multiplicities, the results are shown in wide centrality ranges: for v_3 in the two broad centrality intervals, 0–25 % and 25–60 %, and for v_4 in the full accessible centrality range, 0–25 %. In addition, the results for $v_n\{4\}$ are shown in fine p_T bins

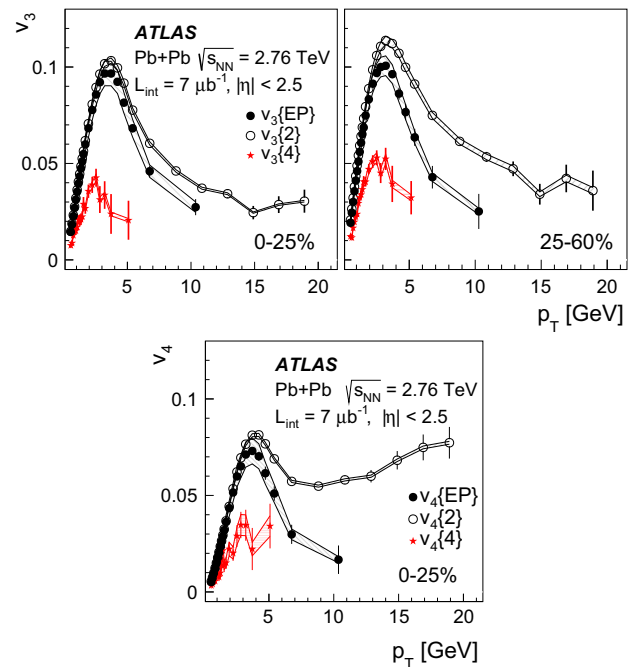


Fig. 5 The transverse momentum dependence of v_3 calculated with two- and four-particle cumulants and with the event-plane method $v_3\{EP\}$ for the centrality interval 0–25 % (*top left plot*) and 25–60 % (*top right plot*). The *bottom plot* shows the same results for v_4 for the centrality interval 0–25 %. Statistical errors are shown as *bars* and systematic uncertainties as *bands*. The highest p_T measurement for $v_n\{4\}$ ($v_n\{EP\}$) is integrated over the p_T range 4–20 (8–20) GeV

at low transverse momenta, up to 4 GeV, while the last p_T point covers the range from 4 GeV to 20 GeV. Similarly to v_2 , smaller short-range jet-like correlations are observed in

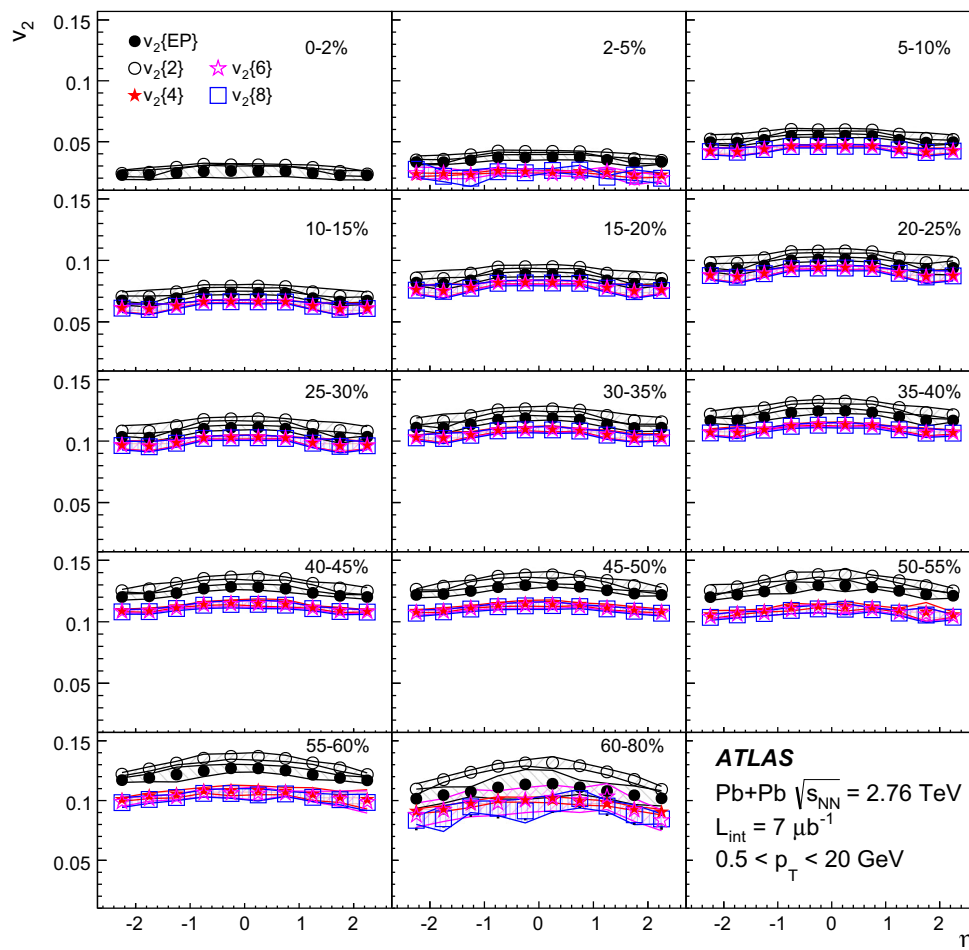


Fig. 6 The second flow harmonic calculated with the two-, four-, six-, and eight-particle cumulants as a function of η in different centrality intervals, integrated over the p_T range $0.5 < p_T < 20$ GeV. The results

for $v_2\{EP\}$ are also shown. Statistical errors are shown as *bars* (too small to be seen on this scale) and systematic uncertainties as *shaded bands*

$v_{3,4}\{EP\}$ as compared to $v_{3,4}\{2\}$. Significantly non-zero values of the third and fourth flow harmonics calculated with four-particle cumulants are observed with a p_T dependence similar to that of v_2 . The $v_n\{4\}$ harmonic is systematically smaller than $v_n\{2\}$, consistent with the suppressed non-flow effects in flow harmonics obtained with cumulants of more than two particles. It is noted that the difference between $v_3\{4\}$ ($v_4\{4\}$) and $v_3\{EP\}$ ($v_4\{EP\}$), which amounts to a factor of about two, is much larger than the difference between $v_2\{4\}$ and $v_2\{EP\}$, which is of the order of 30 %. This indicates that fluctuations of higher-order flow harmonics are much stronger than fluctuations of v_2 .

7.2 Pseudorapidity dependence of flow harmonics

The pseudorapidity dependence of $v_n\{2k\}$ is studied as a function of centrality for flow coefficients integrated over the p_T range from 0.5 GeV to 20 GeV. Figure 6 shows $v_2\{2\}$,

$v_2\{4\}$, $v_2\{6\}$, $v_2\{8\}$ and $v_2\{EP\}$ as a function of η in 14 centrality intervals as indicated in the plots. Observations similar to the case of the p_T dependence can be made: $v_2\{2k\}$ for $k > 1$ is systematically smaller than $v_2\{2\}$ and $v_2\{EP\}$, while the results for $v_2\{2k\}$ with $k > 1$ agree with each other for all centrality intervals. No strong dependence on pseudorapidity is observed for any of the second flow harmonic measurements in any of the centrality bins. Some weak dependence is observed only for $v_2\{2\}$ and can be attributed to the contributions from short-range two-particle correlations. A weak pseudorapidity dependence is observed for $v_3\{4\}$ as shown in Fig. 7 for harmonics averaged over the full accessible centrality range (0–60 %). The fourth-order flow harmonics, $v_4\{4\}$, show no significant dependence on pseudorapidity, within the measurement uncertainties, over the centrality range 0–25 %. A systematic reduction in the non-flow contribution is observed for $v_n\{EP\}$ as compared to $v_n\{2\}$.

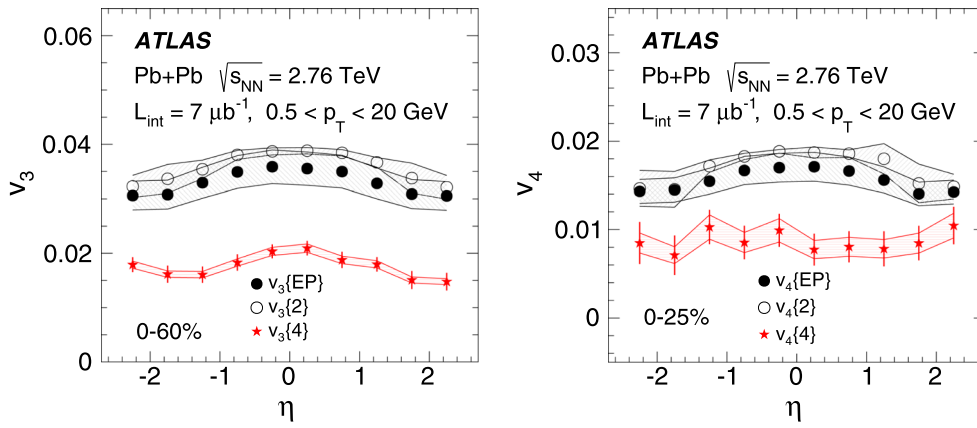


Fig. 7 The pseudorapidity dependence of v_3 (left plot) calculated with two- and four-particle cumulants and with the event-plane method, integrated over p_T from 0.5 GeV to 20 GeV for the centrality range 0–

60 %. The same is shown for v_4 (right plot) for the centrality range 0–25 %. Statistical errors are shown as bars and systematic uncertainties as shaded bands

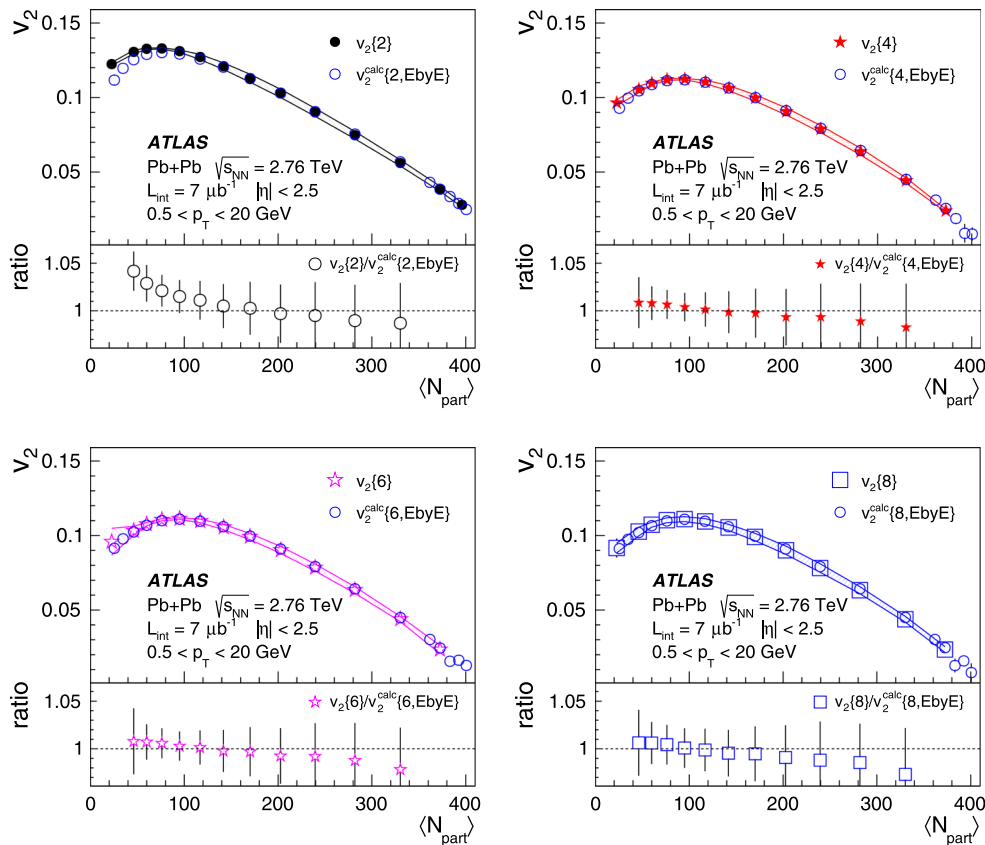


Fig. 8 Comparison of the centrality dependence of $v_2\{2k\}$ for $k = 1–4$ integrated over p_T from 0.5 GeV to 20 GeV and over $|\eta| < 2.5$, and $v_2^{\text{calc}}\{2k, \text{EbyE}\}$ calculated from the measured v_2 distribution [17]. For $v_2\{2k\}$, the statistical errors are shown as bars and the system-

atic uncertainties as shaded bands. For $v_2^{\text{calc}}\{2k, \text{EbyE}\}$, the error bars denote statistical and systematic errors added in quadrature. The bottom panels in each plot show ratios of the results obtained with the two methods. The ratios are calculated for matching centrality intervals

7.3 Centrality dependence of the integrated flow harmonics

The centrality dependence of the elliptic flow harmonic, integrated over the full range in η and p_T and obtained with cumulants of various orders, is shown as a function of $\langle N_{\text{part}} \rangle$ in Fig. 8. The coefficients $v_2\{2k\}$, and in general $v_n\{2k\}$,

can also be calculated from the moments of the distribution, $p(v_n)$, of the event-by-event (EbyE) measured flow harmonics, $\langle v_n^k \rangle = \sum v_n^k p(v_n)$ as:

$$\langle v_n^{\text{calc}}\{2, \text{EbyE}\} \rangle^2 \equiv \langle v_n^2 \rangle, \tag{11}$$

$$\langle v_n^{\text{calc}}\{4, \text{EbyE}\} \rangle^4 \equiv -\langle v_n^4 \rangle + 2\langle v_n^2 \rangle^2, \tag{12}$$

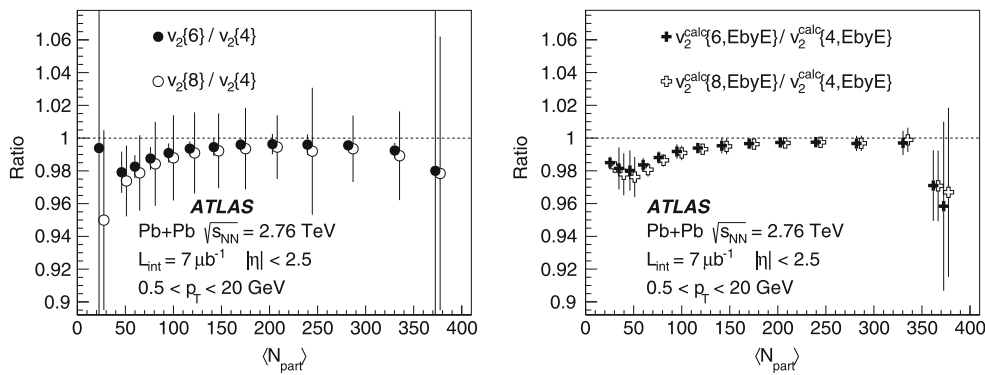


Fig. 9 The ratio of $v_2\{6\}$ and $v_2\{8\}$ to $v_2\{4\}$ as a function of the average number of participating nucleons, $\langle N_{part} \rangle$, for elliptic flow coefficients obtained from the cumulant method (left) and calculated from the mea-

sured $p(v_2)$ distribution [17] (right). The error bars denote statistical and systematic errors added in quadrature. The ratio symbols are shifted horizontally with respect to each other for clarity

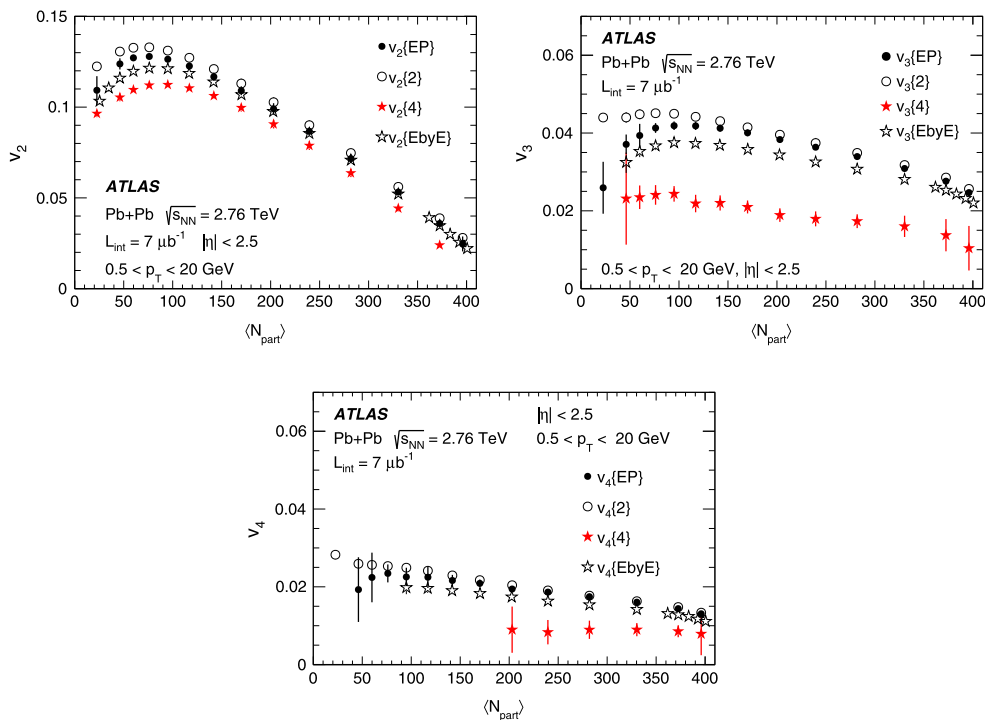


Fig. 10 Comparison of the $\langle N_{part} \rangle$ dependence of the v_2 (top left), v_3 (top right) and v_4 (bottom) harmonics measured with different methods, with $v_n\{EbyE\}$ denoting the mean value of the corresponding $p(v_n)$. The error bars denote statistical and systematic uncertainties added in quadrature

$$\begin{aligned}
 (v_n^{calc}\{6, EbyE\})^6 &\equiv (\langle v_n^6 \rangle - 9\langle v_n^4 \rangle \langle v_n^2 \rangle + 12\langle v_n^2 \rangle^3)/4, \quad (13) \\
 (v_n^{calc}\{8, EbyE\})^8 &\equiv -(\langle v_n^8 \rangle - 16\langle v_n^6 \rangle \langle v_n^2 \rangle - 18\langle v_n^4 \rangle^2)/33 \\
 &\quad - (144\langle v_n^4 \rangle \langle v_n^2 \rangle^2 - 144\langle v_n^2 \rangle^4)/33. \quad (14)
 \end{aligned}$$

ATLAS has measured $p(v_n)$ for $n = 2, 3, 4$ [17]. The comparison of $v_2\{2k\}$ obtained with the cumulant method to $v_2^{calc}\{2k, EbyE\}$ is shown in Fig. 8. Good agreement between the two independent measurements is seen. The cumulant method gives v_2 values larger than those calculated from the $p(v_2)$ distribution only for $v_2\{2\}$ measured in the most peripheral collisions, due to contributions from short-range two-particle correlations in the former. The ratios of $v_2\{6\}$

and $v_2\{8\}$ to $v_2\{4\}$ are shown in Fig. 9. The left panel shows results from the cumulant method. The ratios are systematically below unity, most significantly at low N_{part} . This effect, which is of the order of 1–2 %, is significant for the ratio $v_2\{6\}/v_2\{4\}$ while it is within the present uncertainty of the cumulant measurements for $v_2\{8\}/v_2\{4\}$. Better precision is achieved for $v_2^{calc}\{2k, EbyE\}$ (right panel of Fig. 9). The difference between $v_2\{4\}$ and $v_2\{6\}$ or $v_2\{8\}$ is attributed to the non-Bessel–Gaussian character of the $p(v_2)$ distribution measured in peripheral collisions [17].

It is interesting to compare flow harmonic measurements obtained with different methods, which have different sensi-

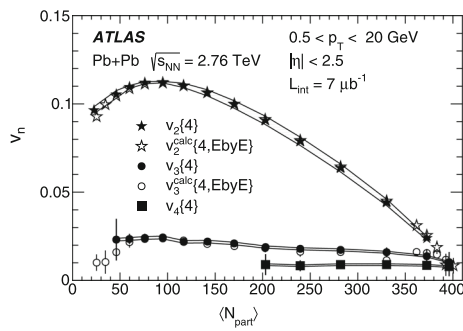


Fig. 11 The harmonics $v_2\{4\}$, $v_3\{4\}$ and $v_4\{4\}$ as a function of $\langle N_{\text{part}} \rangle$. Filled symbols show the results from the cumulant method while open symbols show $v_{2,3}^{\text{calc}}\{4, \text{EbyE}\}$ calculated from the $p(v_2)$ and $p(v_3)$ distributions. Statistical errors are shown as bars and systematic uncertainties as shaded bands

tivities to non-flow correlations and flow harmonic fluctuations. Since the higher-order flow harmonics, $v_n\{2k\}$ ($n > 2$), are measured with the cumulant method with up to four-particle cumulants (see Sect. 5), the $v_n\{2\}$ and $v_n\{4\}$ are only included in the comparison. Figure 10 shows the comparison of v_2 , v_3 and v_4 obtained using the cumulant method with the ATLAS results obtained with the event-plane method, $v_n\{\text{EP}\}$. For $v_n\{\text{EP}\}$, the measurements shown in Figs. 3 and 5 are taken and integrated over $0.5 < p_T < 20$ GeV. The mean values of the measured $p(v_n)$ distributions are also shown and marked as $v_n\{\text{EbyE}\}$. Over the accessible centrality range and for $n = 2, 3, 4$, a systematic pattern is seen with $v_n\{2\} > v_n\{\text{EP}\} \geq v_n\{\text{EbyE}\} > v_n\{4\}$. The $v_n\{2\}$ values are the largest (predominantly) due to large contributions from short-range two-particle correlations, which are suppressed in the event-plane v_n measurements. The v_n coefficients measured with the event-plane method are systematically larger than the mean values of the event-by-event measurement of flow harmonics. This difference is naturally attributed to the flow fluctuations, which contribute to $v_n\{\text{EP}\}$ but are suppressed in $v_n\{\text{EbyE}\}$. The flow coefficients measured with the four-particle cumulant method are the smallest, mainly due to the contribution from flow fluctuations, which is negative for $v_n\{4\}$ and positive for v_n measured with the event-plane method. In addition, some residual two-particle correlations unrelated to the azimuthal asymmetry in the initial geometry contribute to $v_n\{\text{EP}\}$, but are negligibly small in the case of $v_n\{4\}$.

The centrality dependence of $v_n\{4\}$ is shown in Fig. 11 for $n = 2, 3$ and 4. The elliptic flow $v_2\{4\}$ shows a strong centrality dependence, rising with N_{part} until reaching a maximum at $N_{\text{part}} \approx 100$, and then decreasing for more central collisions. This strong centrality dependence is not seen for the higher flow harmonics $v_3\{4\}$ and $v_4\{4\}$. In addition, the magnitude of the third- and fourth-order flow coefficients is much smaller than the magnitude of the elliptic flow; e.g. for $\langle N_{\text{part}} \rangle$ of about 300, $v_n \approx 0.05, 0.02$, and 0.01 for v_2 , v_3 and v_4 , respectively. For smaller N_{part} this difference is even

larger, with v_2 reaching more than 0.1 and v_3 and v_4 staying at the same level as at higher N_{part} . Figure 11 also shows $v_{2,3}^{\text{calc}}\{4, \text{EbyE}\}$ obtained from the measured $p(v_2)$ and $p(v_3)$ distributions. The measured $p(v_4)$ in Ref. [17] is truncated at large values of v_4 and therefore is not used here for the comparison. Good agreement between the two independent measurements is also seen for the third-order flow harmonics.

7.4 Fluctuations of flow harmonics

Measurements of elliptic flow dynamic fluctuations have attracted much interest, since flow fluctuations can be traced back to fluctuations of the initial collision zone. Experimentally, flow fluctuations are difficult to measure due to unavoidable contamination by non-flow effects. The reported elliptic flow fluctuation measurements from RHIC [31–33] are affected by non-flow correlations, despite the attempts made to estimate their contribution. Interestingly, RHIC results indicate that flow fluctuations are mostly determined by initial-state geometry fluctuations, which thus seem to be preserved throughout the system evolution.

The relative flow harmonic fluctuations, defined as $\sigma_{v_n}/\langle v_n \rangle$, can be calculated using the width and mean value of the $p(v_n)$ distributions and compared to the predictions for fluctuations of the initial geometry. The latter can be characterized by the eccentricities, ε_n , which can be estimated from the transverse positions (r, ϕ) of nucleons participating in the collision:

$$\varepsilon_n = \frac{\sqrt{\langle r^n \cos n\phi \rangle^2 + \langle r^n \sin n\phi \rangle^2}}{\langle r^n \rangle}. \quad (15)$$

Such a comparison of $\sigma_{v_n}/\langle v_n \rangle$, derived from the event-by-event measurement of v_n , to the Glauber model [37] and MC-KLN model [46], which combines the Glauber approach with saturated low- x gluon distribution functions, is discussed in Ref. [17]. In general, none of the considered models of the relative fluctuations of ε_n gives a consistent description of the relative flow fluctuations over the entire range of collision centralities.

In this analysis, the measure of relative flow fluctuations, $F(v_n)$, is defined as:

$$F(v_n) = \sqrt{\frac{v_n\{2\}^2 - v_n\{4\}^2}{v_n\{2\}^2 + v_n\{4\}^2}}. \quad (16)$$

The above formula provides a valid estimate of $\sigma_{v_n}/\langle v_n \rangle$ under the assumptions that non-flow correlations are absent in $v_n\{2\}$ and $v_n\{4\}$, and that flow fluctuations are small compared to $\langle v_n \rangle$ ($\sigma_{v_n} \ll \langle v_n \rangle$). The first assumption is obviously not fulfilled by $v_n\{2\}$, which is strongly contaminated by non-flow correlations. Therefore, $v_n\{\text{EP}\}$ is used instead of $v_n\{2\}$, following the approach proposed in Ref. [9]. The second assumption is not valid for fluctuations of third- and

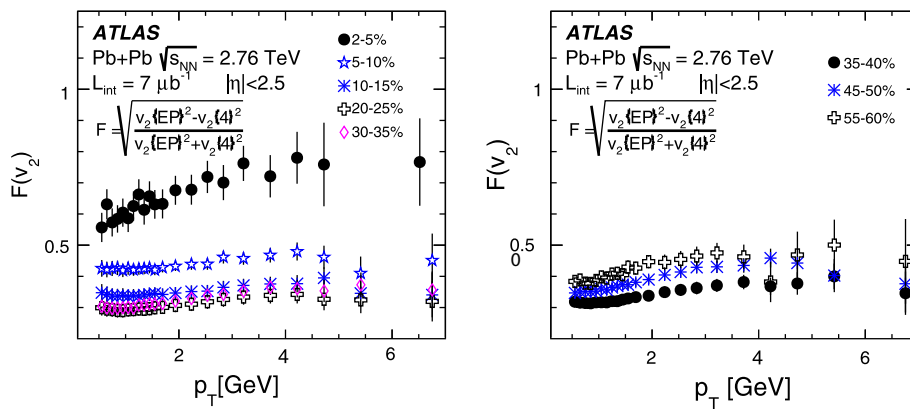


Fig. 12 The transverse momentum dependence of the relative elliptic flow fluctuations, as measured by F with $v_2\{2\}$ replaced by $v_2\{\text{EP}\}$, for central collisions (left panel) and peripheral collisions (right panel). The error bars denote statistical and systematic uncertainties added in quadrature

fourth-order flow harmonics, and also for elliptic flow harmonics measured in the most central Pb+Pb collisions. Nevertheless, it is interesting to study this alternative measure of flow fluctuations and to compare it to the same quantity predicted by initial-state models. For head-on nucleus–nucleus collisions, $\langle N_{\text{part}} \rangle \approx 400$, the prediction for eccentricity fluctuations $\sigma_{\varepsilon_n} / \langle \varepsilon_n \rangle$ reaches the limit of $\sqrt{4/\pi - 1} \approx 0.52$ for the fluctuations-only scenario when the ε_n distribution is described by a two-dimensional Gaussian function in the transverse plane [47]. In Ref. [17] it was shown that this limit is indeed reached by $\sigma_{v_n} / \langle v_n \rangle$ for v_2 measured in the most central Pb+Pb collisions and for v_3 and v_4 over the entire centrality range. For the fluctuations-only scenario, the estimate $F(v_n)$ should be close to one since then $\langle v_n\{4\} \rangle \approx 0$. Thus, it is interesting to compare this alternative measure of flow fluctuations to the same quantity derived from the initial eccentricity distributions, $F(\varepsilon_n)$. It can be seen by comparison with Eq. (16) that the quantity F depends not only on the second moment of the ε_n distribution (as does $\sigma_{\varepsilon_n} / \langle \varepsilon_n \rangle$), but also on the fourth moment and, therefore, can provide a more sensitive test of model assumptions.

Figure 12 shows the p_T dependence of the relative elliptic flow fluctuations calculated for different centrality intervals with Eq. (16), where $v_2\{2\}$ is replaced by $v_2\{\text{EP}\}$. For all centrality intervals, except 2–5 %, the relative elliptic flow fluctuations depend only weakly on p_T over the whole p_T range, indicating that they are predominantly associated with fluctuations of the initial geometry. A similar p_T dependence of the relative elliptic flow fluctuations was recently reported by the ALICE collaboration [9], although the ALICE results for the 0–5 % most central collisions show a much stronger p_T dependence than the present measurement for the centrality interval 2–5 %. This discrepancy may be due to different contributions of non-flow effects to $v_2\{\text{EP}\}$ measured in the two experiments.

The quantity $F(v_n)$ is further investigated as a function of the collision centrality using flow harmonics averaged

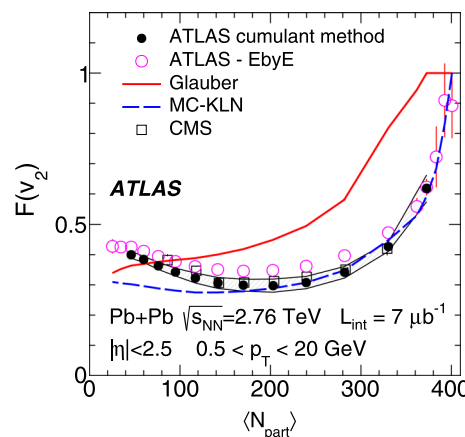


Fig. 13 The relative elliptic flow fluctuations, $F(v_2)$, as a function of $\langle N_{\text{part}} \rangle$, from this analysis (filled circles) with $v_2\{\text{EP}\}$ substituted for $v_2\{2\}$. Statistical errors are shown as bars and systematic uncertainties as shaded bands. $F(v_2)$ obtained from the measured v_2 distribution [17] is shown as open circles (marked in the legend as “EbyE”) with the error bars denoting statistical and systematic uncertainties added in quadrature. The same quantity calculated from the initial eccentricity distributions obtained from the Glauber [37] and MC-KLN [46] models is shown by curves. Open squares show the CMS measurement of $F(v_2)$ [23]

over p_T and η . The dependence of $F(v_2)$ on $\langle N_{\text{part}} \rangle$ is shown in Fig. 13. Two sets of measurements are shown: $F(v_2)$ calculated using $v_2\{4\}$ and $v_2\{2\}$ obtained with the cumulant method with $v_2\{\text{EP}\}$ replacing $v_2\{2\}$, and using $v_2^{\text{calc}}\{4, \text{EbyE}\}$ and $v_2^{\text{calc}}\{2, \text{EbyE}\}$ obtained from the measured $p(v_2)$ distribution [17]. The two measurements show similar centrality dependence, but the estimate based on the cumulant method is systematically smaller (by up to about 15 %) than that calculated from $p(v_2)$.

$F(v_2)$ can also be compared to $\sigma_{v_2} / \langle v_2 \rangle$ determined from the $p(v_2)$ distribution. It was shown in Ref. [17] that the two measures of elliptic flow fluctuations agree for the most peripheral collisions. For semi-central collisions, $\sigma_{v_2} / \langle v_2 \rangle$ is systematically larger than $F(v_2)$. A significant discrepancy

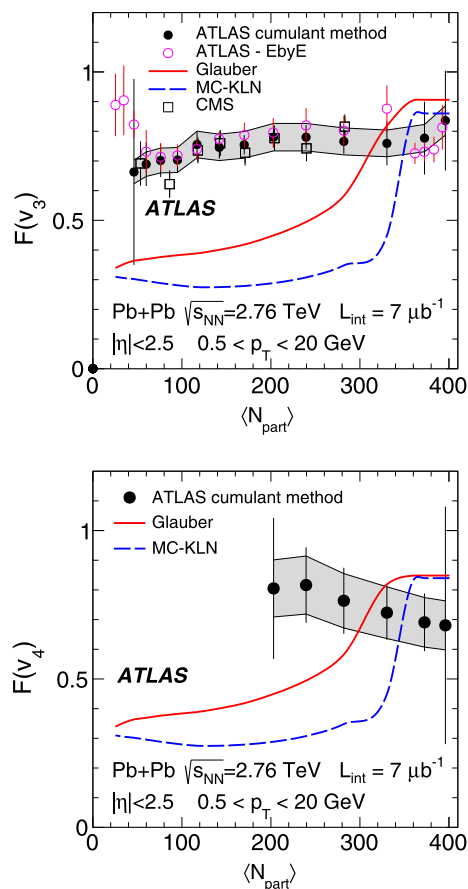


Fig. 14 The relative fluctuations, $F(v_n)$ for $n = 3$ (top) and $n = 4$ (bottom) as a function of $\langle N_{\text{part}} \rangle$, from the ATLAS cumulant method (filled circles) with $v_n\{\text{EP}\}$ substituted for $v_n\{2\}$. Statistical errors are shown as bars and systematic uncertainties as shaded bands. The same quantity calculated from the measured v_3 distributions [17] is shown as open circles in the top plot, with error bars denoting statistical and systematic uncertainties added in quadrature. The top plot also shows $F(v_3)$ as measured by CMS [23] (open squares). F values calculated from the eccentricity distributions obtained from the Glauber [37] and MC-KLN [46] models are shown by curves

was shown for the most central collisions, where $\sigma_{v_2}/\langle v_2 \rangle$ levels off at 0.52, while $F(v_2)$ rises continuously, reaching much higher values.

$F(v_2)$ shows a strong centrality dependence. Starting with the most peripheral collisions, it decreases with $\langle N_{\text{part}} \rangle$, reaching a minimum at $\langle N_{\text{part}} \rangle \approx 200$ and then rises steeply with centrality up to about 1.0 for the most central collisions. A comparison to $F(\epsilon_2)$ calculated from the eccentricity distributions predicted by the Glauber and MC-KLN models is shown in Fig. 13. One can see that the MC-KLN model describes the measurements for Pb+Pb collisions with $\langle N_{\text{part}} \rangle$ above 150 reasonably well, while the Glauber model significantly over-predicts the measured $F(v_2)$ across the entire centrality range. Figure 13 also shows that our results are consistent with the CMS estimate of $F(v_2)$ [23].

The study of $F(v_n)$ is also performed for higher-order flow harmonics, $n = 3, 4$. Figure 14 shows $F(v_3)$ (top plot) and $F(v_4)$ (bottom plot) obtained using the cumulant method with $v_3\{2\}$ and $v_4\{2\}$ replaced by $v_3\{\text{EP}\}$ and $v_4\{\text{EP}\}$, respectively. Large relative fluctuations of the third- and fourth-order harmonics, of the order of 0.7–0.8, are measured over the whole accessible centrality range, with a relatively weak centrality dependence. The results are consistent with the CMS measurement of $F(v_3)$ [23] as well as with F calculated using $v_3^{\text{calc}}\{4, \text{EbyE}\}$ and $v_3^{\text{calc}}\{2, \text{EbyE}\}$ [17]. $F(\epsilon_3)$ and $F(\epsilon_4)$ obtained from the eccentricity distributions predicted by the Glauber and MC-KLN models are also shown. One can see that none of the models gives a consistent description of $F(v_3)$ and $F(v_4)$.

8 Summary

A measurement of flow harmonics of charged particles in Pb+Pb collisions at $\sqrt{s_{\text{NN}}} = 2.76$ TeV from the ATLAS experiment at the LHC is presented using a dataset of approximately $7 \mu\text{b}^{-1}$ collected in 2010. The analysis is based on the cumulant expansion of multi-particle azimuthal correlations, which suppresses correlations not related to the initial-state geometry. Another advantage of the cumulant method is that it provides several different measurements of the same harmonic, v_n , allowing for estimation of the non-flow contributions and for consistency checks. The need for huge computing power in calculating multi-particle correlations is overcome by using the generating function formalism.

Flow coefficients v_n for $n = 2, 3, 4$ were obtained using two- and four-particle cumulants. In addition, for the elliptic flow ($n = 2$), the analysis is for the first time extended to the six- and eight-particle cumulants. The transverse momentum, pseudorapidity and centrality dependence of flow harmonics is presented. An attempt is also made to estimate the flow harmonic fluctuations using the measured $v_n\{4\}$ and v_n obtained with the event-plane method.

The transverse momentum dependence of $v_2\{2\}$ shows significant non-flow contributions. This contribution is reduced in $v_2\{\text{EP}\}$. The elliptic flow obtained with the four-particle cumulants provides a measure of v_2 with non-flow correlations strongly suppressed. Using six- and eight-particle cumulants gives results consistent, within the errors, with those obtained with four-particle cumulants, indicating that four-particle cumulants efficiently suppress non-flow correlations. Similar conclusions can be drawn from the study of the η -dependence of the p_T -integrated v_2 as well as from the centrality dependence of v_2 averaged over p_T and η . As for v_2 , the higher-order flow harmonics determined using four-particle cumulants are significantly reduced compared to the measurement involving two-particle cumulants.

The flow harmonics, $v_n\{4\}$, determined from the four-particle cumulants increase sharply with p_T reaching a maximum at 2–3 GeV. At higher transverse momenta, $v_2\{4\}$ decreases and beyond p_T of about 7 GeV, it plateaus at the level of about 0.04 up to the highest accessible transverse momenta. The higher-order harmonics also decrease above 3 GeV and reach a value of about 0.03 when integrated over p_T from 4 GeV to 20 GeV. The four-particle harmonics, $v_n\{4\}$, are found to depend weakly on the pseudorapidity over the range $|\eta| < 2.5$.

The centrality dependence of the p_T - and η -integrated $v_n\{4\}$ reveals a clear distinction between v_2 and the higher-order harmonics: v_2 strongly depends on the collision centrality, reflecting its sensitivity to the varying shape of the initial collision geometry, while v_3 and v_4 show only a weak centrality dependence, predominantly attributed to geometry fluctuations. Over the studied centrality range, except for the most central collisions, the measured v_3 and v_4 are much smaller than v_2 . For the most central collisions, a similar magnitude is measured for v_2 , v_3 and v_4 because all are dominated by geometry fluctuations. The measured $v_2\{2k\}$ for $k = 2, 3, 4$ and $v_3\{4\}$ are found to agree with the same coefficients calculated from the moments of the measured $p(v_2)$ and $p(v_3)$ distributions.

The relative flow harmonic fluctuations, $F(v_n)$, defined in Eq. (16), are estimated using $v_n\{\text{EP}\}$ and $v_n\{4\}$. For the elliptic flow harmonic, a strong centrality dependence is observed, following a trend similar to that exhibited by F as estimated from the $p(v_2)$ distribution. In contrast, $F(v_3)$ and $F(v_4)$ show a weak centrality dependence. The large magnitudes of F obtained for third- and fourth-order harmonics, and also for the elliptic flow harmonic measured in the most central collisions, indicate the dominant role of initial-state fluctuations. The comparison to the same quantity derived from the initial-state eccentricity distributions, modelled by the Glauber and MC-KLN models, shows that none of these models can describe the flow harmonic fluctuations well, particularly for higher-order flow harmonics. Therefore, the measurements presented in this paper provide valuable constraints on models of initial spatial anisotropy and subsequent hydrodynamic evolution of systems produced in ion–ion collisions with nucleon–nucleon centre-of-mass energies at the TeV energy scale.

Acknowledgments We thank CERN for the very successful operation of the LHC, as well as the support staff from our institutions without whom ATLAS could not be operated efficiently. We acknowledge the support of ANPCyT, Argentina; YerPhI, Armenia; ARC, Australia; BMWFW and FWF, Austria; ANAS, Azerbaijan; SSTC, Belarus; CNPq and FAPESP, Brazil; NSERC, NRC and CFI, Canada; CERN; CONICYT, Chile; CAS, MOST and NSFC, China; COLCIENCIAS, Colombia; MSMT CR, MPO CR and VSC CR, Czech Republic; DNRF, DNSRC and Lundbeck Foundation, Denmark; EPLANET, ERC and NSRF, European Union; IN2P3-CNRS, CEA-DSM/IRFU, France; GNSF, Georgia; BMBF, DFG, HGF, MPG and AvH Foun-

ation, Germany; GSRT and NSRF, Greece; ISF, MINERVA, GIF, I-CORE and Benozio Center, Israel; INFN, Italy; MEXT and JSPS, Japan; CNRST, Morocco; FOM and NWO, Netherlands; BRF and RCN, Norway; MNiSW and NCN, Poland; GRICES and FCT, Portugal; MNE/IFA, Romania; MES of Russia and ROSATOM, Russian Federation; JINR; MSTD, Serbia; MSSR, Slovakia; ARRS and MIZŠ, Slovenia; DST/NRF, South Africa; MINECO, Spain; SRC and Wallenberg Foundation, Sweden; SER, SNSF and Cantons of Bern and Geneva, Switzerland; NSC, Taiwan; TAEK, Turkey; STFC, the Royal Society and Leverhulme Trust, United Kingdom; DOE and NSF, United States of America. The crucial computing support from all WLCG partners is acknowledged gratefully, in particular from CERN and the ATLAS Tier-1 facilities at TRIUMF (Canada), NDGF (Denmark, Norway, Sweden), CC-IN2P3 (France), KIT/GridKA (Germany), INFN-CNAF (Italy), NL-T1 (Netherlands), PIC (Spain), ASGC (Taiwan), RAL (UK) and BNL (USA) and in the Tier-2 facilities worldwide.

Open Access This article is distributed under the terms of the Creative Commons Attribution License which permits any use, distribution, and reproduction in any medium, provided the original author(s) and the source are credited.

Funded by SCOAP³ / License Version CC BY 4.0.

References

1. S. A. Voloshin, A. M. Poskanzer, R. Snellings, Elementary particles, nuclei and atoms (Springer-Verlag) **23**, 293 (2010). [arXiv:0809.2949](#) [nucl-ex].
2. P. Sorensen, Quark-gluon plasma (World Scientific) **4**, 323 (2010). [arXiv:0905.0174](#) [nucl-ex]
3. I. Arsene et al., BRAHMS Collaboration, Nucl. Phys. A **757**, 1–27 (2005). [arXiv:nucl-ex/0410020](#)
4. B.B. Back et al., PHOBOS Collaboration, Nucl. Phys. A **757**, 28–101 (2005). [arXiv:nucl-ex/0410022](#)
5. K. Adox et al., PHENIX Collaboration, Nucl. Phys. A **757**, 184–283 (2005). [arXiv:nucl-ex/0410003](#)
6. J. Adams et al., STAR Collaboration, Nucl. Phys. A **757**, 102–183 (2005). [arXiv:nucl-ex/0501009](#)
7. ALICE Collaboration, Phys. Rev. Lett. **105**, 252302 (2010). [arXiv:1011.3914](#) [nucl-ex]
8. ALICE Collaboration, Phys. Rev. Lett. **107**, 032301 (2011). [arXiv:1105.3865](#) [nucl-ex]
9. ALICE Collaboration, Phys. Lett. B **719**, 18 (2013). [arXiv:1205.5761](#) [nucl-ex]
10. ALICE Collaboration, Phys. Lett. B **708**, 249 (2012). [arXiv:1109.2501](#) [nucl-ex]
11. ALICE Collaboration, Phys. Rev. Lett. **111**, 232302 (2013). [arXiv:1306.4145](#) [nucl-ex]
12. ALICE Collaboration, Phys. Rev. Lett. **111**, 162301 (2013). [arXiv:1303.5880](#) [nucl-ex]
13. ALICE Collaboration, Phys. Rev. Lett. **111**, 102301 (2013). [arXiv:1305.2707](#) [nucl-ex]
14. ALICE Collaboration, [arXiv:1406.2474](#) [nucl-ex]
15. ATLAS Collaboration, Phys. Lett. B **707**, 330 (2012). [arXiv:1108.6018](#) [hep-ex]
16. ATLAS Collaboration, Phys. Rev. C **86**, 014907 (2012). [arXiv:1203.3087](#) [hep-ex]
17. ATLAS Collaboration, JHEP **11**, 183 (2013). [arXiv:1305.2942](#) [hep-ex]
18. ATLAS Collaboration, Phys. Rev. C **90**, 024905 (2014). [arXiv:1403.0489](#) [hep-ex]
19. ATLAS Collaboration, Eur. Phys. J. C **74**, 2982 (2014). [arXiv:1405.3936](#) [hep-ex]

20. CMS Collaboration, Phys. Rev. C **87**, 014902 (2013). [arXiv:1204.1409](#) [nucl-ex]
21. CMS Collaboration, Phys. Rev. Lett. **109**, 022301 (2012). [arXiv:1204.1850](#) [nucl-ex]
22. CMS Collaboration, Phys. Rev. Lett. **110**, 042301 (2013). [arXiv:1208.2470](#) [nucl-ex]
23. CMS Collaboration, Phys. Rev. C **89**, 044906 (2014). [arXiv:1310.8651](#) [nucl-ex]
24. CMS Collaboration, JHEP **02**, 088 (2014). [arXiv:1312.1845](#) [nucl-ex]
25. U. W. Heinz, R. Snellings, Ann. Rev. Nucl. Part. Sci. **63**, 123 (2013). [arXiv:1301.2826](#) [nucl-th]
26. A. M. Poskanzer, S. A. Voloshin, Phys. Rev. C **58**, 1671–1678 (1998). [arXiv:nucl-ex/9805001](#)
27. N. Borghini, P.M. Dinh, J.Y. Ollitrault, Phys. Rev. C **63**, 054906 (2001). [arXiv:nucl-th/0007063](#)
28. N. Borghini, P.M. Dinh, J.Y. Ollitrault, Phys. Rev. C **64**, 054901 (2001). [arXiv:nucl-th/0105040](#)
29. N. Borghini, P. M. Dinh, J. Y. Ollitrault, [arXiv:nucl-ex/0110016](#)
30. A. Bilandzic, R. Snellings, S.A. Voloshin, Phys. Rev. C **83**, 044913 (2011). [arXiv:1010.0233](#) [nucl-ex]
31. B. Alver et al., PHOBOS Collaboration. Phys. Rev. Lett. **104**, 142301 (2010). [arXiv:nucl-ex/0702036](#)
32. B. Alver et al., PHOBOS Collaboration. Phys. Rev. C **81**, 034915 (2010). [arXiv:1002.0534](#) [nucl-ex]
33. P. Sorensen, J. Phys. G **35**, 104102 (2008). [arXiv:0808.0356](#) [nucl-th]
34. C. Alt et al., NA49 Collaboration. Phys. Rev. C **68**, 034903 (2003). [arXiv:nucl-ex/0303001](#)
35. C. Adler et al., STAR Collaboration. Phys. Rev. C **66**, 034904 (2002). [arXiv:nucl-ex/0206001](#)
36. ATLAS Collaboration, JINST **3**, S08003 (2008)
37. M. L. Miller, K. Reygers, S. J. Sanders, P. Steinberg, Ann. Rev. Nucl. Part. Sci. **57**, 205 (2007). [arXiv:nucl-ex/0701025](#)
38. ATLAS Collaboration, Phys. Lett. B **710**, 363 (2012). [arXiv:1108.6027](#) [hep-ex]
39. M. Gyulassy, X.-N. Wang, Comput. Phys. Commun. **83**, 307 (1994). [arXiv:nucl-th/9502021](#)
40. ATLAS Collaboration, Eur. Phys. J. C **70**, 823 (2010). [arXiv:1005.4568](#) [physics.ins-det]
41. S. Agostinelli et al., Nucl. Instr. Method A **506**, 250 (2003)
42. ATLAS Collaboration, ATLAS-CONF-2012-120 (2012). <http://cds.cern.ch/record/1473095>
43. C. Shen, U. Heinz, P. Huovinen, H. Song, Phys. Rev. C **84**, 044903 (2011). [arXiv:1105.3226](#) [nucl-th]
44. C. Gale, S. Jeon, B. Schenke, P. Tribedy, R. Venugopalan, Phys. Rev. Lett. **110**, 012302 (2013). [arXiv:1209.6330](#) [nucl-th]
45. ATLAS Collaboration, Phys. Rev. Lett. **111** (2013). [arXiv:1306.6469](#) [hep-ex]
46. A. Adil, H.J. Drescher, A. Dumitru, A. Hayashigaki, Y. Nara, Phys. Rev. C **74**, 044905 (2006). [arXiv:nucl-th/0605012](#)
47. W. Broniowski, M. Rybczynski, P. Bozek, Phys. Rev. C **76** (2007). [arXiv:0706.4266](#) [nucl-th]

ATLAS Collaboration

G. Aad⁸⁴, B. Abbott¹¹², J. Abdallah¹⁵², S. Abdel Khalek¹¹⁶, O. Abidinov¹¹, R. Aben¹⁰⁶, B. Abi¹¹³, M. Abolins⁸⁹, O. S. AbouZeid¹⁵⁹, H. Abramowicz¹⁵⁴, H. Abreu¹⁵³, R. Abreu³⁰, Y. Abulaiti^{147a,147b}, B. S. Acharya^{165a,165b,a}, L. Adamczyk^{38a}, D. L. Adams²⁵, J. Adelman¹⁷⁷, S. Adomeit⁹⁹, T. Adye¹³⁰, T. Agatonovic-Jovin^{13a}, J. A. Aguilar-Saavedra^{125a,125f}, M. Agustoni¹⁷, S. P. Ahlen²², F. Ahmadov^{64,b}, G. Aielli^{134a,134b}, H. Akerstedt^{147a,147b}, T. P. A. Åkesson⁸⁰, G. Akimoto¹⁵⁶, A. V. Akimov⁹⁵, G. L. Alberghi^{20a,20b}, J. Albert¹⁷⁰, S. Albrand⁵⁵, M. J. Alconada Verzini⁷⁰, M. Aleksa³⁰, I. N. Aleksandrov⁶⁴, C. Alexa^{26a}, G. Alexander¹⁵⁴, G. Alexandre⁴⁹, T. Alexopoulos¹⁰, M. Alhroob^{165a,165c}, G. Alimonti^{90a}, L. Alio⁸⁴, J. Alison³¹, B. M. M. Allbrooke¹⁸, L. J. Allison⁷¹, P. P. Allport⁷³, J. Almond⁸³, A. Aloisio^{103a,103b}, A. Alonso³⁶, F. Alonso⁷⁰, C. Alpigiani⁷⁵, A. Altheimer³⁵, B. Alvarez Gonzalez⁸⁹, M. G. Alvigi^{103a,103b}, K. Amako⁶⁵, Y. Amaral Coutinho^{24a}, C. Amelung²³, D. Amidei⁸⁸, S. P. Amor Dos Santos^{125a,125c}, A. Amorim^{125a,125b}, S. Amoroso⁴⁸, N. Amram¹⁵⁴, G. Amundsen²³, C. Anastopoulos¹⁴⁰, L. S. Ancu⁴⁹, N. Andari³⁰, T. Andeen³⁵, C. F. Anders^{58b}, G. Anders³⁰, K. J. Anderson³¹, A. Andreazza^{90a,90b}, V. Andrei^{58a}, X. S. Anduaga⁷⁰, S. Angelidakis⁹, I. Angelozzi¹⁰⁶, P. Anger⁴⁴, A. Angerami³⁵, F. Anghinolfi³⁰, A. V. Anisenkov¹⁰⁸, N. Anjos^{125a}, A. Annovi⁴⁷, A. Antonaki⁹, M. Antonelli⁴⁷, A. Antonov⁹⁷, J. Antos^{145b}, F. Anulli^{133a}, M. Aoki⁶⁵, L. Aperio Bella¹⁸, R. Apolle^{119,c}, G. Arabidze⁸⁹, I. Aracena¹⁴⁴, Y. Arai⁶⁵, J. P. Araque^{125a}, A. T. H. Arce⁴⁵, J.-F. Arguin⁹⁴, S. Argyropoulos⁴², M. Arik^{19a}, A. J. Armbruster³⁰, O. Arnaez³⁰, V. Arnal⁸¹, H. Arnold⁴⁸, M. Arratia²⁸, O. Arslan²¹, A. Artamonov⁹⁶, G. Artoni²³, S. Asai¹⁵⁶, N. Asbah⁴², A. Ashkenazi¹⁵⁴, B. Åsman^{147a,147b}, L. Asquith⁶, K. Assamagan²⁵, R. Astalos^{145a}, M. Atkinson¹⁶⁶, N. B. Atlay¹⁴², B. Auerbach⁶, K. Augsten¹²⁷, M. Auresseau^{146b}, G. Avolio³⁰, G. Azuelos^{94,d}, Y. Azuma¹⁵⁶, M. A. Baak³⁰, A. E. Baas^{58a}, C. Bacci^{135a,135b}, H. Bachacou¹³⁷, K. Bachas¹⁵⁵, M. Backes³⁰, M. Backhaus³⁰, J. Backus Mayes¹⁴⁴, E. Badescu^{26a}, P. Bagiacchi^{133a,133b}, P. Bagnaia^{133a,133b}, Y. Bai^{33a}, T. Bain³⁵, J. T. Baines¹³⁰, O. K. Baker¹⁷⁷, P. Balek¹²⁸, F. Balli¹³⁷, E. Banas³⁹, Sw. Banerjee¹⁷⁴, A. A. E. Bannoura¹⁷⁶, V. Bansal¹⁷⁰, H. S. Bansil¹⁸, L. Barak¹⁷³, S. P. Baranov⁹⁵, E. L. Barberio⁸⁷, D. Barberis^{50a,50b}, M. Barbero⁸⁴, T. Barillari¹⁰⁰, M. Barisonzi¹⁷⁶, T. Barklow¹⁴⁴, N. Barlow²⁸, B. M. Barnett¹³⁰, R. M. Barnett¹⁵, Z. Barnovska⁵, A. Baroncelli^{135a}, G. Barone⁴⁹, A. J. Barr¹¹⁹, F. Barreiro⁸¹, J. Barreiro Guimarães da Costa⁵⁷, R. Bartoldus¹⁴⁴, A. E. Barton⁷¹, P. Bartos^{145a}, V. Bartsch¹⁵⁰, A. Bassalat¹¹⁶, A. Basye¹⁶⁶, R. L. Bates⁵³, J. R. Batley²⁸, M. Battaglia¹³⁸, M. Battistin³⁰, F. Bauer¹³⁷, H. S. Bawa^{144,e}, M. D. Beattie⁷¹, T. Beau⁷⁹, P. H. Beauchemin¹⁶², R. Beccherle^{123a,123b}, P. Bechtel²¹, H. P. Beck¹⁷, K. Becker¹⁷⁶, S. Becker⁹⁹, M. Beckingham¹⁷¹, C. Becot¹¹⁶, A. J. Beddall^{19c}, A. Beddall^{19c}, S. Bedikian¹⁷⁷, V. A. Bednyakov⁶⁴, C. P. Bee¹⁴⁹,

L. J. Beemster¹⁰⁶, T. A. Beermann¹⁷⁶, M. Begel²⁵, K. Behr¹¹⁹, C. Belanger-Champagne⁸⁶, P. J. Bell⁴⁹, W. H. Bell⁴⁹, G. Bella¹⁵⁴, L. Bellagamba^{20a}, A. Bellerive²⁹, M. Bellomo⁸⁵, K. Belotskiy⁹⁷, O. Beltramello³⁰, O. Benary¹⁵⁴, D. Benchechrout^{136a}, K. Bendtz^{147a,147b}, N. Benekos¹⁶⁶, Y. Benhammou¹⁵⁴, E. Benhar Nocchioli⁴⁹, J. A. Benitez Garcia^{160b}, D. P. Benjamin⁴⁵, J. R. Bensinger²³, K. Benslama¹³¹, S. Bentvelsen¹⁰⁶, D. Berge¹⁰⁶, E. Bergeaas Kuutmann¹⁶, N. Berger⁵, F. Berghaus¹⁷⁰, J. Beringer¹⁵, C. Bernard²², P. Bernal⁷⁷, C. Bernius⁷⁸, F. U. Bernlochner¹⁷⁰, T. Berry⁷⁶, P. Berta¹²⁸, C. Bertella⁸⁴, G. Bertoli^{147a,147b}, F. Bertolucci^{123a,123b}, C. Bertsche¹¹², D. Bertsche¹¹², M. I. Besana^{90a}, G. J. Besjes¹⁰⁵, O. Bessidskaia^{147a,147b}, M. Bessner⁴², N. Besson¹³⁷, C. Betancourt⁴⁸, S. Bethke¹⁰⁰, W. Bhimji⁴⁶, R. M. Bianchi¹²⁴, L. Bianchini²³, M. Bianco³⁰, O. Biebel⁹⁹, S. P. Bieniek⁷⁷, K. Bierwagen⁵⁴, J. Biesiada¹⁵, M. Biglietti^{135a}, J. Bilbao De Mendizabal⁴⁹, H. Bilokon⁴⁷, M. Bindi⁵⁴, S. Binet¹¹⁶, A. Bingul^{19c}, C. Bini^{133a,133b}, C. W. Black¹⁵¹, J. E. Black¹⁴⁴, K. M. Black²², D. Blackburn¹³⁹, R. E. Blair⁶, J.-B. Blanchard¹³⁷, T. Blazek^{145a}, I. Bloch⁴², C. Blocker²³, W. Blum^{82,*}, U. Blumenschein⁵⁴, G. J. Bobbink¹⁰⁶, V. S. Bobrovnikov¹⁰⁸, S. S. Bocchetta⁸⁰, A. Bocci⁴⁵, C. Bock⁹⁹, C. R. Boddy¹¹⁹, M. Boehler⁴⁸, T. T. Boek¹⁷⁶, J. A. Bogaerts³⁰, A. G. Bogdanchikov¹⁰⁸, A. Bogouch^{91,*}, C. Bohm^{147a}, J. Bohm¹²⁶, V. Boisvert⁷⁶, T. Bold^{38a}, V. Boldea^{26a}, A. S. Boldyrev⁹⁸, M. Bomben⁷⁹, M. Bona⁷⁵, M. Boonekamp¹³⁷, A. Borisov¹²⁹, G. Borissov⁷¹, M. Borri⁸³, S. Borroni⁴², J. Bortfeldt⁹⁹, V. Bortolotto^{135a,135b}, K. Bos¹⁰⁶, D. Boscherini^{20a}, M. Bosman¹², H. Boterenbrood¹⁰⁶, J. Boudreau¹²⁴, J. Bouffard², E. V. Bouhova-Thacker⁷¹, D. Boumediene³⁴, C. Bourdarios¹¹⁶, N. Bousson¹¹³, S. Boutouil^{136d}, A. Boveia³¹, J. Boyd³⁰, I. R. Boyko⁶⁴, J. Bracik¹⁸, A. Brandt⁸, G. Brandt¹⁵, O. Brandt^{58a}, U. Bratzler¹⁵⁷, B. Brau⁸⁵, J. E. Brau¹¹⁵, H. M. Braun^{176,*}, S. F. Brazzale^{165a,165c}, B. Brelief¹⁵⁹, K. Brendlinger¹²¹, A. J. Brennan⁸⁷, R. Brenner¹⁶⁷, S. Bressler¹⁷³, K. Bristow^{146c}, T. M. Bristow⁴⁶, D. Britton⁵³, F. M. Brochu²⁸, I. Brock²¹, R. Brock⁸⁹, C. Bromberg⁸⁹, J. Bronner¹⁰⁰, G. Brooijmans³⁵, T. Brooks⁷⁶, W. K. Brooks^{32b}, J. Brosamer¹⁵, E. Brost¹¹⁵, J. Brown⁵⁵, P. A. Bruckman de Renstrom³⁹, D. Bruncko^{145b}, R. Bruneliere⁴⁸, S. Brunet⁶⁰, A. Bruni^{20a}, G. Bruni^{20a}, M. Bruschi^{20a}, L. Bryngemark⁸⁰, T. Buanes¹⁴, Q. Buat¹⁴³, F. Bucci⁴⁹, P. Buchholz¹⁴², R. M. Buckingham¹¹⁹, A. G. Buckley⁵³, S. I. Buda^{26a}, I. A. Budagov⁶⁴, F. Buehrer⁴⁸, L. Bugge¹¹⁸, M. K. Bugge¹¹⁸, O. Bulekov⁹⁷, A. C. Bundock⁷³, H. Burckhart³⁰, S. Burdin⁷³, B. Burghgrave¹⁰⁷, S. Burke¹³⁰, I. Burmeister⁴³, E. Busato³⁴, D. Buischer⁴⁸, V. Buischer⁸², P. Bussey⁵³, C. P. Buszello¹⁶⁷, B. Butler⁵⁷, J. M. Butler²², A. I. Butt³, C. M. Buttar⁵³, J. M. Butterworth⁷⁷, P. Butti¹⁰⁶, W. Buttinger²⁸, A. Buzatu⁵³, M. Byszewski¹⁰, S. Cabrera Urbán¹⁶⁸, D. Caforio^{20a,20b}, O. Cakir^{4a}, P. Calafiura¹⁵, A. Calandri¹³⁷, G. Calderini⁷⁹, P. Calfayan⁹⁹, R. Calkins¹⁰⁷, L. P. Caloba^{24a}, D. Calvet³⁴, S. Calvet³⁴, R. Camacho Toro⁴⁹, S. Camarda⁴², D. Cameron¹¹⁸, L. M. Caminada¹⁵, R. Caminal Armadans¹², S. Campana³⁰, M. Campanelli⁷⁷, A. Campoverde¹⁴⁹, V. Canale^{103a,103b}, A. Canepa^{160a}, M. Cano Bret⁷⁵, J. Cantero⁸¹, R. Cantrill^{125a}, T. Cao⁴⁰, M. D. M. Capeans Garrido³⁰, I. Caprini^{26a}, M. Caprini^{26a}, M. Capua^{37a,37b}, R. Caputo⁸², R. Cardarelli^{134a}, T. Carli³⁰, G. Carlino^{103a}, L. Carminati^{90a,90b}, S. Caron¹⁰⁵, E. Carquin^{32a}, G. D. Carrillo-Montoya^{146c}, J. R. Carter²⁸, J. Carvalho^{125a,125c}, D. Casadei⁷⁷, M. P. Casado¹², M. Casolino¹², E. Castaneda-Miranda^{146b}, A. Castelli¹⁰⁶, V. Castillo Gimenez¹⁶⁸, N. F. Castro^{125a}, P. Catastini⁵⁷, A. Catinaccio³⁰, J. R. Catmore¹¹⁸, A. Cattai³⁰, G. Cattani^{134a,134b}, S. Caughron⁸⁹, V. Cavaliere¹⁶⁶, D. Cavalli^{90a}, M. Cavalli-Sforza¹², V. Cavasinni^{123a,123b}, F. Ceradini^{135a,135b}, B. C. Cerio⁴⁵, K. Cerny¹²⁸, A. S. Cerqueira^{24b}, A. Cerri¹⁵⁰, L. Cerrito⁷⁵, F. Cerutti¹⁵, M. Cerv³⁰, A. Cervelli¹⁷, S. A. Cetin^{19b}, A. Chafaq^{136a}, D. Chakraborty¹⁰⁷, I. Chalupkova¹²⁸, P. Chang¹⁶⁶, B. Chapleau⁸⁶, J. D. Chapman²⁸, D. Charfeddine¹¹⁶, D. G. Charlton¹⁸, C. C. Chau¹⁵⁹, C. A. Chavez Barajas¹⁵⁰, S. Cheatham⁸⁶, A. Chegwidan⁸⁹, S. Chekanov⁶, S. V. Chekulaev^{160a}, G. A. Chelkov^{64,f}, M. A. Chelstowska⁸⁸, C. Chen⁶³, H. Chen²⁵, K. Chen¹⁴⁹, L. Chen^{33d,g}, S. Chen^{33c}, X. Chen^{146c}, Y. Chen⁶⁶, Y. Chen³⁵, H. C. Cheng⁸⁸, Y. Cheng³¹, A. Cheplakov⁶⁴, R. Cherkaoui El Moursli^{136e}, V. Chernyatin^{25,*}, E. Cheu⁷, L. Chevalier¹³⁷, V. Chiarella⁴⁷, G. Chiefari^{103a,103b}, J. T. Childers⁶, A. Chilingarov⁷¹, G. Chiodini^{72a}, A. S. Chisholm¹⁸, R. T. Chislett⁷⁷, A. Chitan^{26a}, M. V. Chizhov⁶⁴, S. Chouridou⁹, B. K. B. Chow⁹⁹, D. Chromek-Burckhart³⁰, M. L. Chu¹⁵², J. Chudoba¹²⁶, J. J. Chwastowski³⁹, L. Chytka¹¹⁴, G. Ciapetti^{133a,133b}, A. K. Ciftci^{4a}, R. Ciftci^{4a}, D. Cinca⁵³, V. Cindro⁷⁴, A. Ciocio¹⁵, P. Cirkovic^{13b}, Z. H. Citron¹⁷³, M. Citterio^{90a}, M. Ciubancan^{26a}, A. Clark⁴⁹, P. J. Clark⁴⁶, R. N. Clarke¹⁵, W. Cleland¹²⁴, J. C. Clemens⁸⁴, C. Clement^{147a,147b}, Y. Coadou⁸⁴, M. Cobal^{165a,165c}, A. Coccaro¹³⁹, J. Cochran⁶³, L. Coffey²³, J. G. Cogan¹⁴⁴, J. Coggeshall¹⁶⁶, B. Cole³⁵, S. Cole¹⁰⁷, A. P. Colijn¹⁰⁶, J. Collot⁵⁵, T. Colombo^{58c}, G. Colon⁸⁵, G. Compostella¹⁰⁰, P. Conde Muino^{125a,125b}, E. Coniavitis⁴⁸, M. C. Conidi¹², S. H. Connell^{146b}, I. A. Connelly⁷⁶, S. M. Consonni^{90a,90b}, V. Consorti⁴⁸, S. Constantinescu^{26a}, C. Conta^{120a,120b}, G. Conti⁵⁷, F. Conventi^{103a,h}, M. Cooke¹⁵, B. D. Cooper⁷⁷, A. M. Cooper-Sarkar¹¹⁹, N. J. Cooper-Smith⁷⁶, K. Copic¹⁵, T. Cornelissen¹⁷⁶, M. Corradi^{20a}, F. Corriveau^{86,i}, A. Corso-Radu¹⁶⁴, A. Cortes-Gonzalez¹², G. Cortiana¹⁰⁰, G. Costa^{90a}, M. J. Costa¹⁶⁸, D. Costanzo¹⁴⁰, D. Côté⁸, G. Cottin²⁸, G. Cowan⁷⁶, B. E. Cox⁸³, K. Cranmer¹⁰⁹, G. Cree²⁹, S. Crépe-Renaudin⁵⁵, F. Crescioli⁷⁹, W. A. Cribbs^{147a,147b}, M. Crispin Ortuzar¹¹⁹, M. Cristinziani²¹, V. Croft¹⁰⁵, G. Crosetti^{37a,37b}, C.-M. Cuciuc^{26a}, T. Cuhadar Donszelmann¹⁴⁰, J. Cummings¹⁷⁷, M. Curatolo⁴⁷, C. Cuthbert¹⁵¹, H. Czirz¹⁴², P. Czodrowski³, Z. Czynula¹⁷⁷, S. D'Auria⁵³, M. D'Onofrio⁷³, M. J. Da Cunha Sargedas De Sousa^{125a,125b}, C. Da Via⁸³, W. Dabrowski^{38a}, A. Dafinca¹¹⁹, T. Dai⁸⁸,

O. Dale¹⁴, F. Dallaire⁹⁴, C. Dallapiccola⁸⁵, M. Dam³⁶, A. C. Daniells¹⁸, M. Dano Hoffmann¹³⁷, V. Dao⁴⁸, G. Darbo^{50a}, S. Darmora⁸, J. A. Dassoulas⁴², A. Dattagupta⁶⁰, W. Davey²¹, C. David¹⁷⁰, T. Davidek¹²⁸, E. Davies^{119,c}, M. Davies¹⁵⁴, O. Davignon⁷⁹, A. R. Davison⁷⁷, P. Davison⁷⁷, Y. Davygora^{58a}, E. Dawe¹⁴³, I. Dawson¹⁴⁰, R. K. Daya-Ishmukhametova⁸⁵, K. De⁸, R. de Asmundis^{103a}, S. De Castro^{20a,20b}, S. De Cecco⁷⁹, N. De Groot¹⁰⁵, P. de Jong¹⁰⁶, H. De la Torre⁸¹, F. De Lorenzi⁶³, L. De Nooij¹⁰⁶, D. De Pedis^{133a}, A. De Salvo^{133a}, U. De Sanctis^{165a,165b}, A. De Santo¹⁵⁰, J. B. De Vivie De Regie¹¹⁶, W. J. Dearnaley⁷¹, R. Debebe²⁵, C. Debenedetti¹³⁸, B. Dechenaux⁵⁵, D. V. Dedovich⁶⁴, I. Deigaard¹⁰⁶, J. Del Peso⁸¹, T. Del Prete^{123a,123b}, F. Deliot¹³⁷, C. M. Delitzsch⁴⁹, M. Deliyergiyev⁷⁴, A. Dell'Acqua³⁰, L. Dell'Asta²², M. Dell'Orso^{123a,123b}, M. Della Pietra^{103a,h}, D. della Volpe⁴⁹, M. Delmastro⁵, P. A. Delsart⁵⁵, C. Deluca¹⁰⁶, S. Demers¹⁷⁷, M. Demichev⁶⁴, A. Demilly⁷⁹, S. P. Denisov¹²⁹, D. Derendarz³⁹, J. E. Derkaoui^{136d}, F. Derue⁷⁹, P. Dervan⁷³, K. Desch²¹, C. Deterre⁴², P. O. Deviveiros¹⁰⁶, A. Dewhurst¹³⁰, S. Dhaliwal¹⁰⁶, A. Di Ciaccio^{134a,134b}, L. Di Ciaccio⁵, A. Di Domenico^{133a,133b}, C. Di Donato^{103a,103b}, A. Di Girolamo³⁰, B. Di Girolamo³⁰, A. Di Mattia¹⁵³, B. Di Micco^{135a,135b}, R. Di Nardo⁴⁷, A. Di Simone⁴⁸, R. Di Sipio^{20a,20b}, D. Di Valentino²⁹, F. A. Dias⁴⁶, M. A. Diaz^{32a}, E. B. Diehl⁸⁸, J. Dietrich⁴², T. A. Dietzsch^{58a}, S. Diglio⁸⁴, A. Dimitrievska^{13a}, J. Dingfelder²¹, C. Dionisi^{133a,133b}, P. Dita^{26a}, S. Dita^{26a}, F. Dittus³⁰, F. Djama⁸⁴, T. Djobava^{51b}, M. A. B. do Vale^{24c}, A. Do Valle Wemans^{125a,125g}, T. K. O. Doan⁵, D. Dobos³⁰, C. Doglioni⁴⁹, T. Doherty⁵³, T. Dohmae¹⁵⁶, J. Dolejsi¹²⁸, Z. Dolezal¹²⁸, B. A. Dolgoshein^{97,*}, M. Donadelli^{24d}, S. Donati^{123a,123b}, P. Dondero^{120a,120b}, J. Donini³⁴, J. Dopke¹³⁰, A. Doria^{103a}, M. T. Dova⁷⁰, A. T. Doyle⁵³, M. Dris¹⁰, J. Dubbert⁸⁸, S. Dube¹⁵, E. Dubreuil³⁴, E. Duchovni¹⁷³, G. Duckeck⁹⁹, O. A. Ducu^{26a}, D. Duda¹⁷⁶, A. Dudarev³⁰, F. Dudziak⁶³, L. Duflot¹¹⁶, L. Duguid⁷⁶, M. Dührssen³⁰, M. Dunford^{58a}, H. Duran Yildiz^{4a}, M. Düren⁵², A. Durglishvili^{51b}, M. Dwuznik^{38a}, M. Dyndal^{38a}, J. Ebke⁹⁹, W. Edson², N. C. Edwards⁴⁶, W. Ehrenfeld²¹, T. Eifert¹⁴⁴, G. Eigen¹⁴, K. Einsweiler¹⁵, T. Ekelof¹⁶⁷, M. El Kacimi^{136c}, M. Ellert¹⁶⁷, S. Elles⁵, F. Ellinghaus⁸², N. Ellis³⁰, J. Elmsheuser⁹⁹, M. Elsing³⁰, D. Emelianov¹³⁰, Y. Enari¹⁵⁶, O. C. Endner⁸², M. Endo¹¹⁷, R. Engelmann¹⁴⁹, J. Erdmann¹⁷⁷, A. Ereditato¹⁷, D. Eriksson^{147a}, G. Ernis¹⁷⁶, J. Ernst², M. Ernst², J. Ernwein¹³⁷, D. Errede¹⁶⁶, S. Errede¹⁶⁶, E. Ertel⁸², M. Escalier¹¹⁶, H. Esch⁴³, C. Escobar¹²⁴, B. Esposito⁴⁷, A. I. Etienne¹³⁷, E. Etzion¹⁵⁴, H. Evans⁶⁰, A. Ezhilov¹²², L. Fabbri^{20a,20b}, G. Facini³¹, R. M. Fakhruddinov¹²⁹, S. Falciano^{133a}, R. J. Falla⁷⁷, J. Faltova¹²⁸, Y. Fang^{33a}, M. Fanti^{90a,90b}, A. Farbin⁸, A. Farilla^{135a}, T. Faroouque¹², S. Farrell¹⁵, S. M. Farrington¹⁷¹, P. Farthouat³⁰, F. Fassi^{136e}, P. Fassnacht³⁰, D. Fassoulitis⁹, A. Favareto^{50a,50b}, L. Fayard¹¹⁶, P. Federic^{145a}, O. L. Fedin^{122,j}, W. Fedorko¹⁶⁹, M. Fehling-Kaschek⁴⁸, S. Feigl³⁰, L. Felgioni⁸⁴, C. Feng^{33d}, E. J. Feng⁶, H. Feng⁸⁸, A. B. Fenyuk¹²⁹, S. Fernandez Perez³⁰, S. Ferrag⁵³, J. Ferrando⁵³, A. Ferrari¹⁶⁷, P. Ferrari¹⁰⁶, R. Ferrari^{120a}, D. E. Ferreira de Lima⁵³, A. Ferrer¹⁶⁸, D. Ferrere⁴⁹, C. Ferretti⁸⁸, A. Ferretto Parodi^{50a,50b}, M. Fiascaris³¹, F. Fiedler⁸², A. Filipčić⁷⁴, M. Filipuzzi⁴², F. Filthaut¹⁰⁵, M. Fincke-Keeler¹⁷⁰, K. D. Finelli¹⁵¹, M. C. N. Fiolhais^{125a,125c}, L. Fiorini¹⁶⁸, A. Firan⁴⁰, A. Fischer², J. Fischer¹⁷⁶, W. C. Fisher⁸⁹, E. A. Fitzgerald²³, M. Flechl⁴⁸, I. Fleck¹⁴², P. Fleischmann⁸⁸, S. Fleischmann¹⁷⁶, G. T. Fletcher¹⁴⁰, G. Fletcher⁷⁵, T. Flick¹⁷⁶, A. Floderus⁸⁰, L. R. Flores Castillo^{174,k}, A. C. Florez Bustos^{160b}, M. J. Flowerdew¹⁰⁰, A. Formica¹³⁷, A. Forti⁸³, D. Fortin^{160a}, D. Fournier¹¹⁶, H. Fox⁷¹, S. Fracchia¹², P. Francavilla⁷⁹, M. Franchini^{20a,20b}, S. Franchino³⁰, D. Francis³⁰, M. Franklin⁵⁷, S. Franz⁶¹, M. Fraternali^{120a,120b}, S. T. French²⁸, C. Friedrich⁴², F. Friedrich⁴⁴, D. Froidevaux³⁰, J. A. Frost²⁸, C. Fukunaga¹⁵⁷, E. Fullana Torregrosa⁸², B. G. Fulsom¹⁴⁴, J. Fuster¹⁶⁸, C. Gabaldon⁵⁵, O. Gabizon¹⁷³, A. Gabrielli^{20a,20b}, A. Gabrielli^{133a,133b}, S. Gadatsch¹⁰⁶, S. Gadomski⁴⁹, G. Gagliardi^{50a,50b}, P. Gagnon⁶⁰, C. Galea¹⁰⁵, B. Galhardo^{125a,125c}, E. J. Gallas¹¹⁹, V. Gallo¹⁷, B. J. Gallop¹³⁰, P. Gallus¹²⁷, G. Galster³⁶, K. K. Gan¹¹⁰, R. P. Gandrajula⁶², J. Gao^{33b,g}, Y. S. Gao^{144,e}, F. M. Garay Walls⁴⁶, F. Garbersson¹⁷⁷, C. García¹⁶⁸, J. E. García Navarro¹⁶⁸, M. Garcia-Sciveres¹⁵, R. W. Gardner³¹, N. Garelli¹⁴⁴, V. Garonne³⁰, C. Gatti⁴⁷, G. Gaudio^{120a}, B. Gaur¹⁴², L. Gauthier⁹⁴, P. Gauzzi^{133a,133b}, I. L. Gavrilenko⁹⁵, C. Gay¹⁶⁹, G. Gaycken²¹, E. N. Gazis¹⁰, P. Ge^{33d}, Z. Gece¹⁶⁹, C. N. P. Gee¹³⁰, D. A. A. Geerts¹⁰⁶, Ch. Geich-Gimbel²¹, K. Gellerstedt^{147a,147b}, C. Gemme^{50a}, A. Gemmell⁵³, M. H. Genest⁵⁵, S. Gentile^{133a,133b}, M. George⁵⁴, S. George⁷⁶, D. Gerbaudo¹⁶⁴, A. Gershon¹⁵⁴, H. Ghazlane^{136b}, N. Ghodbane³⁴, B. Giacobbe^{20a}, S. Giagu^{133a,133b}, V. Giangiobbe¹², P. Giannetti^{123a,123b}, F. Gianotti³⁰, B. Gibbard²⁵, S. M. Gibson⁷⁶, M. Gilchriese¹⁵, T. P. S. Gillam²⁸, D. Gillberg³⁰, G. Gilles³⁴, D. M. Gingrich^{3,d}, N. Giokaris⁹, M. P. Giordani^{165a,165c}, R. Giordano^{103a,103b}, F. M. Giorgi^{20a}, F. M. Giorgi¹⁶, P. F. Giraud¹³⁷, D. Giugni^{90a}, C. Giuliani⁴⁸, M. Giuliani^{58b}, B. K. Gjelsten¹¹⁸, S. Gkaitatzis¹⁵⁵, I. Gkialas^{155,1}, L. K. Gladilin⁹⁸, C. Glasman⁸¹, J. Glatzer³⁰, P. C. F. Glaysher⁴⁶, A. Glazov⁴², G. L. Glonti⁶⁴, M. Goblirsch-Kolb¹⁰⁰, J. R. Goddard⁷⁵, J. Godfrey¹⁴³, J. Godlewski³⁰, C. Goeringer⁸², S. Goldfarb⁸⁸, T. Golling¹⁷⁷, D. Golubkov¹²⁹, A. Gomes^{125a,125b,125d}, L. S. Gomez Fajardo⁴², R. Gonçalves^{125a}, J. Goncalves Pinto Firmino Da Costa¹³⁷, L. Gonella²¹, S. González de la Hoz¹⁶⁸, G. Gonzalez Parra¹², S. Gonzalez-Sevilla⁴⁹, L. Goossens³⁰, P. A. Gorbounov⁹⁶, H. A. Gordon²⁵, I. Gorelov¹⁰⁴, B. Gorini³⁰, E. Gorini^{72a,72b}, A. Gorišek⁷⁴, E. Gornicki³⁹, A. T. Goshaw⁶, C. Gössling⁴³, M. I. Gostkin⁶⁴, M. Gouighri^{136a}, D. Goujdami^{136c}, M. P. Goulette⁴⁹, A. G. Goussiou¹³⁹, C. Goy⁵, S. Gozpinar²³, H. M. X. Grabas¹³⁷, L. Graber⁵⁴, I. Grabowska-Bold^{38a}, P. Grafström^{20a,20b}, K.-J. Grahn⁴², J. Gramling⁴⁹, E. Gramstad¹¹⁸, S. Grancagnolo¹⁶, V. Grassi¹⁴⁹, V. Gratchev¹²²,

H. M. Gray³⁰, E. Graziani^{135a}, O. G. Grebenyuk¹²², Z. D. Greenwood^{78,m}, K. Gregersen⁷⁷, I. M. Gregor⁴², P. Grenier¹⁴⁴, J. Griffiths⁸, A. A. Grillo¹³⁸, K. Grimm⁷¹, S. Grinstein^{12,n}, Ph. Gris³⁴, Y. V. Grishkevich⁹⁸, J.-F. Grivaz¹¹⁶, J. P. Grohs⁴⁴, A. Grohsjean⁴², E. Gross¹⁷³, J. Grosse-Knetter⁵⁴, G. C. Grossi^{134a,134b}, J. Groth-Jensen¹⁷³, Z. J. Grout¹⁵⁰, L. Guan^{33b}, F. Guescini⁴⁹, D. Guest¹⁷⁷, O. Gueta¹⁵⁴, C. Guicheney³⁴, E. Guido^{50a,50b}, T. Guillemin¹¹⁶, S. Guindon², U. Gul⁵³, C. Gumpert⁴⁴, J. Gunther¹²⁷, J. Guo³⁵, S. Gupta¹¹⁹, P. Gutierrez¹¹², N. G. Gutierrez Ortiz⁵³, C. Gutsche⁷⁷, N. Guttman¹⁵⁴, C. Guyot¹³⁷, C. Gwenlan¹¹⁹, C. B. Gwilliam⁷³, A. Haas¹⁰⁹, C. Haber¹⁵, H. K. Hadavand⁸, N. Haddad^{136e}, P. Haefner²¹, S. Hageböeck²¹, Z. Hajduk³⁹, H. Hakobyan¹⁷⁸, M. Haleem⁴², D. Hall¹¹⁹, G. Halladjian⁸⁹, K. Hamacher¹⁷⁶, P. Hamal¹¹⁴, K. Hamano¹⁷⁰, M. Hamer⁵⁴, A. Hamilton^{146a}, S. Hamilton¹⁶², G. N. Hamity^{146c}, P. G. Hamnett⁴², L. Han^{33b}, K. Hanagaki¹¹⁷, K. Hanawa¹⁵⁶, M. Hance¹⁵, P. Hanke^{58a}, R. Hann¹³⁷, J. B. Hansen³⁶, J. D. Hansen³⁶, P. H. Hansen³⁶, K. Hara¹⁶¹, A. S. Hard¹⁷⁴, T. Harenberg¹⁷⁶, F. Hariri¹¹⁶, S. Harkusha⁹¹, D. Harper⁸⁸, R. D. Harrington⁴⁶, O. M. Harris¹³⁹, P. F. Harrison¹⁷¹, F. Hartjes¹⁰⁶, M. Hasegawa⁶⁶, S. Hasegawa¹⁰², Y. Hasegawa¹⁴¹, A. Hasib¹¹², S. Hassani¹³⁷, S. Haug¹⁷, M. Hauschild³⁰, R. Hauser⁸⁹, M. Havranek¹²⁶, C. M. Hawkes¹⁸, R. J. Hawkins³⁰, A. D. Hawkins⁸⁰, T. Hayashi¹⁶¹, D. Hayden⁸⁹, C. P. Hays¹¹⁹, H. S. Hayward⁷³, S. J. Haywood¹³⁰, S. J. Head¹⁸, T. Heck⁸², V. Hedberg⁸⁰, L. Heelan⁸, S. Heim¹²¹, T. Heim¹⁷⁶, B. Heinemann¹⁵, L. Heinrich¹⁰⁹, J. Hejbal¹²⁶, L. Helary²², C. Heller⁹⁹, M. Heller³⁰, S. Hellman^{147a,147b}, D. Hellmich²¹, C. Helsens³⁰, J. Henderson¹¹⁹, R. C. W. Henderson⁷¹, Y. Heng¹⁷⁴, C. Hengler⁴², A. Henrichs¹⁷⁷, A. M. Henriques Correia³⁰, S. Henrot-Versille¹¹⁶, C. Hensel⁵⁴, G. H. Herbert¹⁶, Y. Hernández Jiménez¹⁶⁸, R. Herrberg-Schubert¹⁶, G. Herten⁴⁸, R. Hertenberger⁹⁹, L. Hervas³⁰, G. G. Hesketh⁷⁷, N. P. Hessey¹⁰⁶, R. Hickling⁷⁵, E. Higón-Rodríguez¹⁶⁸, E. Hill¹⁷⁰, J. C. Hill²⁸, K. H. Hiller⁴², S. Hillert²¹, S. J. Hillier¹⁸, I. Hinchliffe¹⁵, E. Hines¹²¹, M. Hirose¹⁵⁸, D. Hirschbuehl¹⁷⁶, J. Hobbs¹⁴⁹, N. Hod¹⁰⁶, M. C. Hodgkinson¹⁴⁰, P. Hodgson¹⁴⁰, A. Hoecker³⁰, M. R. Hoferkamp¹⁰⁴, J. Hoffman⁴⁰, D. Hoffmann⁸⁴, J. I. Hofmann^{58a}, M. Hohlfield⁸², T. R. Holmes¹⁵, T. M. Hong¹²¹, L. Hooft van Huysduynen¹⁰⁹, J.-Y. Hostachy⁵⁵, S. Hou¹⁵², A. Houmada^{136a}, J. Howard¹¹⁹, J. Howarth⁴², M. Hrabovsky¹¹⁴, I. Hristova¹⁶, J. Hrivnac¹¹⁶, T. Hryn'ova⁵, C. Hsu^{146c}, P. J. Hsu⁸², S.-C. Hsu¹³⁹, D. Hu³⁵, X. Hu²⁵, Y. Huang⁴², Z. Hubacek³⁰, F. Hubaut⁸⁴, F. Huegging²¹, T. B. Huffman¹¹⁹, E. W. Hughes³⁵, G. Hughes⁷¹, M. Huhtinen³⁰, T. A. Hülsing⁸², M. Hurwitz¹⁵, N. Huseynov^{64,b}, J. Huston⁸⁹, J. Huth⁵⁷, G. Iacobucci⁴⁹, G. Iakovidis¹⁰, I. Ibragimov¹⁴², L. Iconomidou-Fayard¹¹⁶, E. Ideal¹⁷⁷, P. Iengo^{103a}, O. Igonkina¹⁰⁶, T. Iizawa¹⁷², Y. Ikegami⁶⁵, K. Ikematsu¹⁴², M. Ikeno⁶⁵, Y. Ilchenko^{31,o}, D. Iliadis¹⁵⁵, N. Ilic¹⁵⁹, Y. Inamaru⁶⁶, T. Ince¹⁰⁰, P. Ioannou⁹, M. Iodice^{135a}, K. Iordanidou⁹, V. Ippolito⁵⁷, A. Irls Quiles¹⁶⁸, C. Isaksson¹⁶⁷, M. Ishino⁶⁷, M. Ishitsuka¹⁵⁸, R. Ishmukhametov¹¹⁰, C. Issever¹¹⁹, S. Istin^{19a}, J. M. Iturbe Ponce⁸³, R. Iuppa^{134a,134b}, J. Ivarsson⁸⁰, W. Iwanski³⁹, H. Iwasaki⁶⁵, J. M. Izen⁴¹, V. Izzo^{103a}, B. Jackson¹²¹, M. Jackson⁷³, P. Jackson¹, M. R. Jaekel³⁰, V. Jain², K. Jakobs⁴⁸, S. Jakobsen³⁰, T. Jakoubek¹²⁶, J. Jakubek¹²⁷, D. O. Jamin¹⁵², D. K. Jana⁷⁸, E. Jansen⁷⁷, H. Jansen³⁰, J. Janssen²¹, M. Janus¹⁷¹, G. Jarlskog⁸⁰, N. Javadov^{64,b}, T. Javůrek⁴⁸, L. Jeanty¹⁵, J. Jejelava^{51a,p}, G.-Y. Jeng¹⁵¹, D. Jennens⁸⁷, P. Jenni^{48,q}, J. Jentsch⁴³, C. Jeske¹⁷¹, S. Jézéquel⁵, H. Ji¹⁷⁴, J. Jia¹⁴⁹, Y. Jiang^{33b}, M. Jimenez Belenguer⁴², S. Jin^{33a}, A. Jinaru^{26a}, O. Jinnouchi¹⁵⁸, M. D. Joergensen³⁶, K. E. Johansson^{147a,147b}, P. Johansson¹⁴⁰, K. A. Johns⁷, K. Jon-And^{147a,147b}, G. Jones¹⁷¹, R. W. L. Jones⁷¹, T. J. Jones⁷³, J. Jongmanns^{58a}, P. M. Jorge^{125a,125b}, K. D. Joshi⁸³, J. Jovicevic¹⁴⁸, X. Ju¹⁷⁴, C. A. Jung⁴³, R. M. Jungst³⁰, P. Jussel⁶¹, A. Juste Rozas^{12,n}, M. Kaci¹⁶⁸, A. Kaczmarska³⁹, M. Kado¹¹⁶, H. Kagan¹¹⁰, M. Kagan¹⁴⁴, E. Kajomovitz⁴⁵, C. W. Kalderon¹¹⁹, S. Kama⁴⁰, A. Kamenshchikov¹²⁹, N. Kanaya¹⁵⁶, M. Kaneda³⁰, S. Kaneti²⁸, V. A. Kantserov⁹⁷, J. Kanzaki⁶⁵, B. Kaplan¹⁰⁹, A. Kapliy³¹, D. Kar⁵³, K. Karakostas¹⁰, N. Karastathis¹⁰, M. Karnevskiy⁸², S. N. Karpov⁶⁴, Z. M. Karpova⁶⁴, K. Karthik¹⁰⁹, V. Kartvelishvili⁷¹, A. N. Karyukhin¹²⁹, L. Kashif¹⁷⁴, G. Kasieczka^{58b}, R. D. Kass¹¹⁰, A. Kastanas¹⁴, Y. Kataoka¹⁵⁶, A. Katre⁴⁹, J. Katzy⁴², V. Kaushik⁷, K. Kawagoe⁶⁹, T. Kawamoto¹⁵⁶, G. Kawamura⁵⁴, S. Kazama¹⁵⁶, V. F. Kazanin¹⁰⁸, M. Y. Kazarinov⁶⁴, R. Keeler¹⁷⁰, R. Kehoe⁴⁰, M. Keil⁵⁴, J. S. Keller⁴², J. J. Kempster⁷⁶, H. Keoshkerian⁵, O. Kepka¹²⁶, B. P. Kerševan⁷⁴, S. Kersten¹⁷⁶, K. Kessoku¹⁵⁶, J. Keung¹⁵⁹, F. Khalil-zada¹¹, H. Khandanyan^{147a,147b}, A. Khanov¹¹³, A. Khodinov⁹⁷, A. Khomich^{58a}, T. J. Khoo²⁸, G. Khorialuli²¹, A. Khoroshilov¹⁷⁶, V. Khovanskiy⁹⁶, E. Khramov⁶⁴, J. Khubua^{51b}, H. Y. Kim⁸, H. Kim^{147a,147b}, S. H. Kim¹⁶¹, N. Kimura¹⁷², O. Kind¹⁶, B. T. King⁷³, M. King¹⁶⁸, R. S. B. King¹¹⁹, S. B. King¹⁶⁹, J. Kirk¹³⁰, A. E. Kiryunin¹⁰⁰, T. Kishimoto⁶⁶, D. Kisielewska^{38a}, F. Kiss⁴⁸, T. Kittelmann¹²⁴, K. Kiuchi¹⁶¹, E. Kladiva^{145b}, M. Klein⁷³, U. Klein⁷³, K. Kleinknecht⁸², P. Klimek^{147a,147b}, A. Klimentov²⁵, R. Klingenberg⁴³, J. A. Klinger⁸³, T. Klioutchnikova³⁰, P. F. Klok¹⁰⁵, E.-E. Kluge^{58a}, P. Kluit¹⁰⁶, S. Kluth¹⁰⁰, E. Kneringer⁶¹, E. B. F. G. Knoops⁸⁴, A. Knue⁵³, D. Kobayashi¹⁵⁸, T. Kobayashi¹⁵⁶, M. Kobel⁴⁴, M. Kocian¹⁴⁴, P. Kodys¹²⁸, P. Koesvesarki²¹, T. Koffas²⁹, E. Koffeman¹⁰⁶, L. A. Kogan¹¹⁹, S. Kohlmann¹⁷⁶, Z. Kohout¹²⁷, T. Kohriki⁶⁵, T. Koi¹⁴⁴, H. Kolanoski¹⁶, I. Koletsou⁵, J. Koll⁸⁹, A. A. Komar^{95,*}, Y. Komori¹⁵⁶, T. Kondo⁶⁵, N. Kondrashova⁴², K. Köneke⁴⁸, A. C. König¹⁰⁵, S. König⁸², T. Kono^{65,r}, R. Konoplich^{109,s}, N. Konstantinidis⁷⁷, R. Kopeliainsky¹⁵³, S. Koperny^{38a}, L. Köpke⁸², A. K. Kopp⁴⁸, K. Korcyl³⁹, K. Kordas¹⁵⁵, A. Korn⁷⁷, A. A. Korol^{108,t}, I. Korolkov¹², E. V. Korolkova¹⁴⁰, V. A. Korotkov¹²⁹, O. Kortner¹⁰⁰, S. Kortner¹⁰⁰, V. V. Kostyukhin²¹, V. M. Kotov⁶⁴, A. Kotwal⁴⁵, C. Kourkoumelis⁹, V. Kouskoura¹⁵⁵,

A. Koutsman^{160a}, R. Kowalewski¹⁷⁰, T. Z. Kowalski^{38a}, W. Kozanecki¹³⁷, A. S. Kozhin¹²⁹, V. Kral¹²⁷, V. A. Kramarenko⁹⁸, G. Kramberger⁷⁴, D. Krasnopevtsev⁹⁷, M. W. Krasny⁷⁹, A. Krasznahorkay³⁰, J. K. Kraus²¹, A. Kravchenko²⁵, S. Kreiss¹⁰⁹, M. Kretz^{58c}, J. Kretzschmar⁷³, K. Kreutzfeldt⁵², P. Krieger¹⁵⁹, K. Kroeninger⁵⁴, H. Kroha¹⁰⁰, J. Kroll¹²¹, J. Kroseberg²¹, J. Krstic^{13a}, U. Kruchonak⁶⁴, H. Krüger²¹, T. Kruker¹⁷, N. Krumnack⁶³, Z. V. Krumshteyn⁶⁴, A. Kruse¹⁷⁴, M. C. Kruse⁴⁵, M. Kruskal²², T. Kubota⁸⁷, S. Kuday^{4a}, S. Kuehn⁴⁸, A. Kugel^{58c}, A. Kuhl¹³⁸, T. Kuhl⁴², V. Kukhtin⁶⁴, Y. Kulchitsky⁹¹, S. Kuleshov^{32b}, M. Kuna^{133a,133b}, J. Kunkle¹²¹, A. Kupco¹²⁶, H. Kurashige⁶⁶, Y. A. Kurochkin⁹¹, R. Kurumida⁶⁶, V. Kus¹²⁶, E. S. Kuwertz¹⁴⁸, M. Kuze¹⁵⁸, J. Kvita¹¹⁴, A. La Rosa⁴⁹, L. La Rotonda^{37a,37b}, C. Lacasta¹⁶⁸, F. Lacava^{133a,133b}, J. Lacey²⁹, H. Lacker¹⁶, D. Lacour⁷⁹, V. R. Lacuesta¹⁶⁸, E. Ladygin⁶⁴, R. Lafaye⁵, B. Laforge⁷⁹, T. Lagouri¹⁷⁷, S. Lai⁴⁸, H. Laier^{58a}, L. Lambourne⁷⁷, S. Lammers⁶⁰, C. L. Lampen⁷, W. Lampl⁷, E. Lançon¹³⁷, U. Landgraf⁴⁸, M. P. J. Landon⁷⁵, V. S. Lang^{58a}, A. J. Lankford¹⁶⁴, F. Lanni²⁵, K. Lantzsch³⁰, S. Laplace⁷⁹, C. Lapoire²¹, J. F. Laporte¹³⁷, T. Lari^{90a}, M. Lassnig³⁰, P. Laurelli⁴⁷, W. Lavrijsen¹⁵, A. T. Law¹³⁸, P. Laycock⁷³, O. Le Dortz⁷⁹, E. Le Guirriec⁸⁴, E. Le Menedeu¹², T. LeCompte⁶, F. Ledroit-Guillon⁵⁵, C. A. Lee¹⁵², H. Lee¹⁰⁶, J. S. H. Lee¹¹⁷, S. C. Lee¹⁵², L. Lee¹⁷⁷, G. Lefebvre⁷⁹, M. Lefebvre¹⁷⁰, F. Legger⁹⁹, C. Leggett¹⁵, A. Lehan⁷³, M. Lehmacher²¹, G. Lehmann Miotto³⁰, X. Lei⁷, W. A. Leight²⁹, A. Leisos¹⁵⁵, A. G. Leister¹⁷⁷, M. A. L. Leite^{24d}, R. Leitner¹²⁸, D. Lellouch¹⁷³, B. Lemmer⁵⁴, K. J. C. Leney⁷⁷, T. Lenz¹⁰⁶, G. Lenzen¹⁷⁶, B. Lenzi³⁰, R. Leone⁷, S. Leone^{123a,123b}, K. Leonhardt⁴⁴, C. Leonidopoulos⁴⁶, S. Leontsinis¹⁰, C. Leroy⁹⁴, C. G. Lester²⁸, C. M. Lester¹²¹, M. Levchenko¹²², J. Levêque⁵, D. Levin⁸⁸, L. J. Levinson¹⁷³, M. Levy¹⁸, A. Lewis¹¹⁹, G. H. Lewis¹⁰⁹, A. M. Leyko²¹, M. Leyton⁴¹, B. Li^{33b,u}, B. Li⁸⁴, H. Li¹⁴⁹, H. L. Li³¹, L. Li⁴⁵, L. Li^{33e}, S. Li⁴⁵, Y. Li^{33c,v}, Z. Liang¹³⁸, H. Liao³⁴, B. Liberti^{134a}, P. Lichard³⁰, K. Lie¹⁶⁶, J. Liebal²¹, W. Liebig¹⁴, C. Limbach²¹, A. Limosani⁸⁷, S. C. Lin^{152,w}, T. H. Lin⁸², F. Linde¹⁰⁶, B. E. Lindquist¹⁴⁹, J. T. Linnemann⁸⁹, E. Lipeles¹²¹, A. Lipniacka¹⁴, M. Lisovsky⁴², T. M. Liss¹⁶⁶, D. Lissauer²⁵, A. Lister¹⁶⁹, A. M. Litke¹³⁸, B. Liu¹⁵², D. Liu¹⁵², J. B. Liu^{33b}, K. Liu^{33b,x}, L. Liu⁸⁸, M. Liu⁴⁵, M. Liu^{33b}, Y. Liu^{33b}, M. Livan^{120a,120b}, S. S. A. Livermore¹¹⁹, A. Lleres⁵⁵, J. Llorente Merino⁸¹, S. L. Lloyd⁷⁵, F. Lo Sterzo¹⁵², E. Lobodzinska⁴², P. Loch⁷, W. S. Lockman¹³⁸, T. Loddenkoetter²¹, F. K. Loebinger⁸³, A. E. Loevschall-Jensen³⁶, A. Loginov¹⁷⁷, T. Lohse¹⁶, K. Lohwasser⁴², M. Lokajicek¹²⁶, V. P. Lombardo⁵, B. A. Long²², J. D. Long⁸⁸, R. E. Long⁷¹, L. Lopes^{125a}, D. Lopez Mateos⁵⁷, B. Lopez Paredes¹⁴⁰, I. Lopez Paz¹², J. Lorenz⁹⁹, N. Lorenzo Martinez⁶⁰, M. Losada¹⁶³, P. Loscutoff¹⁵, X. Lou⁴¹, A. Lounis¹¹⁶, J. Love⁶, P. A. Love⁷¹, A. J. Lowe^{144,e}, F. Lu^{33a}, N. Lu⁸⁸, H. J. Lubatti¹³⁹, C. Luci^{133a,133b}, A. Lucotte⁵⁵, F. Luehring⁶⁰, W. Lukas⁶¹, L. Luminari^{133a}, O. Lundberg^{147a,147b}, B. Lund-Jensen¹⁴⁸, M. Lungwitz⁸², D. Lynn²⁵, R. Lysak¹²⁶, E. Lytken⁸⁰, H. Ma²⁵, L. L. Ma^{33d}, G. Maccarrone⁴⁷, A. Macchiolo¹⁰⁰, J. Machado Miguens^{125a,125b}, D. Macina³⁰, D. Madaffari⁸⁴, R. Madar⁴⁸, H. J. Maddocks⁷¹, W. F. Mader⁴⁴, A. Madsen¹⁶⁷, M. Maeno⁸, T. Maeno²⁵, E. Magradze⁵⁴, K. Mahboubi⁴⁸, J. Mahlstedt¹⁰⁶, S. Mahmoud⁷³, C. Maiani¹³⁷, C. Maidantchik^{24a}, A. A. Maier¹⁰⁰, A. Maio^{125a,125b,125d}, S. Majewski¹¹⁵, Y. Makida⁶⁵, N. Makovec¹¹⁶, P. Mal^{137,y}, B. Malaescu⁷⁹, Pa. Malecki³⁹, V. P. Maleev¹²², F. Malek⁵⁵, U. Mallik⁶², D. Malon⁶, C. Malone¹⁴⁴, S. Maltezos¹⁰, V. M. Malyshev¹⁰⁸, S. Malyukov³⁰, J. Mamuzic^{13b}, B. Mandelli³⁰, L. Mandelli^{90a}, I. Mandic⁷⁴, R. Mandrysch⁶², J. Maneira^{125a,125b}, A. Manfredini¹⁰⁰, L. Manhaes de Andrade Filho^{24b}, J. A. Manjarres Ramos^{160b}, A. Mann⁹⁹, P. M. Manning¹³⁸, A. Manousakis-Katsikakis⁹, B. Mansoulie¹³⁷, R. Mantifel⁸⁶, L. Mapelli³⁰, L. March^{146c}, J. F. Marchand²⁹, G. Marchiori⁷⁹, M. Marcisovsky¹²⁶, C. P. Marino¹⁷⁰, M. Marjanovic^{13a}, C. N. Marques^{125a}, F. Marroquim^{24a}, S. P. Marsden⁸³, Z. Marshall¹⁵, L. F. Marti¹⁷, S. Marti-Garcia¹⁶⁸, B. Martin³⁰, B. Martin⁸⁹, T. A. Martin¹⁷¹, V. J. Martin⁴⁶, B. Martin dit Latour¹⁴, H. Martinez¹³⁷, M. Martinez^{12,n}, S. Martin-Haugh¹³⁰, A. C. Martyniuk⁷⁷, M. Marx¹³⁹, F. Marzano^{133a}, A. Marzin³⁰, L. Masetti⁸², T. Mashimo¹⁵⁶, R. Mashinistov⁹⁵, J. Masik⁸³, A. L. Maslennikov¹⁰⁸, I. Massa^{20a,20b}, L. Massa^{20a,20b}, N. Massol⁵, P. Mastrandrea¹⁴⁹, A. Mastroberardino^{37a,37b}, T. Masubuchi¹⁵⁶, P. Mättig¹⁷⁶, J. Mattmann⁸², J. Maurer^{26a}, S. J. Maxfield⁷³, D. A. Maximov^{108,t}, R. Mazini¹⁵², L. Mazzaferro^{134a,134b}, G. Mc Goldrick¹⁵⁹, S. P. Mc Kee⁸⁸, A. McCann⁸⁸, R. L. McCarthy¹⁴⁹, T. G. McCarthy²⁹, N. A. McCubbin¹³⁰, K. W. McFarlane^{56,*}, J. A. McFayden⁷⁷, G. Mchedlidze⁵⁴, S. J. McMahon¹³⁰, R. A. McPherson^{170,i}, A. Meade⁸⁵, J. Mechnich¹⁰⁶, M. Medinnis⁴², S. Meehan³¹, S. Mehlhase⁹⁹, A. Mehta⁷³, K. Meier^{58a}, C. Meineck⁹⁹, B. Meirose⁸⁰, C. Melachrinos³¹, B. R. Mellado Garcia^{146c}, F. Meloni¹⁷, A. Mengarelli^{20a,20b}, S. Menke¹⁰⁰, E. Meoni¹⁶², K. M. Mercurio⁵⁷, S. Mergelmeyer²¹, N. Meric¹³⁷, P. Mermoud⁴⁹, L. Merola^{103a,103b}, C. Meroni^{90a}, F. S. Merritt³¹, H. Merritt¹¹⁰, A. Messina^{30,z}, J. Metcalfe²⁵, A. S. Mete¹⁶⁴, C. Meyer⁸², C. Meyer¹²¹, J.-P. Meyer¹³⁷, J. Meyer³⁰, R. P. Middleton¹³⁰, S. Migas⁷³, L. Mijovic²¹, G. Mikenberg¹⁷³, M. Mikesikova¹²⁶, M. Mikuž⁷⁴, A. Milic³⁰, D. W. Miller³¹, C. Mills⁴⁶, A. Milov¹⁷³, D. A. Milstead^{147a,147b}, D. Milstein¹⁷³, A. A. Minaenko¹²⁹, I. A. Minashvili⁶⁴, A. I. Mincer¹⁰⁹, B. Mindur^{38a}, M. Mineev⁶⁴, Y. Ming¹⁷⁴, L. M. Mir¹², G. Mirabelli^{133a}, T. Mitani¹⁷², J. Mitrevski⁹⁹, V. A. Mitsou¹⁶⁸, S. Mitsui⁶⁵, A. Miucci⁴⁹, P. S. Miyagawa¹⁴⁰, J. U. Mjörnmark⁸⁰, T. Moa^{147a,147b}, K. Mochizuki⁸⁴, S. Mohapatra³⁵, W. Mohr⁴⁸, S. Molander^{147a,147b}, R. Moles-Valls¹⁶⁸, K. Mönig⁴², C. Monini⁵⁵, J. Monk³⁶, E. Monnier⁸⁴, J. Montejo Berlingen¹², F. Monticelli⁷⁰, S. Monzani^{133a,133b}, R. W. Moore³, A. Moraes⁵³, N. Morange⁶², D. Moreno⁸², M. Moreno Llácer⁵⁴, P. Morettini^{50a}, M. Morgenstern⁴⁴, M. Morii⁵⁷, S. Moritz⁸², A. K. Morley¹⁴⁸, G. Mornacchi³⁰

J. D. Morris⁷⁵, L. Morvaj¹⁰², H. G. Moser¹⁰⁰, M. Mosidze^{51b}, J. Moss¹¹⁰, K. Motohashi¹⁵⁸, R. Mount¹⁴⁴, E. Mountricha²⁵, S. V. Mouraviev^{95,*}, E. J. W. Moyse⁸⁵, S. Muanza⁸⁴, R. D. Mudd¹⁸, F. Mueller^{58a}, J. Mueller¹²⁴, K. Mueller²¹, T. Mueller²⁸, T. Mueller⁸², D. Muenstermann⁴⁹, Y. Munwes¹⁵⁴, J. A. Murillo Quijada¹⁸, W. J. Murray^{130,171}, H. Musheghyan⁵⁴, E. Musto¹⁵³, A. G. Myagkov^{129,aa}, M. Myska¹²⁷, O. Nackenhorst⁵⁴, J. Nadal⁵⁴, K. Nagai⁶¹, R. Nagai¹⁵⁸, Y. Nagai⁸⁴, K. Nagano⁶⁵, A. Nagarkar¹¹⁰, Y. Nagasaka⁵⁹, M. Nagel¹⁰⁰, A. M. Nairz³⁰, Y. Nakahama³⁰, K. Nakamura⁶⁵, T. Nakamura¹⁵⁶, I. Nakano¹¹¹, H. Namasivayam⁴¹, G. Nanava²¹, R. Narayan^{58b}, T. Nattermann²¹, T. Naumann⁴², G. Navarro¹⁶³, R. Nayyar⁷, H. A. Neal⁸⁸, P. Yu. Nechaeva⁹⁵, T. J. Neep⁸³, P. D. Nef¹⁴⁴, A. Negri^{120a,120b}, G. Negri³⁰, M. Negrini^{20a}, S. Nektarijevic⁴⁹, A. Nelson¹⁶⁴, T. K. Nelson¹⁴⁴, S. Nemecek¹²⁶, P. Nemethy¹⁰⁹, A. A. Nepomuceno^{24a}, M. Nessi^{30,ab}, M. S. Neubauer¹⁶⁶, M. Neumann¹⁷⁶, R. M. Neves¹⁰⁹, P. Nevski²⁵, P. R. Newman¹⁸, D. H. Nguyen⁶, R. B. Nickerson¹¹⁹, R. Nicolaidou¹³⁷, B. Nicquevert³⁰, J. Nielsen¹³⁸, N. Nikiforou³⁵, A. Nikiforov¹⁶, V. Nikolaenko^{129,aa}, I. Nikolic-Audit⁷⁹, K. Nikolics⁴⁹, K. Nikolopoulos¹⁸, P. Nilsson⁸, Y. Ninomiya¹⁵⁶, A. Nisati^{133a}, R. Nisius¹⁰⁰, T. Nobe¹⁵⁸, L. Nodulman⁶, M. Nomachi¹¹⁷, I. Nomidis²⁹, S. Norberg¹¹², M. Nordberg³⁰, O. Novgorodova⁴⁴, S. Nowak¹⁰⁰, M. Nozaki⁶⁵, L. Nozka¹¹⁴, K. Ntekas¹⁰, G. Nunes Hanninger⁸⁷, T. Nunnemann⁹⁹, E. Nurse⁷⁷, F. Nuti⁸⁷, B. J. O'Brien⁴⁶, F. O'grady⁷, D. C. O'Neil¹⁴³, V. O'Shea⁵³, F. G. Oakham^{29,d}, H. Oberlack¹⁰⁰, T. Obermann²¹, J. Ocariz⁷⁹, A. Ochi⁶⁶, M. I. Ochoa⁷⁷, S. Oda⁶⁹, S. Odaka⁶⁵, H. Ogren⁶⁰, A. Oh⁸³, S. H. Oh⁴⁵, C. C. Ohm¹⁵, H. Ohman¹⁶⁷, W. Okamura¹¹⁷, H. Okawa²⁵, Y. Okumura³¹, T. Okuyama¹⁵⁶, A. Olariu^{26a}, A. G. Olchevski⁶⁴, S. A. Olivares Pino⁴⁶, D. Oliveira Damazio²⁵, E. Oliver Garcia¹⁶⁸, A. Olszewski³⁹, J. Olszowska³⁹, A. Onofre^{125a,125c}, P. U. E. Onyisi^{31,o}, C. J. Oram^{160a}, M. J. Oreglia³¹, Y. Oren¹⁵⁴, D. Orestano^{135a,135b}, N. Orlando^{72a,72b}, C. Oropeza Barrera⁵³, R. S. Ori¹⁵⁹, B. Osculati^{50a,50b}, R. Ospanov¹²¹, G. Otero y Garzon²⁷, H. Otono⁶⁹, M. Ouchrif^{136d}, E. A. Ouellette¹⁷⁰, F. Ould-Saada¹¹⁸, A. Ouraou¹³⁷, K. P. Oussoren¹⁰⁶, Q. Ouyang^{33a}, A. Ovcharova¹⁵, M. Owen⁸³, V. E. Ozcan^{19a}, N. Ozturk⁸, K. Pachal¹¹⁹, A. Pacheco Pages¹², C. Padilla Aranda¹², M. Pagáčová⁴⁸, S. Pagan Griso¹⁵, E. Paganis¹⁴⁰, C. Pahl¹⁰⁰, F. Paige²⁵, P. Pais⁸⁵, K. Pajchel¹¹⁸, G. Palacino^{160b}, S. Palestini³⁰, M. Palka^{38b}, D. Pallin³⁴, A. Palma^{125a,125b}, J. D. Palmer¹⁸, Y. B. Pan¹⁷⁴, E. Panagiotopoulou¹⁰, J. G. Panduro Vazquez⁷⁶, P. Pani¹⁰⁶, N. Panikashvili⁸⁸, S. Panitkin²⁵, D. Pantea^{26a}, L. Paolozzi^{134a,134b}, Th. D. Papadopoulou¹⁰, K. Papageorgiou^{155,i}, A. Paramonov⁶, D. Paredes Hernandez³⁴, M. A. Parker²⁸, F. Parodi^{50a,50b}, J. A. Parsons³⁵, U. Parzefall⁴⁸, E. Pasqualucci^{133a}, S. Passaggio^{50a}, A. Passeri^{135a}, F. Pastore^{135a,135b,*}, Fr. Pastore⁷⁶, G. Pásztor²⁹, S. Pataraiia¹⁷⁶, N. D. Patel¹⁵¹, J. R. Pater⁸³, S. Patricelli^{103a,103b}, T. Pauly³⁰, J. Pearce¹⁷⁰, M. Pedersen¹¹⁸, S. Pedraza Lopez¹⁶⁸, R. Pedro^{125a,125b}, S. V. Peleganchuk¹⁰⁸, D. Pelikan¹⁶⁷, H. Peng^{33b}, B. Penning³¹, J. Penwell⁶⁰, D. V. Perepelitsa²⁵, E. Perez Codina^{160a}, M. T. Pérez García-Estañ¹⁶⁸, V. Perez Reale³⁵, L. Perini^{90a,90b}, H. Pernegger³⁰, R. Perrino^{72a}, R. Peschke⁴², V. D. Peshekhonov⁶⁴, K. Peters³⁰, R. F. Y. Peters⁸³, B. A. Petersen³⁰, T. C. Petersen³⁶, E. Petit⁴², A. Petridis^{147a,147b}, C. Petridou¹⁵⁵, E. Petrolo^{133a}, F. Petrucci^{135a,135b}, N. E. Pettersson¹⁵⁸, R. Pezoa^{32b}, P. W. Phillips¹³⁰, G. Piacquadio¹⁴⁴, E. Pianori¹⁷¹, A. Picazio⁴⁹, E. Piccaro⁷⁵, M. Piccinini^{20a,20b}, R. Piegai²⁷, D. T. Pignotti¹¹⁰, J. E. Pilcher³¹, A. D. Pilkington⁷⁷, J. Pina^{125a,125b,125d}, M. Pinamonti^{165a,165c,ac}, A. Pinder¹¹⁹, J. L. Pinfold³, A. Pingel³⁶, B. Pinto^{125a}, S. Pires⁷⁹, M. Pitt¹⁷³, C. Pizio^{90a,90b}, L. Plazak^{145a}, M.-A. Pleier²⁵, V. Pleskot¹²⁸, E. Plotnikova⁶⁴, P. Plucinski^{147a,147b}, S. Poddar^{58a}, F. Podlyski³⁴, R. Poettgen⁸², L. Poggioli¹¹⁶, D. Pohl²¹, M. Pohl⁴⁹, G. Polesello^{120a}, A. Policicchio^{37a,37b}, R. Polifka¹⁵⁹, A. Polini^{20a}, C. S. Pollard⁴⁵, V. Polychronakos²⁵, K. Pommès³⁰, L. Pontecorvo^{133a}, B. G. Pope⁸⁹, G. A. Popeneciu^{26b}, D. S. Popovic^{13a}, A. Poppleton³⁰, X. Portell Bueso¹², S. Pospisil¹²⁷, K. Potamianos¹⁵, I. N. Potrap⁶⁴, C. J. Potter¹⁵⁰, C. T. Potter¹¹⁵, G. Poulard³⁰, J. Poveda⁶⁰, V. Pozdnyakov⁶⁴, P. Pralavorio⁸⁴, A. Pranko¹⁵, S. Prasad³⁰, R. Pravahan⁸, S. Prell⁶³, D. Price⁸³, J. Price⁷³, L. E. Price⁶, D. Prieur¹²⁴, M. Primavera^{72a}, M. Proissl⁴⁶, K. Prokofiev⁴⁷, F. Prokoshin^{32b}, E. Protopapadaki¹³⁷, S. Protopopescu²⁵, J. Proudfoot⁶, M. Przybycien^{38a}, H. Przysiezniak⁵, E. Ptacek¹¹⁵, D. Puddu^{135a,135b}, E. Pueschel⁸⁵, D. Puldon¹⁴⁹, M. Purohit^{25,ad}, P. Puzo¹¹⁶, J. Qian⁸⁸, G. Qin⁵³, Y. Qin⁸³, A. Quadt⁵⁴, D. R. Quarrie¹⁵, W. B. Quayle^{165a,165b}, M. Queitsch-Maitland⁸³, D. Quilty⁵³, A. Qureshi^{160b}, V. Radeka²⁵, V. Radescu⁴², S. K. Radhakrishnan¹⁴⁹, P. Radloff¹¹⁵, P. Rados⁸⁷, F. Ragusa^{90a,90b}, G. Rahal¹⁷⁹, S. Rajagopalan²⁵, M. Rammensee³⁰, A. S. Randle-Conde⁴⁰, C. Rangel-Smith¹⁶⁷, K. Rao¹⁶⁴, F. Rauscher⁹⁹, T. C. Rave⁴⁸, T. Ravenscroft⁵³, M. Raymond³⁰, A. L. Read¹¹⁸, N. P. Readioff⁷³, D. M. Rebuffi^{120a,120b}, A. Redelbach¹⁷⁵, G. Redlinger²⁵, R. Reece¹³⁸, K. Reeves⁴¹, L. Rehnisch¹⁶, H. Reisin²⁷, M. Relich¹⁶⁴, C. Rembser³⁰, H. Ren^{33a}, Z. L. Ren¹⁵², A. Renaud¹¹⁶, M. Rescigno^{133a}, S. Resconi^{90a}, O. L. Rezanova^{108,t}, P. Reznicek¹²⁸, R. Rezvani⁹⁴, R. Richter¹⁰⁰, M. Ridel⁷⁹, P. Rieck¹⁶, J. Rieger⁵⁴, M. Rijssenbeek¹⁴⁹, A. Rimoldi^{120a,120b}, L. Rinaldi^{20a}, E. Ritsch⁶¹, I. Riu¹², F. Rizatdinova¹¹³, E. Rizvi⁷⁵, S. H. Robertson^{86,i}, A. Robichaud-Veronneau⁸⁶, D. Robinson²⁸, J. E. M. Robinson⁸³, A. Robson⁵³, C. Roda^{123a,123b}, L. Rodrigues³⁰, S. Roe³⁰, O. Røhne¹¹⁸, S. Rolli¹⁶², A. Romaniouk⁹⁷, M. Romano^{20a,20b}, E. Romero Adam¹⁶⁸, N. Rompotis¹³⁹, M. Ronzani⁴⁸, L. Roos⁷⁹, E. Ros¹⁶⁸, S. Rosati^{133a}, K. Rosbach⁴⁹, M. Rose⁷⁶, P. Rose¹³⁸, P. L. Rosendahl¹⁴, O. Rosenthal¹⁴², V. Rossetti^{147a,147b}, E. Rossi^{103a,103b}, L. P. Rossi^{50a}, R. Rosten¹³⁹, M. Rotaru^{26a}, I. Roth¹⁷³, J. Rothberg¹³⁹, D. Rousseau¹¹⁶, C. R. Royon¹³⁷, A. Rozanov⁸⁴, Y. Rozen¹⁵³, X. Ruan^{146c}, F. Rubbo¹², I. Rubinskiy⁴², V. I. Rud⁹⁸, C. Rudolph⁴⁴, M. S. Rudolph¹⁵⁹, F. Rühr⁴⁸, A. Ruiz-Martinez³⁰, Z. Rurikova⁴⁸, N. A. Rusakovich⁶⁴,

A. Ruschke⁹⁹, J. P. Rutherford⁷, N. Ruthmann⁴⁸, Y. F. Ryabov¹²², M. Rybar¹²⁸, G. Rybkin¹¹⁶, N. C. Ryder¹¹⁹, A. F. Saavedra¹⁵¹, S. Sacerdoti²⁷, A. Saddique³, I. Sadeh¹⁵⁴, H. F.-W. Sadrozinski¹³⁸, R. Sadykov⁶⁴, F. Safai Tehrani^{133a}, H. Sakamoto¹⁵⁶, Y. Sakurai¹⁷², G. Salamanna^{135a,135b}, A. Salamon^{134a}, M. Saleem¹¹², D. Salek¹⁰⁶, P. H. Sales De Bruin¹³⁹, D. Salihagic¹⁰⁰, A. Salnikov¹⁴⁴, J. Salt¹⁶⁸, D. Salvatore^{37a,37b}, F. Salvatore¹⁵⁰, A. Salvucci¹⁰⁵, A. Salzburger³⁰, D. Sampsonidis¹⁵⁵, A. Sanchez^{103a,103b}, J. Sánchez¹⁶⁸, V. Sanchez Martinez¹⁶⁸, H. Sandaker¹⁴, R. L. Sandbach⁷⁵, H. G. Sander⁸², M. P. Sanders⁹⁹, M. Sandhoff¹⁷⁶, T. Sandoval²⁸, C. Sandoval¹⁶³, R. Sandstroem¹⁰⁰, D. P. C. Sankey¹³⁰, A. Sansoni⁴⁷, C. Santoni³⁴, R. Santonico^{134a,134b}, H. Santos^{125a}, I. Santoyo Castillo¹⁵⁰, K. Sapp¹²⁴, A. Saprnov⁶⁴, J. G. Saraiva^{125a,125d}, B. Sarrazin²¹, G. Sartisohn¹⁷⁶, O. Sasaki⁶⁵, Y. Sasaki¹⁵⁶, G. Sauvage^{5,*}, E. Sauvan⁵, P. Savard^{159,d}, D. O. Savu³⁰, C. Sawyer¹¹⁹, L. Sawyer^{78,m}, D. H. Saxon⁵³, J. Saxon¹²¹, C. Sbarra^{20a}, A. Sbrizzi³, T. Scanlon⁷⁷, D. A. Scannicchio¹⁶⁴, M. Scarcella¹⁵¹, V. Scarfone^{37a,37b}, J. Schaarschmidt¹⁷³, P. Schacht¹⁰⁰, D. Schaefer³⁰, R. Schaefer⁴², S. Schaepe²¹, S. Schaezel^{58b}, U. Schäfer⁸², A. C. Schaffer¹¹⁶, D. Schaile⁹⁹, R. D. Schamberger¹⁴⁹, V. Scharf^{58a}, V. A. Schegelsky¹²², D. Scheirich¹²⁸, M. Schernau¹⁶⁴, M. I. Scherzer³⁵, C. Schiavi^{50a,50b}, J. Schieck⁹⁹, C. Schillo⁴⁸, M. Schioppa^{37a,37b}, S. Schlenker³⁰, E. Schmidt⁴⁸, K. Schmieden³⁰, C. Schmitt⁸², S. Schmitt^{58b}, B. Schneider¹⁷, Y. J. Schnellbach⁷³, U. Schnoor⁴⁴, L. Schoeffel¹³⁷, A. Schoening^{58b}, B. D. Schoenrock⁸⁹, A. L. S. Schorlemmer⁵⁴, M. Schott⁸², D. Schouten^{160a}, J. Schovancova²⁵, S. Schramm¹⁵⁹, M. Schreyer¹⁷⁵, C. Schroeder⁸², N. Schuh⁸², M. J. Schultens²¹, H.-C. Schultz-Coulon^{58a}, H. Schulz¹⁶, M. Schumacher⁴⁸, B. A. Schumm¹³⁸, Ph. Schune¹³⁷, C. Schwanenberger⁸³, A. Schwartzman¹⁴⁴, Ph. Schwegler¹⁰⁰, Ph. Schwemling¹³⁷, R. Schwienhorst⁸⁹, J. Schwindling¹³⁷, T. Schwindt²¹, M. Schwoerer⁵, F. G. Sciacca¹⁷, E. Scifo¹¹⁶, G. Sciolla²³, W. G. Scott¹³⁰, F. Scuri^{123a,123b}, F. Scutti²¹, J. Searcy⁸⁸, G. Sedov⁴², E. Sedykh¹²², S. C. Seidel¹⁰⁴, A. Seiden¹³⁸, F. Seifert¹²⁷, J. M. Seixas^{24a}, G. Sekhniaidze^{103a}, S. J. Sekula⁴⁰, K. E. Selbach⁴⁶, D. M. Seliverstov^{122,*}, G. Sellers⁷³, N. Semprini-Cesari^{20a,20b}, C. Serfon³⁰, L. Serin¹¹⁶, L. Serkin⁵⁴, T. Serre⁸⁴, R. Seuster^{160a}, H. Severini¹¹², T. Sfiligoy⁷⁴, F. Sforza¹⁰⁰, A. Sfyrla³⁰, E. Shabalina⁵⁴, M. Shamim¹¹⁵, L. Y. Shan^{33a}, R. Shang¹⁶, J. T. Shank²², M. Shapiro¹⁵, P. B. Shatalov⁹⁶, K. Shaw^{165a,165b}, C. Y. Shehu¹⁵⁰, P. Sherwood⁷⁷, L. Shi^{152,ae}, S. Shimizu⁶⁶, C. O. Shimmin¹⁶⁴, M. Shimojima¹⁰¹, M. Shiyakova⁶⁴, A. Shmeleva⁹⁵, M. J. Shochet³¹, D. Short¹¹⁹, S. Shrestha⁶³, E. Shulga⁹⁷, M. A. Shupe⁷, S. Shushkevich⁴², P. Sicho¹²⁶, O. Sidiropoulou¹⁵⁵, D. Sidorov¹¹³, A. Sidoti^{133a}, F. Siegert⁴⁴, Dj. Sijacki^{13a}, J. Silva^{125a,125d}, Y. Silver¹⁵⁴, D. Silverstein¹⁴⁴, S. B. Silverstein^{147a}, V. Simak¹²⁷, O. Simard⁵, Lj. Simic^{13a}, S. Simion¹¹⁶, E. Simioni⁸², B. Simmons⁷⁷, R. Simoniello^{90a,90b}, M. Simonyan³⁶, P. Sinervo¹⁵⁹, N. B. Sinev¹¹⁵, V. Sipica¹⁴², G. Siragusa¹⁷⁵, A. Sircar⁷⁸, A. N. Sisakyan^{64,*}, S. Yu. Sivoklov⁹⁸, J. Sjölin^{147a,147b}, T. B. Sjursen¹⁴, H. P. Skottowe⁵⁷, K. Yu. Skovpen¹⁰⁸, P. Skubic¹¹², M. Slater¹⁸, T. Slavicek¹²⁷, K. Sliwa¹⁶², V. Smakhtin¹⁷³, B. H. Smart⁴⁶, L. Smestad¹⁴, S. Yu. Smirnov⁹⁷, Y. Smirnov⁹⁷, L. N. Smirnova^{98,af}, O. Smirnova⁸⁰, K. M. Smith⁵³, M. Smizanska⁷¹, K. Smolek¹²⁷, A. A. Snesarev⁹⁵, G. Snidero⁷⁵, S. Snyder²⁵, R. Sobie^{170,i}, F. Socher⁴⁴, A. Soffer¹⁵⁴, D. A. Soh^{152,ae}, C. A. Solans³⁰, M. Solar¹²⁷, J. Solc¹²⁷, E. Yu. Soldatov⁹⁷, U. Soldevila¹⁶⁸, A. A. Solodkov¹²⁹, A. Soloshenko⁶⁴, O. V. Solovyanov¹²⁹, V. Solovyev¹²², P. Sommer⁴⁸, H. Y. Song^{33b}, N. Soni¹, A. Sood¹⁵, A. Sopczak¹²⁷, B. Sopko¹²⁷, V. Sopko¹²⁷, V. Sorin¹², M. Sosebee⁸, R. Soualah^{165a,165c}, P. Soueid⁹⁴, A. M. Soukharev¹⁰⁸, D. South⁴², S. Spagnolo^{72a,72b}, F. Spanò⁷⁶, W. R. Spearman⁵⁷, F. Spettel¹⁰⁰, R. Spighi^{20a}, G. Spigo³⁰, L. A. Spiller⁸⁷, M. Spousta¹²⁸, T. Spreitzer¹⁵⁹, B. Spurlock⁸, R. D. St. Denis^{53,*}, S. Staerz⁴⁴, J. Stahlman¹²¹, R. Stamen^{58a}, S. Stamm¹⁶, E. Stanecka³⁹, R. W. Stanek⁶, C. Stanescu^{135a}, M. Stanescu-Bellu⁴², M. M. Stanitzki⁴², S. Stapnes¹¹⁸, E. A. Starchenko¹²⁹, J. Stark⁵⁵, P. Staroba¹²⁶, P. Starovoitov⁴², R. Staszewski³⁹, P. Stavina^{145a,*}, P. Steinberg²⁵, B. Stelzer¹⁴³, H. J. Stelzer³⁰, O. Stelzer-Chilton^{160a}, H. Stenzel⁵², S. Stern¹⁰⁰, G. A. Stewart⁵³, J. A. Stillings²¹, M. C. Stockton⁸⁶, M. Stoebe⁸⁶, G. Stoica^{26a}, P. Stolte⁵⁴, S. Stonjek¹⁰⁰, A. R. Stradling⁸, A. Straessner⁴⁴, M. E. Stramaglia¹⁷, J. Strandberg¹⁴⁸, S. Strandberg^{147a,147b}, A. Strandlie¹¹⁸, E. Strauss¹⁴⁴, M. Strauss¹¹², P. Strizenc^{145b}, R. Ströhmer¹⁷⁵, D. M. Strom¹¹⁵, R. Stroynowski⁴⁰, S. A. Stucci¹⁷, B. Stugu¹⁴, N. A. Styles⁴², D. Su¹⁴⁴, J. Su¹²⁴, R. Subramaniam⁷⁸, A. Succurro¹², Y. Sugaya¹¹⁷, C. Suhr¹⁰⁷, M. Suk¹²⁷, V. V. Sulin⁹⁵, S. Sultansoy^{4c}, T. Sumida⁶⁷, S. Sun⁵⁷, X. Sun^{33a}, J. E. Sundermann⁴⁸, K. Suruliz¹⁴⁰, G. Susinno^{37a,37b}, M. R. Sutton¹⁵⁰, Y. Suzuki⁶⁵, M. Svatos¹²⁶, S. Swedish¹⁶⁹, M. Swiatlowski¹⁴⁴, I. Sykora^{145a}, T. Sykora¹²⁸, D. Ta⁸⁹, C. Taccini^{135a,135b}, K. Tackmann⁴², J. Taenzer¹⁵⁹, A. Taffard¹⁶⁴, R. Tahirout^{160a}, N. Taiblum¹⁵⁴, H. Takai²⁵, R. Takashima⁶⁸, H. Takeda⁶⁶, T. Takeshita¹⁴¹, Y. Takubo⁶⁵, M. Talby⁸⁴, A. A. Talyshv^{108,t}, J. Y. C. Tam¹⁷⁵, K. G. Tan⁸⁷, J. Tanaka¹⁵⁶, R. Tanaka¹¹⁶, S. Tanaka¹³², S. Tanaka⁶⁵, A. J. Tanasijczuk¹⁴³, B. B. Tannenwald¹¹⁰, N. Tannoury²¹, S. Tapprogge⁸², S. Tarem¹⁵³, F. Tarrade²⁹, G. F. Tartarelli^{90a}, P. Tas¹²⁸, M. Tasevsky¹²⁶, T. Tashiro⁶⁷, E. Tassi^{37a,37b}, A. Tavares Delgado^{125a,125b}, Y. Tayalati^{136d}, F. E. Taylor⁹³, G. N. Taylor⁸⁷, W. Taylor^{160b}, F. A. Teischinger³⁰, M. Teixeira Dias Castanheira⁷⁵, P. Teixeira-Dias⁷⁶, K. K. Temming⁴⁸, H. Ten Kate³⁰, P. K. Teng¹⁵², J. J. Teoh¹¹⁷, S. Terada⁶⁵, K. Terashi¹⁵⁶, J. Terron⁸¹, S. Terzo¹⁰⁰, M. Testa⁴⁷, R. J. Teuscher^{159,i}, J. Therhaag²¹, T. Thevenaux-Pelzer³⁴, J. P. Thomas¹⁸, J. Thomas-Wilsker⁷⁶, E. N. Thompson³⁵, P. D. Thompson¹⁸, P. D. Thompson¹⁵⁹, R. J. Thompson⁸³, A. S. Thompson⁵³, L. A. Thomsen³⁶, E. Thomson¹²¹, M. Thomson²⁸, W. M. Thong⁸⁷, R. P. Thun^{88,*}, F. Tian³⁵, M. J. Tibbetts¹⁵, V. O. Tikhomirov^{95,ag}, Yu. A. Tikhonov^{108,t}

S. Timoshenko⁹⁷, E. Tiouchichine⁸⁴, P. Tipton¹⁷⁷, S. Tisserant⁸⁴, T. Todorov⁵, S. Todorova-Nova¹²⁸, B. Toggerson⁷, J. Tojo⁶⁹, S. Tokár^{145a}, K. Tokushuku⁶⁵, K. Tollefson⁸⁹, L. Tomlinson⁸³, M. Tomoto¹⁰², L. Tompkins³¹, K. Toms¹⁰⁴, N. D. Topilin⁶⁴, E. Torrence¹¹⁵, H. Torres¹⁴³, E. Torró Pastor¹⁶⁸, J. Toth^{84,ah}, F. Touchard⁸⁴, D. R. Tovey¹⁴⁰, H. L. Tran¹¹⁶, T. Trefzger¹⁷⁵, L. Tremblet³⁰, A. Tricoli³⁰, I. M. Trigger^{160a}, S. Trincaz-Duvoid⁷⁹, M. F. Tripijana¹², W. Trischuk¹⁵⁹, B. Trocme⁵⁵, C. Troncon^{90a}, M. Trotter-McDonald¹⁴³, M. Trovatelli^{135a,135b}, P. True⁸⁹, M. Trzebinski³⁹, A. Trzupek³⁹, C. Tsarouchas³⁰, J. C.-L. Tseng¹¹⁹, P. V. Tsiarshka⁹¹, D. Tsionou¹³⁷, G. Tsipolitis¹⁰, N. Tsirintanis⁹, S. Tsiskaridze¹², V. Tsiskaridze⁴⁸, E. G. Tskhadadze^{51a}, I. I. Tsukerman⁹⁶, V. Tsulaia¹⁵, S. Tsuno⁶⁵, D. Tsybychev¹⁴⁹, A. Tudorache^{26a}, V. Tudorache^{26a}, A. N. Tuna¹²¹, S. A. Tuppuri^{20a,20b}, S. Turchikhin^{98,af}, D. Turecek¹²⁷, I. Turk Cakir^{4d}, R. Turra^{90a,90b}, P. M. Tuts³⁵, A. Tykhonov⁴⁹, M. Tylmad^{147a,147b}, M. Tyndel¹³⁰, K. Uchida²¹, I. Ueda¹⁵⁶, R. Ueno²⁹, M. Ughetto⁸⁴, M. Ugland¹⁴, M. Uhlenbrock²¹, F. Ukegawa¹⁶¹, G. Unal³⁰, A. Undrus²⁵, G. Unel¹⁶⁴, F. C. Ungaro⁴⁸, Y. Unno⁶⁵, C. Unverdorben⁹⁹, D. Urbaniec³⁵, P. Urquijo⁸⁷, G. Usai⁸, A. Usanova⁶¹, L. Vacavant⁸⁴, V. Vacek¹²⁷, B. Vachon⁸⁶, N. Valencic¹⁰⁶, S. Valentinetti^{20a,20b}, A. Valero¹⁶⁸, L. Valery³⁴, S. Valkar¹²⁸, E. Valladolid Gallego¹⁶⁸, S. Vallecorsa⁴⁹, J. A. Valls Ferrer¹⁶⁸, W. Van Den Wollenberg¹⁰⁶, P. C. Van Der Deijl¹⁰⁶, R. van der Geer¹⁰⁶, H. van der Graaf¹⁰⁶, R. Van Der Leeuw¹⁰⁶, D. van der Ster³⁰, N. van Eldik³⁰, P. van Gemmeren⁶, J. Van Nieuwkoop¹⁴³, I. van Vulpen¹⁰⁶, M. C. van Woerden³⁰, M. Vanadia^{133a,133b}, W. Vandelli³⁰, R. Vanguri¹²¹, A. Vaniachine⁶, P. Vankov⁴², F. Vannucci⁷⁹, G. Vardanyan¹⁷⁸, R. Vari^{133a}, E. W. Varnes⁷, T. Varol⁸⁵, D. Varouchas⁷⁹, A. Vartapetian⁸, K. E. Varvell¹⁵¹, F. Vazeille³⁴, T. Vazquez Schroeder⁵⁴, J. Veatch⁷, F. Veloso^{125a,125c}, S. Veneziano^{133a}, A. Ventura^{72a,72b}, D. Ventura⁸⁵, M. Venturi¹⁷⁰, N. Venturi¹⁵⁹, A. Venturini²³, V. Vercesi^{120a}, M. Verducci^{133a,133b}, W. Verkerke¹⁰⁶, J. C. Vermeulen¹⁰⁶, A. Vest⁴⁴, M. C. Vetterli^{143,d}, O. Viazlo⁸⁰, I. Vichou¹⁶⁶, T. Vickey^{146c,ai}, O. E. Vickey Boeriu^{146c}, G. H. A. Viehhauser¹¹⁹, S. Viel¹⁶⁹, R. Vigne³⁰, M. Villa^{20a,20b}, M. Villaplana Perez^{90a,90b}, E. Vilucchi⁴⁷, M. G. Vincter²⁹, V. B. Vinogradov⁶⁴, J. Virzi¹⁵, I. Vivarelli¹⁵⁰, F. Vives Vaque³, S. Vlachos¹⁰, D. Vladoiu⁹⁹, M. Vlasak¹²⁷, A. Vogel²¹, M. Vogel^{32a}, P. Vokac¹²⁷, G. Volpi^{123a,123b}, M. Volpi⁸⁷, H. von der Schmitt¹⁰⁰, H. von Radziewski⁴⁸, E. von Toerne²¹, V. Vorobel¹²⁸, K. Vorobev⁹⁷, M. Vos¹⁶⁸, R. Voss³⁰, J. H. Vossebeld⁷³, N. Vranjes¹³⁷, M. Vranjes Milosavljevic¹⁰⁶, V. Vrba¹²⁶, M. Vreeswijk¹⁰⁶, T. Vu Anh⁴⁸, R. Vuillermet³⁰, I. Vukotic³¹, Z. Vykydal¹²⁷, P. Wagner²¹, W. Wagner¹⁷⁶, H. Wahlberg⁷⁰, S. Wahrmund⁴⁴, J. Wakabayashi¹⁰², J. Walder⁷¹, R. Walker⁹⁹, W. Walkowiak¹⁴², R. Wall¹⁷⁷, P. Waller⁷³, B. Walsh¹⁷⁷, C. Wang^{152,aj}, C. Wang⁴⁵, F. Wang¹⁷⁴, H. Wang¹⁵, H. Wang⁴⁰, J. Wang⁴², J. Wang^{33a}, K. Wang⁸⁶, R. Wang¹⁰⁴, S. M. Wang¹⁵², T. Wang²¹, X. Wang¹⁷⁷, C. Wanotayaroj¹¹⁵, A. Warburton⁸⁶, C. P. Ward²⁸, D. R. Wardrope⁷⁷, M. Warsinsky⁴⁸, A. Washbrook⁴⁶, C. Wasicki⁴², P. M. Watkins¹⁸, A. T. Watson¹⁸, I. J. Watson¹⁵¹, M. F. Watson¹⁸, G. Watts¹³⁹, S. Watts⁸³, B. M. Waugh⁷⁷, S. Webb⁸³, M. S. Weber¹⁷, S. W. Weber¹⁷⁵, J. S. Webster³¹, A. R. Weidberg¹¹⁹, P. Weigell¹⁰⁰, B. Weinert⁶⁰, J. Weingarten⁵⁴, C. Weiser⁴⁸, H. Weits¹⁰⁶, P. S. Wells³⁰, T. Wenaus²⁵, D. Wendland¹⁶, Z. Weng^{152,ae}, T. Wengler³⁰, S. Wenig³⁰, N. Vermes²¹, M. Werner⁴⁸, P. Werner³⁰, M. Wessels^{58a}, J. Wetter¹⁶², K. Whalen²⁹, A. White⁸, M. J. White¹, R. White^{32b}, S. White^{123a,123b}, D. Whiteson¹⁶⁴, D. Wicke¹⁷⁶, F. J. Wickens¹³⁰, W. Wiedenmann¹⁷⁴, M. Wielers¹³⁰, P. Wienemann²¹, C. Wiglesworth³⁶, L. A. M. Wiik-Fuchs²¹, P. A. Wijeratne⁷⁷, A. Wildauer¹⁰⁰, M. A. Wildt^{42,ak}, H. G. Wilkens³⁰, J. Z. Will⁹⁹, H. H. Williams¹²¹, S. Williams²⁸, C. Willis⁸⁹, S. Willocq⁸⁵, A. Wilson⁸⁸, J. A. Wilson¹⁸, I. Wingerter-Seez⁵, F. Winklmeier¹¹⁵, B. T. Winter²¹, M. Wittgen¹⁴⁴, T. Wittig⁴³, J. Wittkowski⁹⁹, S. J. Wollstadt⁸², M. W. Wolter³⁹, H. Wolters^{125a,125c}, B. K. Wosiek³⁹, J. Wotschack³⁰, M. J. Woudstra⁸³, K. W. Wozniak³⁹, M. Wright⁵³, M. Wu⁵⁵, S. L. Wu¹⁷⁴, X. Wu⁴⁹, Y. Wu⁸⁸, E. Wulf³⁵, T. R. Wyatt⁸³, B. M. Wynne⁴⁶, S. Xella³⁶, M. Xiao¹³⁷, D. Xu^{33a}, L. Xu^{33b,al}, B. Yabsley¹⁵¹, S. Yacoub^{146b,am}, R. Yakabe⁶⁶, M. Yamada⁶⁵, H. Yamaguchi¹⁵⁶, Y. Yamaguchi¹¹⁷, A. Yamamoto⁶⁵, K. Yamamoto⁶³, S. Yamamoto¹⁵⁶, T. Yamamura¹⁵⁶, T. Yamanaka¹⁵⁶, K. Yamauchi¹⁰², Y. Yamazaki⁶⁶, Z. Yan²², H. Yang^{33e}, H. Yang¹⁷⁴, U. K. Yang⁸³, Y. Yang¹¹⁰, S. Yanush⁹², L. Yao^{33a}, W.-M. Yao¹⁵, Y. Yasu⁶⁵, E. Yatsenko⁴², K. H. Yau Wong²¹, J. Ye⁴⁰, S. Ye²⁵, I. Yeletsikhin⁶⁴, A. L. Yen⁵⁷, E. Yildirim⁴², M. Yilmaz^{4b}, R. Yoosoofmiya¹²⁴, K. Yorita¹⁷², R. Yoshida⁶, K. Yoshihara¹⁵⁶, C. Young¹⁴⁴, C. J. S. Young³⁰, S. Youssef²², D. R. Yu¹⁵, J. Yu⁸, J. M. Yu⁸⁸, J. Yu¹¹³, L. Yuan⁶⁶, A. Yurkewicz¹⁰⁷, I. Yusuff^{28,an}, B. Zabinski³⁹, R. Zaidan⁶², A. M. Zaitsev^{129,aa}, A. Zaman¹⁴⁹, S. Zambito²³, L. Zanello^{133a,133b}, D. Zanzi¹⁰⁰, C. Zeitnitz¹⁷⁶, M. Zeman¹²⁷, A. Zemla^{38a}, K. Zengel²³, O. Zenin¹²⁹, T. Ženiš^{145a}, D. Zerwas¹¹⁶, G. Zevi della Porta⁵⁷, D. Zhang⁸⁸, F. Zhang¹⁷⁴, H. Zhang⁸⁹, J. Zhang⁶, L. Zhang¹⁵², X. Zhang^{33d}, Z. Zhang¹¹⁶, Z. Zhao^{33b}, A. Zhemchugov⁶⁴, J. Zhong¹¹⁹, B. Zhou⁸⁸, L. Zhou³⁵, N. Zhou¹⁶⁴, C. G. Zhu^{33d}, H. Zhu^{33a}, J. Zhu⁸⁸, Y. Zhu^{33b}, X. Zhuang^{33a}, K. Zhukov⁹⁵, A. Zibell¹⁷⁵, D. Ziemska⁶⁰, N. I. Zimine⁶⁴, C. Zimmermann⁸², R. Zimmermann²¹, S. Zimmermann²¹, S. Zimmermann⁴⁸, Z. Zinonos⁵⁴, M. Ziolkowski¹⁴², G. Zobernig¹⁷⁴, A. Zoccoli^{20a,20b}, M. zur Nedden¹⁶, G. Zurzolo^{103a,103b}, V. Zutshi¹⁰⁷, L. Zwalinski³⁰

¹ Department of Physics, University of Adelaide, Adelaide, Australia

² Physics Department, SUNY Albany, Albany, NY, USA

³ Department of Physics, University of Alberta, Edmonton, AB, Canada

- ⁴ (a) Department of Physics, Ankara University, Ankara, Turkey; (b) Department of Physics, Gazi University, Ankara, Turkey; (c) Division of Physics, TOBB University of Economics and Technology, Ankara, Turkey; (d) Turkish Atomic Energy Authority, Ankara, Turkey
- ⁵ LAPP, CNRS/IN2P3 and Université de Savoie, Annecy-le-Vieux, France
- ⁶ High Energy Physics Division, Argonne National Laboratory, Argonne, IL, USA
- ⁷ Department of Physics, University of Arizona, Tucson, AZ, USA
- ⁸ Department of Physics, The University of Texas at Arlington, Arlington, TX, USA
- ⁹ Physics Department, University of Athens, Athens, Greece
- ¹⁰ Physics Department, National Technical University of Athens, Zografou, Greece
- ¹¹ Institute of Physics, Azerbaijan Academy of Sciences, Baku, Azerbaijan
- ¹² Institut de Física d'Altes Energies and Departament de Física de la Universitat Autònoma de Barcelona, Barcelona, Spain
- ¹³ (a) Institute of Physics, University of Belgrade, Belgrade, Serbia; (b) Vinca Institute of Nuclear Sciences, University of Belgrade, Belgrade, Serbia
- ¹⁴ Department for Physics and Technology, University of Bergen, Bergen, Norway
- ¹⁵ Physics Division, Lawrence Berkeley National Laboratory, University of California, Berkeley, CA, USA
- ¹⁶ Department of Physics, Humboldt University, Berlin, Germany
- ¹⁷ Albert Einstein Center for Fundamental Physics and Laboratory for High Energy Physics, University of Bern, Bern, Switzerland
- ¹⁸ School of Physics and Astronomy, University of Birmingham, Birmingham, UK
- ¹⁹ (a) Department of Physics, Bogazici University, Istanbul, Turkey; (b) Department of Physics, Dogus University, Istanbul, Turkey; (c) Department of Physics Engineering, Gaziantep University, Gaziantep, Turkey
- ²⁰ (a) INFN Sezione di Bologna, Bologna, Italy; (b) Dipartimento di Fisica e Astronomia, Università di Bologna, Bologna, Italy
- ²¹ Physikalisches Institut, University of Bonn, Bonn, Germany
- ²² Department of Physics, Boston University, Boston, MA, USA
- ²³ Department of Physics, Brandeis University, Waltham, MA, USA
- ²⁴ (a) Universidade Federal do Rio De Janeiro COPPE/EE/IF, Rio de Janeiro, Brazil; (b) Federal University of Juiz de Fora (UFJF), Juiz de Fora, Brazil; (c) Federal University of Sao Joao del Rei (UFSJ), Sao Joao del Rei, Brazil; (d) Instituto de Física, Universidade de Sao Paulo, São Paulo, Brazil
- ²⁵ Physics Department, Brookhaven National Laboratory, Upton, NY, USA
- ²⁶ (a) National Institute of Physics and Nuclear Engineering, Bucharest, Romania; (b) Physics Department, National Institute for Research and Development of Isotopic and Molecular Technologies, Cluj Napoca, Romania; (c) University Politehnica Bucharest, Bucharest, Romania; (d) West University in Timisoara, Timisoara, Romania
- ²⁷ Departamento de Física, Universidad de Buenos Aires, Buenos Aires, Argentina
- ²⁸ Cavendish Laboratory, University of Cambridge, Cambridge, UK
- ²⁹ Department of Physics, Carleton University, Ottawa, ON, Canada
- ³⁰ CERN, Geneva, Switzerland
- ³¹ Enrico Fermi Institute, University of Chicago, Chicago, IL, USA
- ³² (a) Departamento de Física, Pontificia Universidad Católica de Chile, Santiago, Chile; (b) Departamento de Física, Universidad Técnica Federico Santa María, Valparaiso, Chile
- ³³ (a) Institute of High Energy Physics, Chinese Academy of Sciences, Beijing, China; (b) Department of Modern Physics, University of Science and Technology of China, Hefei, Anhui, China; (c) Department of Physics, Nanjing University, Nanjing, Jiangsu, China; (d) School of Physics, Shandong University, Jinan, Shandong, China; (e) Physics Department, Shanghai Jiao Tong University, Shanghai, China
- ³⁴ Laboratoire de Physique Corpusculaire, Clermont Université and Université Blaise Pascal and CNRS/IN2P3, Clermont-Ferrand, France
- ³⁵ Nevis Laboratory, Columbia University, Irvington, NY, USA
- ³⁶ Niels Bohr Institute, University of Copenhagen, Copenhagen, Denmark
- ³⁷ (a) INFN Gruppo Collegato di Cosenza, Laboratori Nazionali di Frascati, Frascati, Italy; (b) Dipartimento di Fisica, Università della Calabria, Rende, Italy
- ³⁸ (a) Faculty of Physics and Applied Computer Science, AGH University of Science and Technology, Kraków, Poland; (b) Marian Smoluchowski Institute of Physics, Jagiellonian University, Kraków, Poland

- ³⁹ The Henryk Niewodniczanski Institute of Nuclear Physics, Polish Academy of Sciences, Kraków, Poland
- ⁴⁰ Physics Department, Southern Methodist University, Dallas, TX, USA
- ⁴¹ Physics Department, University of Texas at Dallas, Richardson, TX, USA
- ⁴² DESY, Hamburg and Zeuthen, Germany
- ⁴³ Institut für Experimentelle Physik IV, Technische Universität Dortmund, Dortmund, Germany
- ⁴⁴ Institut für Kern- und Teilchenphysik, Technische Universität Dresden, Dresden, Germany
- ⁴⁵ Department of Physics, Duke University, Durham, NC, USA
- ⁴⁶ SUPA-School of Physics and Astronomy, University of Edinburgh, Edinburgh, UK
- ⁴⁷ INFN Laboratori Nazionali di Frascati, Frascati, Italy
- ⁴⁸ Fakultät für Mathematik und Physik, Albert-Ludwigs-Universität, Freiburg, Germany
- ⁴⁹ Section de Physique, Université de Genève, Geneva, Switzerland
- ⁵⁰ ^(a) INFN Sezione di Genova, Genoa, Italy; ^(b) Dipartimento di Fisica, Università di Genova, Genoa, Italy
- ⁵¹ ^(a) E. Andronikashvili Institute of Physics, Iv. Javakishvili Tbilisi State University, Tbilisi, Georgia; ^(b) High Energy Physics Institute, Tbilisi State University, Tbilisi, Georgia
- ⁵² II Physikalisches Institut, Justus-Liebig-Universität Giessen, Giessen, Germany
- ⁵³ SUPA-School of Physics and Astronomy, University of Glasgow, Glasgow, UK
- ⁵⁴ II Physikalisches Institut, Georg-August-Universität, Göttingen, Germany
- ⁵⁵ Laboratoire de Physique Subatomique et de Cosmologie, Université Grenoble-Alpes, CNRS/IN2P3, Grenoble, France
- ⁵⁶ Department of Physics, Hampton University, Hampton, VA, USA
- ⁵⁷ Laboratory for Particle Physics and Cosmology, Harvard University, Cambridge, MA, USA
- ⁵⁸ ^(a) Kirchhoff-Institut für Physik, Ruprecht-Karls-Universität Heidelberg, Heidelberg, Germany; ^(b) Physikalisches Institut, Ruprecht-Karls-Universität Heidelberg, Heidelberg, Germany; ^(c) ZITI Institut für technische Informatik, Ruprecht-Karls-Universität Heidelberg, Mannheim, Germany
- ⁵⁹ Faculty of Applied Information Science, Hiroshima Institute of Technology, Hiroshima, Japan
- ⁶⁰ Department of Physics, Indiana University, Bloomington, IN, USA
- ⁶¹ Institut für Astro- und Teilchenphysik, Leopold-Franzens-Universität, Innsbruck, Austria
- ⁶² University of Iowa, Iowa City, IA, USA
- ⁶³ Department of Physics and Astronomy, Iowa State University, Ames, IA, USA
- ⁶⁴ Joint Institute for Nuclear Research, JINR Dubna, Dubna, Russia
- ⁶⁵ KEK, High Energy Accelerator Research Organization, Tsukuba, Japan
- ⁶⁶ Graduate School of Science, Kobe University, Kobe, Japan
- ⁶⁷ Faculty of Science, Kyoto University, Kyoto, Japan
- ⁶⁸ Kyoto University of Education, Kyoto, Japan
- ⁶⁹ Department of Physics, Kyushu University, Fukuoka, Japan
- ⁷⁰ Instituto de Física La Plata, Universidad Nacional de La Plata and CONICET, La Plata, Argentina
- ⁷¹ Physics Department, Lancaster University, Lancaster, UK
- ⁷² ^(a) INFN Sezione di Lecce, Lecce, Italy; ^(b) Dipartimento di Matematica e Fisica, Università del Salento, Lecce, Italy
- ⁷³ Oliver Lodge Laboratory, University of Liverpool, Liverpool, UK
- ⁷⁴ Department of Physics, Jožef Stefan Institute and University of Ljubljana, Ljubljana, Slovenia
- ⁷⁵ School of Physics and Astronomy, Queen Mary University of London, London, UK
- ⁷⁶ Department of Physics, Royal Holloway University of London, Surrey, UK
- ⁷⁷ Department of Physics and Astronomy, University College London, London, UK
- ⁷⁸ Louisiana Tech University, Ruston, LA, USA
- ⁷⁹ Laboratoire de Physique Nucléaire et de Hautes Energies, UPMC and Université Paris-Diderot and CNRS/IN2P3, Paris, France
- ⁸⁰ Fysiska institutionen, Lunds Universitet, Lund, Sweden
- ⁸¹ Departamento de Física Teórica C-15, Universidad Autónoma de Madrid, Madrid, Spain
- ⁸² Institut für Physik, Universität Mainz, Mainz, Germany
- ⁸³ School of Physics and Astronomy, University of Manchester, Manchester, UK
- ⁸⁴ CPPM, Aix-Marseille Université and CNRS/IN2P3, Marseille, France
- ⁸⁵ Department of Physics, University of Massachusetts, Amherst, MA, USA
- ⁸⁶ Department of Physics, McGill University, Montreal, QC, Canada
- ⁸⁷ School of Physics, University of Melbourne, Parkville, VIC, Australia

- 88 Department of Physics, The University of Michigan, Ann Arbor, MI, USA
- 89 Department of Physics and Astronomy, Michigan State University, East Lansing, MI, USA
- 90 (a) INFN Sezione di Milano, Milan, Italy; (b) Dipartimento di Fisica, Università di Milano, Milan, Italy
- 91 B.I. Stepanov Institute of Physics, National Academy of Sciences of Belarus, Minsk, Republic of Belarus
- 92 National Scientific and Educational Centre for Particle and High Energy Physics, Minsk, Republic of Belarus
- 93 Department of Physics, Massachusetts Institute of Technology, Cambridge, MA, USA
- 94 Group of Particle Physics, University of Montreal, Montreal, QC, Canada
- 95 P.N. Lebedev Institute of Physics, Academy of Sciences, Moscow, Russia
- 96 Institute for Theoretical and Experimental Physics (ITEP), Moscow, Russia
- 97 Moscow Engineering and Physics Institute (MEPhI), Moscow, Russia
- 98 D.V. Skobeltsyn Institute of Nuclear Physics, M.V. Lomonosov Moscow State University, Moscow, Russia
- 99 Fakultät für Physik, Ludwig-Maximilians-Universität München, Munich, Germany
- 100 Max-Planck-Institut für Physik (Werner-Heisenberg-Institut), Munich, Germany
- 101 Nagasaki Institute of Applied Science, Nagasaki, Japan
- 102 Graduate School of Science and Kobayashi-Maskawa Institute, Nagoya University, Nagoya, Japan
- 103 (a) INFN Sezione di Napoli, Naples, Italy; (b) Dipartimento di Fisica, Università di Napoli, Naples, Italy
- 104 Department of Physics and Astronomy, University of New Mexico, Albuquerque, NM, USA
- 105 Institute for Mathematics, Astrophysics and Particle Physics, Radboud University Nijmegen/Nikhef, Nijmegen, The Netherlands
- 106 Nikhef National Institute for Subatomic Physics and University of Amsterdam, Amsterdam, The Netherlands
- 107 Department of Physics, Northern Illinois University, DeKalb, IL, USA
- 108 Budker Institute of Nuclear Physics, SB RAS, Novosibirsk, Russia
- 109 Department of Physics, New York University, New York, NY, USA
- 110 Ohio State University, Columbus, OH, USA
- 111 Faculty of Science, Okayama University, Okayama, Japan
- 112 Homer L. Dodge Department of Physics and Astronomy, University of Oklahoma, Norman, OK, USA
- 113 Department of Physics, Oklahoma State University, Stillwater, OK, USA
- 114 Palacký University, RCPTM, Olomouc, Czech Republic
- 115 Center for High Energy Physics, University of Oregon, Eugene, OR, USA
- 116 LAL, Université Paris-Sud and CNRS/IN2P3, Orsay, France
- 117 Graduate School of Science, Osaka University, Osaka, Japan
- 118 Department of Physics, University of Oslo, Oslo, Norway
- 119 Department of Physics, Oxford University, Oxford, UK
- 120 (a) INFN Sezione di Pavia, Pavia, Italy; (b) Dipartimento di Fisica, Università di Pavia, Pavia, Italy
- 121 Department of Physics, University of Pennsylvania, Philadelphia, PA, USA
- 122 Petersburg Nuclear Physics Institute, Gatchina, Russia
- 123 (a) INFN Sezione di Pisa, Pisa, Italy; (b) Dipartimento di Fisica E. Fermi, Università di Pisa, Pisa, Italy
- 124 Department of Physics and Astronomy, University of Pittsburgh, Pittsburgh, PA, USA
- 125 (a) Laboratório de Instrumentação e Física Experimental de Partículas-LIP, Lisbon, Portugal; (b) Faculdade de Ciências, Universidade de Lisboa, Lisbon, Portugal; (c) Department of Physics, University of Coimbra, Coimbra, Portugal; (d) Centro de Física Nuclear da Universidade de Lisboa, Lisbon, Portugal; (e) Departamento de Física, Universidade do Minho, Braga, Portugal; (f) Departamento de Física Teórica y del Cosmos and CAFPE, Universidad de Granada, Granada, Spain; (g) Dep Física and CEFITEC of Faculdade de Ciências e Tecnologia, Universidade Nova de Lisboa, Caparica, Portugal
- 126 Institute of Physics, Academy of Sciences of the Czech Republic, Prague, Czech Republic
- 127 Czech Technical University in Prague, Prague, Czech Republic
- 128 Faculty of Mathematics and Physics, Charles University in Prague, Prague, Czech Republic
- 129 State Research Center Institute for High Energy Physics, Protvino, Russia
- 130 Particle Physics Department, Rutherford Appleton Laboratory, Didcot, UK
- 131 Physics Department, University of Regina, Regina, SK, Canada
- 132 Ritsumeikan University, Kusatsu, Shiga, Japan
- 133 (a) INFN Sezione di Roma, Rome, Italy; (b) Dipartimento di Fisica, Sapienza Università di Roma, Rome, Italy

- 134 (a) INFN Sezione di Roma Tor Vergata, Rome, Italy; (b) Dipartimento di Fisica, Università di Roma Tor Vergata, Rome, Italy
- 135 (a) INFN Sezione di Roma Tre, Rome, Italy; (b) Dipartimento di Matematica e Fisica, Università Roma Tre, Rome, Italy
- 136 (a) Faculté des Sciences Ain Chock, Réseau Universitaire de Physique des Hautes Energies-Université Hassan II, Casablanca, Morocco; (b) Centre National de l'Énergie des Sciences Techniques Nucleaires, Rabat, Morocco; (c) Faculté des Sciences Semlalia, Université Cadi Ayyad, LPHEA-Marrakech, Marrakech, Morocco; (d) Faculté des Sciences, Université Mohamed Premier and LPTPM, Oujda, Morocco; (e) Faculté des Sciences, Université Mohammed V-Agdal, Rabat, Morocco
- 137 DSM/IRFU (Institut de Recherches sur les Lois Fondamentales de l'Univers), CEA Saclay (Commissariat à l'Énergie Atomique et aux Énergies Alternatives), Gif-sur-Yvette, France
- 138 Santa Cruz Institute for Particle Physics, University of California Santa Cruz, Santa Cruz, CA, USA
- 139 Department of Physics, University of Washington, Seattle, WA, USA
- 140 Department of Physics and Astronomy, University of Sheffield, Sheffield, UK
- 141 Department of Physics, Shinshu University, Nagano, Japan
- 142 Fachbereich Physik, Universität Siegen, Siegen, Germany
- 143 Department of Physics, Simon Fraser University, Burnaby, BC, Canada
- 144 SLAC National Accelerator Laboratory, Stanford, CA, USA
- 145 (a) Faculty of Mathematics, Physics and Informatics, Comenius University, Bratislava, Slovak Republic; (b) Department of Subnuclear Physics, Institute of Experimental Physics of the Slovak Academy of Sciences, Kosice, Slovak Republic
- 146 (a) Department of Physics, University of Cape Town, Cape Town, South Africa; (b) Department of Physics, University of Johannesburg, Johannesburg, South Africa; (c) School of Physics, University of the Witwatersrand, Johannesburg, South Africa
- 147 (a) Department of Physics, Stockholm University, Stockholm, Sweden; (b) The Oskar Klein Centre, Stockholm, Sweden
- 148 Physics Department, Royal Institute of Technology, Stockholm, Sweden
- 149 Departments of Physics and Astronomy and Chemistry, Stony Brook University, Stony Brook, NY, USA
- 150 Department of Physics and Astronomy, University of Sussex, Brighton, UK
- 151 School of Physics, University of Sydney, Sydney, Australia
- 152 Institute of Physics, Academia Sinica, Taipei, Taiwan
- 153 Department of Physics, Technion, Israel Institute of Technology, Haifa, Israel
- 154 Raymond and Beverly Sackler School of Physics and Astronomy, Tel Aviv University, Tel Aviv, Israel
- 155 Department of Physics, Aristotle University of Thessaloniki, Thessaloniki, Greece
- 156 International Center for Elementary Particle Physics and Department of Physics, The University of Tokyo, Tokyo, Japan
- 157 Graduate School of Science and Technology, Tokyo Metropolitan University, Tokyo, Japan
- 158 Department of Physics, Tokyo Institute of Technology, Tokyo, Japan
- 159 Department of Physics, University of Toronto, Toronto, ON, Canada
- 160 (a) TRIUMF, Vancouver, BC, Canada; (b) Department of Physics and Astronomy, York University, Toronto, ON, Canada
- 161 Faculty of Pure and Applied Sciences, University of Tsukuba, Tsukuba, Japan
- 162 Department of Physics and Astronomy, Tufts University, Medford, MA, USA
- 163 Centro de Investigaciones, Universidad Antonio Narino, Bogota, Colombia
- 164 Department of Physics and Astronomy, University of California Irvine, Irvine, CA, USA
- 165 (a) INFN Gruppo Collegato di Udine, Sezione di Trieste, Udine, Italy; (b) ICTP, Trieste, Italy; (c) Dipartimento di Chimica, Fisica e Ambiente, Università di Udine, Udine, Italy
- 166 Department of Physics, University of Illinois, Urbana, IL, USA
- 167 Department of Physics and Astronomy, University of Uppsala, Uppsala, Sweden
- 168 Instituto de Física Corpuscular (IFIC) and Departamento de Física Atómica, Molecular y Nuclear and Departamento de Ingeniería Electrónica and Instituto de Microelectrónica de Barcelona (IMB-CNM), University of Valencia and CSIC, Valencia, Spain
- 169 Department of Physics, University of British Columbia, Vancouver, BC, Canada
- 170 Department of Physics and Astronomy, University of Victoria, Victoria, BC, Canada
- 171 Department of Physics, University of Warwick, Coventry, UK
- 172 Waseda University, Tokyo, Japan
- 173 Department of Particle Physics, The Weizmann Institute of Science, Rehovot, Israel
- 174 Department of Physics, University of Wisconsin, Madison, WI, USA

- ¹⁷⁵ Fakultät für Physik und Astronomie, Julius-Maximilians-Universität, Würzburg, Germany
- ¹⁷⁶ Fachbereich C Physik, Bergische Universität Wuppertal, Wuppertal, Germany
- ¹⁷⁷ Department of Physics, Yale University, New Haven, CT, USA
- ¹⁷⁸ Yerevan Physics Institute, Yerevan, Armenia
- ¹⁷⁹ Centre de Calcul de l'Institut National de Physique Nucléaire et de Physique des Particules (IN2P3), Villeurbanne, France
- ^a Also at Department of Physics, King's College London, London, UK
- ^b Also at Institute of Physics, Azerbaijan Academy of Sciences, Baku, Azerbaijan
- ^c Also at Particle Physics Department, Rutherford Appleton Laboratory, Didcot, UK
- ^d Also at TRIUMF, Vancouver, BC, Canada
- ^e Also at Department of Physics, California State University, Fresno, CA, USA
- ^f Also at Tomsk State University, Tomsk, Russia
- ^g Also at CPPM, Aix-Marseille Université and CNRS/IN2P3, Marseille, France
- ^h Also at Università di Napoli Parthenope, Naples, Italy
- ⁱ Also at Institute of Particle Physics (IPP), Victoria, Canada
- ^j Also at Department of Physics, St. Petersburg State Polytechnical University, St. Petersburg, Russia
- ^k Also at Chinese University of Hong Kong, Hong Kong, China
- ^l Also at Department of Financial and Management Engineering, University of the Aegean, Chios, Greece
- ^m Also at Louisiana Tech University, Ruston, LA, USA
- ⁿ Also at Institutio Catalana de Recerca i Estudis Avancats, ICREA, Barcelona, Spain
- ^o Also at Department of Physics, The University of Texas at Austin, Austin, TX, USA
- ^p Also at Institute of Theoretical Physics, Ilia State University, Tbilisi, Georgia
- ^q Also at CERN, Geneva, Switzerland
- ^r Also at O Chadai Academic Production, Ochanomizu University, Tokyo, Japan
- ^s Also at Manhattan College, New York, NY, USA
- ^t Also at Novosibirsk State University, Novosibirsk, Russia
- ^u Also at Institute of Physics, Academia Sinica, Taipei, Taiwan
- ^v Also at LAL, Université Paris-Sud and CNRS/IN2P3, Orsay, France
- ^w Also at Academia Sinica Grid Computing, Institute of Physics, Academia Sinica, Taipei, Taiwan
- ^x Also at Laboratoire de Physique Nucléaire et de Hautes Energies, UPMC and Université Paris-Diderot and CNRS/IN2P3, Paris, France
- ^y Also at School of Physical Sciences, National Institute of Science Education and Research, Bhubaneswar, India
- ^z Also at Dipartimento di Fisica, Sapienza Università di Roma, Rome, Italy
- ^{aa} Also at Moscow Institute of Physics and Technology State University, Dolgoprudny, Russia
- ^{ab} Also at Section de Physique, Université de Genève, Geneva, Switzerland
- ^{ac} Also at International School for Advanced Studies (SISSA), Trieste, Italy
- ^{ad} Also at Department of Physics and Astronomy, University of South Carolina, Columbia, SC, USA
- ^{ae} Also at School of Physics and Engineering, Sun Yat-sen University, Guangzhou, China
- ^{af} Also at Faculty of Physics, M.V. Lomonosov Moscow State University, Moscow, Russia
- ^{ag} Also at Moscow Engineering and Physics Institute (MEPhI), Moscow, Russia
- ^{ah} Also at Institute for Particle and Nuclear Physics, Wigner Research Centre for Physics, Budapest, Hungary
- ^{ai} Also at Department of Physics, Oxford University, Oxford, UK
- ^{aj} Also at Department of Physics, Nanjing University, Jiangsu, China
- ^{ak} Also at Institut für Experimentalphysik, Universität Hamburg, Hamburg, Germany
- ^{al} Also at Department of Physics, The University of Michigan, Ann Arbor, MI, USA
- ^{am} Also at Discipline of Physics, University of KwaZulu-Natal, Durban, South Africa
- ^{an} Also at Department of Physics, University of Malaya, Kuala Lumpur, Malaysia
- * Deceased